OCULAR FINDINGS AND INTRAOCULAR LENS POWER IN CAPTIVE CHIMPANZEES (*Pan troglodytes*)

by

Keri-Lee Shannon Dobbie

Submitted in partial fulfilment in accordance with the requirements for the degree of

Master Of Veterinary Medicine (MMedVet)

in the subject

OPHTHALMOLOGY

at the

UNIVERSITY OF PRETORIA

SUPERVISOR: Prof Gerhard Steenkamp
CO-SUPERVISOR: Dr Izak Venter

AUGUST 2020

DECLARATION

I, Keri-Lee Shannon Dobbie, student number 04296385 hereby declare that this dissertation, "Ocular findings and intraocular lens power in captive chimpanzees *(Pan troglodytes)*", is submitted in accordance with the requirements for the Master of Veterinary Medicine (MMedVet) degree at University of Pretoria, is my own original work and has not previously been submitted to any other institution of higher learning. All sources cited or quoted in this research paper are indicated and acknowledged with a comprehensive list of references. Ethics clearance for this research was obtained from the University of Pretoria Animal Ethics Committee (V089-18) and Research Ethics Committee (REC088-18) on 30 October 2018 and 5 November 2018 respectively.

.....

Keri-Lee Shannon Dobbie

15 August 2020

AEC CERTIFICATE

UNIVERSITEIT VAN PRETORIA
UNIVERSITY OF PRETORIA
YUNIBESITHI YA PRETORIA

Animal Ethics Committee

PROJECT TITLE	**Ocular findings and reference values for tonometry in the chimpanzee (*Pan troglodytes*)**
PROJECT NUMBER	**V089-18**
RESEARCHER/PRINCIPAL INVESTIGATOR	**Dr. K-L Dobbie**

STUDENT NUMBER (where applicable)	**U_04297385**
DISSERTATION/THESIS SUBMITTED FOR	**MMedVet**

ANIMAL SPECIES/SAMPLE	**Chimpanzee (*Pan troglodytes*)**
NUMBER OF SAMPLES	**33**
Approval period to use animals for research/testing purposes	**October 2018 – October 2019**
SUPERVISOR	**Prof. G Steenkamp**

KINDLY NOTE:

Should there be a change in the species or number of animal/s required, or the experimental procedure/s - please submit an amendment form to the UP Animal Ethics Committee for approval before commencing with the experiment

APPROVED	Date 30 October 2018
CHAIRMAN: UP Animal Ethics Committee	Signature

S4285-15

REC CERTIFICATE

UNIVERSITEIT VAN PRETORIA
UNIVERSITY OF PRETORIA
YUNIBESITHI YA PRETORIA

Research Ethics Committee

PROJECT TITLE	**Ocular findings and reference values for tonometry in the chimpanzee (*Pan troglodytes*)**
PROJECT NUMBER	**REC088-18**
RESEARCHER/PRINCIPAL INVESTIGATOR	**Keri-Lee Dobbie**

DISSERTATION/THESIS SUBMITTED FOR	**MMedVet**

SUPERVISOR	**Gerhard Steenkamp**

APPROVED	Date **05 November 2018**
CHAIRMAN: UP Research Ethics Committee	Signature M. M. Duncan

DEDICATION

I dedicate this research to the chimpanzees of Chimp Eden. It has been a humbling experience to work with these magnificent individuals and I am so very grateful for the opportunity to have been part of the health examination team for the past four years.

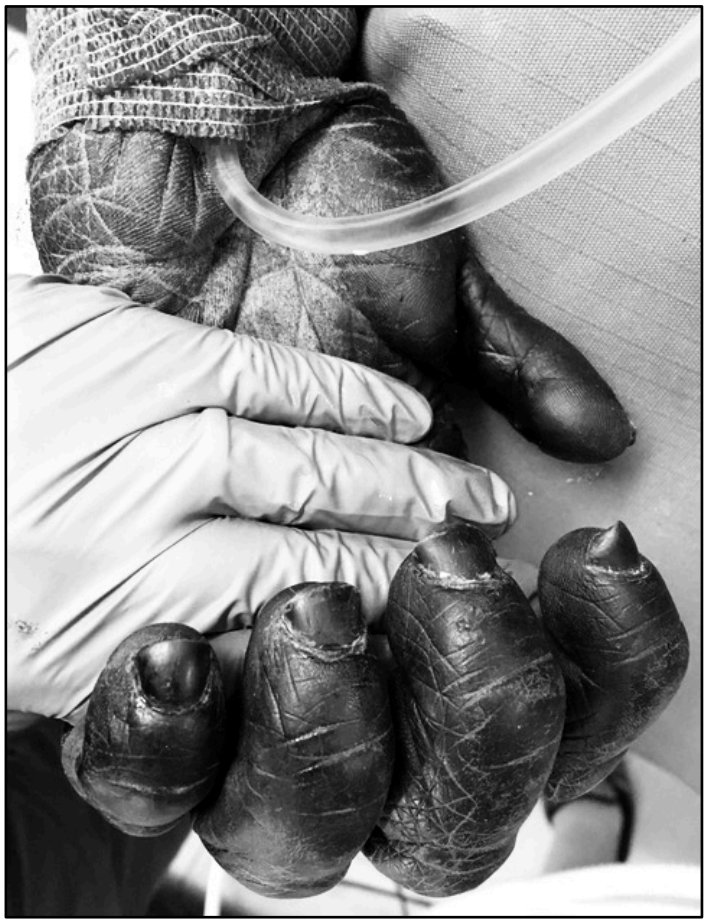

ACKNOWLEDGEMENTS

To have achieved this milestone in my life, I would like to express my sincere gratitude to the following people:

- Dr Izak Venter, clinical supervisor and mentor, who has helped nurtured my passion for ophthalmology, selflessly shared his knowledge, adventured with me to Congo and back, and has taught me so much.
- Prof Gerhard Steenkamp, research supervisor, for his thoughtful insights and constructive criticism.
- Prof Adrian Tordiffe for assisting with the statistical analyses.
- Dr Katja Koeppel, chief veterinarian for Chimp Eden, for giving me the opportunity to join the veterinary team, for safely anaesthetising the patients and co-ordinating the bi-annual health assessments.
- The team at the Jane Goodall Institute, Chimp Eden, South Africa, for their tireless work in rehabilitating and providing a forever home for these chimpanzees, for their help and support during the health examinations, and for educating the public on great ape conservation.
- Mrs Jana Pretorius, manager of Chimp Eden, for her incredible dedication to the animals under her care and for her support of this research project.
- Ms Estelle Mayhew of Creative Studios (Onderstepoort) for her assistance with annotating some of the figures included in this manuscript.
- VetdentSA for generously covering logistical and transportation costs.
- Medequip South Africa and Mr Simon van Heerden, for the generous loan of diagnostic equipment.
- Genop South Africa and Mr Willie Trollip, for the generous loan of diagnostic equipment.
- IMV Imaging South Africa and Mr Tim Perks, for the generous loan of diagnostic equipment.
- Drs Antony Goodhead, Christie Boucher, Lo-An Odayar and the team at Johannesburg Animal Eye Hospital, who each had an important impact on shaping me into the ophthalmologist I am today.
- Ophthalmology colleagues and friends from abroad, Drs Ann Gratzek, Sinisa Grozdanic, Lana Linton, Kristina Burling, Helga Kecova and Stamatina Giannikaki, for always being so ready with their advice and support, for broadening my horizons and teaching me so much.
- Dr Ramona Allen, my resident mate and friend, who kept me sane and never stopped supporting me during this test of endurance.
- Mrs Ursula Dobbie, my mother, for her unwavering support, for investing so heavily in my education, for her unconditional love and for assisting as a scribe during the data collection.
- Dr Jose Carlos Almansa Ruiz, my husband, partner in life, best friend and soul mate, who has supported me throughout this project, worked alongside me at every health examination, encouraged me throughout the write-up and continues to inspire me every day.

ABSTRACT

Purpose. To perform a descriptive investigation of the chimpanzee (*Pan troglodytes*) eye, conduct selected ophthalmic diagnostic tests, document intraocular measurements and determine the intraocular lens (IOL) power for this species.

Methods. Thirty-three anaesthetised captive chimpanzees (20 females with a mean age of 21.8 ± 7.06 years and a median age of 15 years, 13 males with a mean age of 16.4 ± 17.48 years and a median age of 15 years) underwent ophthalmic examination as part of routine health examinations. Selected diagnostic tests performed: intraocular pressure (IOP) by rebound tonometry (TonoVet®), central corneal thickness (CCT) by ultrasonic pachymetry, keratometry using a handheld automatic keratometer, A- and B-mode ultrasonography. IOL power was calculated using the Retzlaff and Binkhorst theoretical formulas.

Results. Most common ophthalmic findings (eyes): iridal melanosis (11), dyscoria (3) and mature cataracts (2). IOP: 22.59 ± 5.34 mmHg ("d" setting), 14.34 ± 4.03 mmHg ("P" setting). Mean horizontal corneal radius: 7.35 ± 0.47, mean vertical corneal radius: 6.55 ± 0.55 mm. Mean horizontal and vertical corneal curvatures were 46.19 ± 2.80 D and 51.74 ± 4.39 D respectively. CCT: 0.45 ± 0.04 mm. No significant differences were found between right and left eyes, age or sex for any parameter evaluated except for a sex difference in IOP where males had lower IOP than females. Ocular biometry: axial globe length: 21.41 ± 0.76 mm, anterior chamber depth (ACD): 3.63 ± 0.47 mm, crystalline lens thickness (LT): 3.81 ± 0.68 mm, posterior segment depth: 13.98 ± 1.00 mm. The estimated postoperative ACD (PACD) was calculated as ACD + 0.5 x LT. To address the effect of IOL position on lens power, additional calculations using PACD +2mm and PACD -2mm were performed. Calculated IOL powers (using the Retzlaff and Binkhorst formulas respectively): PACD: 21.86 ± 5.73 D and 22.81 ± 5.79 D; PACD +2mm: 27.67 ± 7.36 D and 28.83 ± 7.43 D; PACD -2mm: 17.71 ± 4.59 D and 18.51 ± 4.65 D.

Conclusions. Normal parameters described in this study will aid in the identification of ocular pathology in chimpanzees. Determination of the IOL power will facilitate correct IOL selection for the phacoemulsification candidate, although further studies evaluating pseudophakic refraction and determination of actual PACD are required.

TABLE OF CONTENTS

LIST OF FIGURES

LIST OF TABLES

LIST OF ABBREVIATIONS AND CONVENTIONS

ACD	Anterior chamber depth
AGL	Axial globe length
CCT	Central corneal thickness
CLT	Crystalline lens thickness
CITES	Convention of International Trade in Endangered Species of Wild Fauna and Flora
D	Diopter
DNA	Deoxyribonucleic acid
ERG	Electroretinogram
IOL	Intraocular lens
IOP	Intraocular pressure
IUCN	International Union for Conservation of Nature
JGI	Jane Goodall Institute
LD	Lens depth
LCOR	Low-coherence optical reflectometry
m	Metre
mm	Millimetre
mmHg	Millimetre mercury
OCT	Optical coherence tomography
PACD	Post-operative anterior chamber depth
PASA	Pan African Sanctuary Alliance
PCI	Partial coherence interferometry
Physician-based ophthalmology	Human ophthalmology
PSD	Posterior segment depth
SD	Standard deviation
VCD	Vitreous chamber depth

CHAPTER 1. INTRODUCTION & LITERATURE REVIEW

1.1 INTRODUCTION

The common chimpanzee (*Pan troglodytes*) belongs to the family Hominidae, the great apes, which also include humans, gorillas, orang-utans and bonobos [1]. Chimpanzees are human's closest living relatives, sharing >98% of the same DNA and are the most intelligent and social of all nonhuman primates [2, 3]. Chimpanzees are classified as "Endangered" on the International Union for Conservation of Nature (IUCN) Red List and listed in Appendix 1 of Convention on International Trade in Endangered Species of Wild Fauna and Flora (CITES) [4]. They are under threat from poaching, habitat destruction and the illegal pet trade. Chimpanzees are native to the Congolese forests and heavily forested regions of Central and West Africa. There are four subspecies of the common chimpanzee, based on geographical distribution: Central, Western, Nigeria-Cameroon and Eastern chimpanzee [1, 5], with the possibility of a fifth subspecies, the Southeastern chimpanzee [6, 7]. Chimpanzees live in social groups called "communities", led by an alpha male with a definite social hierarchy [8]. They exhibit complex social interactions and communicate with vocalizations, hand gestures, facial expressions and eye contact, making the sense of vision particularly important for normal behavioural performance [9]. Intraspecies aggression is common and poorly visual individuals suffer increased difficulties in their social interactions and may lose their position in the social hierarchy [10, 11]. Chimpanzees live up to 30 years-of-age in the wild and the average life span in captivity is approximately 25-years for males and 34-years for females [12], although rarely they may exceed 70 years-of-age in captivity.

Glaucoma is a leading cause of blindness in both animals and humans [13]. Glaucoma, an important vision-threatening disease, is a group of optic neuropathies, resulting in optic nerve degeneration [14]. Disruption to the axoplasmic flow in the optic nerve head and death of retinal ganglion cells and their axons, results in a progressive loss of retinal sensitivity and function, leading to reduction in the visual field and ultimately blindness [15]. Increased intraocular pressure (IOP) is the most important risk factor for glaucoma [16]. Although the mechanisms by which the retinal ganglion cells are lost is not yet fully understood, treatments aimed at lowering IOP have been demonstrated to be effective [17-19]. Mean IOP is specific for each species, with large interspecies variation being recorded, making extrapolation of IOP values invalid [20].

There is a paucity of published data on ophthalmic parameters in the common chimpanzee (*Pan troglodytes*). Determining reference values for rebound tonometry in this species is of great clinical importance and had not yet been published at the time of the primary investigator undertaking this research. Confirming mean IOP for the chimpanzee and determining if there are significant effects of age, gender and refractive error in this species, will be a valid contribution to the literature and will assist veterinarians in diagnosing and treating glaucoma in chimpanzees. While it has been reported in the literature that sedation and general anaesthesia

may have an effect on IOP [21-29] there is still clinical value in describing the IOP under immobilisation conditions, since veterinarians will most commonly have to anaesthetise these patients in order to conduct a clinical examination.

Determining corneal curvature, refractive characteristics and corneal thickness values, together with the ocular biometric measurements for the chimpanzee, will serve as a standard set of measurements which can be used as reference values in clinical veterinary ophthalmology. Establishing these normal ophthalmic parameters for various exotic, wild and laboratory species is a fundamental component of descriptive vision research [30]. Moreover, there is little reported on the incidence of general ocular pathology in chimpanzees and descriptive data gathered in this relatively large survey could fill this information gap.

Due to the longevity of these great apes in captivity, the incidence of cataracts is increased [12]. Despite being most often age-related, cataracts have also been described in young orang-utans and gorillas [10, 31-33]. Reports exist of both captive and wild middle-aged gorillas affected by cataracts as well as a report of a zoo-housed 29-year-old chimpanzee with cataracts [10, 11, 31-33]. Performing cataract surgery (phacoemulsification) in nonhuman primates enhances their quality of life and has been associated with dramatic behavioural improvements [10, 31, 33]. Affected animals have been described to become more active and social post-surgery and often regain their place in the social hierarchy [31, 33]. Restoring optimal vision post phacoemulsification would include the implantation of an appropriate intraocular lens to allow better near vision. Leaving the patient aphakic (without a lens) would affect their visual acuity and accommodation and render them hyperopic (far-sighted). In human medicine, the appropriate intraocular lens power is typically calculated for each individual patient undergoing cataract surgery, using biometric and keratometric measurements that are incorporated into various intraocular lens (IOL) power calculation formulae. In contrast, in veterinary medicine IOL power is not predicted for the individual but instead pre-established powers are commonly used and have been predicted for dogs [34], cats [35], horses [36, 37], bald eagles [38] and tigers [39].

Although there are case reports documenting phacoemulsification and IOL implantation (after individual IOL power prediction using keratometry and biometry) in captive western lowland gorillas [10, 31], there has not been a documented case of a chimpanzee undergoing IOL implantation post-phacoemulsification where the IOL power has been predicted, and there are no studies predicting IOL power in any nonhuman primate species. A further aim of our study is to use our data in order to determine the IOL power for the chimpanzee. Medical and veterinary ophthalmologists performing phacoemulsification on chimpanzees will be able to use this data to select an appropriate IOL for their patient to achieve as close to optimal vision as is possible, in the absence of performing A-mode biometry and keratometry.

1.2 LITERATURE REVIEW

1.2.1 Ophthalmic Examination

1.2.1.1 Tonometry

The intraocular pressure may be measured via direct and indirect methods. While being the most accurate and the gold standard technique by which tonometric instruments are calibrated, direct tonometry via manometry is invasive and impractical for clinical cases. In contrast, indirect tonometry, where the corneal tension is measured, is quick, simple and non-invasive [40]. Indirect methods include digital tonometry and instrumental tonometry (the standard method in clinical practice). Techniques of indirect instrumental tonometry include indentation, applanation and rebound tonometry.

Digital tonometry is a highly subjective, insensitive and inaccurate method for gauging the IOP and should only be considered when no other method is available. The examiner places their index or middle finger on both of the patient´s closed upper eyelids simultaneously, and applies slight pressure to the globes. By comparing the feel or resistance to the slight pressure applied, the examiner can get a sense of whether the globe is “hard” or “soft” [40].

Indentation tonometry can be performed using a Schiotz tonometer (J. Sklar Manufacturing Company, Long Island, NY, USA). This instrument has a large footplate that is placed directly on the cornea and requires use of topical anaesthesia. The curvature of the footplate is specific for that of human patients. The footplate is attached to a scale and used with a specific weight. The scale measures the indentation of the cornea produced by a specific weight. This scale measurement is then read on a specific table (“1955 Friedenwald Nomogram” [41]) that converts the scale reading to mmHg. This instrument is not deemed accurate or safe to use on diseased or fragile corneas. It is practically difficult to use in veterinary patients due to the patient´s head needing to be directed upwards and the fact that globe, eyelid and third eyelid movement can affect the results [40]. The only published data, at the time of the primary investigator embarking on this study, for intraocular pressure in the chimpanzee was obtained in 1964 using a Schiotz tonometer [29].

Applanation tonometry can be performed using a Tono-Pen® (iCare Oy, Finland). This instrument estimates IOP by measuring the forced required to flatten an area of cornea (corresponding the size of the instrument´s footplate), but also requires the use of topical anaesthesia [40]. The instrument is held perpendicular to the cornea and gently tapped on the central corneal surface by the examiner, without causing indentation of the cornea [40].

In rebound tonometry, a small metal probe with plastic tip makes contact with the central corneal surface and

returns to the device. The deceleration of the returning probe is then used to calculate the IOP. Due to the brevity of the contact and the small footprint of the probe, topical anaesthesia is not required. The TonoVet® (iCare Oy, Finland) is a commercially available handheld tonometer measuring IOP using rebound tonometry technology [42] and is based on the induction/impact principle first described by Kontiola [43-45]. Both the TonoVet® and the iCare PRO® (iCare Oy, Finland) are set to take 6 measurements. Of the 6 measurements obtained, the highest and lowest readings are excluded and an average of the remaining 4 readings is automatically calculated by the instrument. An error message (and corresponding sound) is displayed when there is a problem with probe motion, misalignment with the central cornea, or excessive differences between readings [46]. These instruments will also indicate on the display whether or not the final intra-ocular pressure value is an accurate or valid reading. The TonoVet® displays this as the absence or presence of a horizontal line next to the IOP reading. If there is no line present, or if the line is "down" on the display, then the reading is of an acceptable standard deviation as per the manufacturer (≤ 2.5 mmHg). The iCare PRO® displays the acceptability of readings as "OK" (<15% of the IOP), "Deviation" (15-25% of the IOP) or "Remeasure" (>25% of the IOP).

A disadvantage of the TonoVet® is that the instrument must be held upright, perpendicular to the ground, so that the probe is propelled horizontally [47]. This can make measuring IOP in anaesthetised animals difficult, since they may need to be re-positioned into either lateral recumbency or have their heads held upright to facilitate the measurement. The TonoVet® has been calibrated for dogs, cats and horses with a strong linear correlation with direct manometry [46, 48], but underestimates IOP by 37-60% in rabbit and porcine (enucleated) eyes compared with direct manometry [49]. The TonoVet® has three different settings: Dog/Cat, Horse and P (undetermined). According to the manufacturers, the "P" setting is intended for service use and is an adjusted human calibration. When the instrument is used on any other species for which it is not calibrated, the manufacturers advise using the setting that corresponds most closely to the eye size of that species.

Reliable and accurate IOP measurements have been obtained using rebound tonometry and are reported in humans [50, 51], nonhuman primates including the chimpanzee [52], rhesus macaques [53], cynomolgus macaques [54], and many other non-primate animals including: dogs [46, 55, 56], cats [57] horses [46], pygmy goats [58], rabbits [49, 59], pigs [49], mice [60], deer [61], guinea pigs [62, 63], bats [64], bearded dragons [65], penguins (66, 67), and various birds of prey [68-74]. These studies were either clinical studies to establish reference values, comparisons between different tonometers or instrument validation studies where IOP readings obtained manometrically have been compared to those obtained with the rebound tonometer. The highest IOP published is in the rhinoceros (32.1 ± 10.4 mmHg) [20, 23] and the lowest in the chinchilla (2.9 ± 1.8 mmHg) [75]. Anatomical differences in terms of corneal structure, curvature and thickness, as well as physiological differences in terms of aqueous humor drainage pathways, are put forward as explanations as to why these readings show such variation between different species [20].

Instrumental tonometry may be affected by various examiner factors, including pressure by the fingers of the examiner on the eyelids or globe [76] as well as excessive patient restraint and pressure on the jugular veins [76, 77]. Several patient factors have also been shown to affect IOP measurement, including sedation and general anaesthesia [21, 22, 24-28], body position [52, 78], tonometer position [79], head position [80-85], corneal thickness [86-94], age [66, 94-99], gender and reproductive status [20, 29, 98, 100-103], refractive error [29], circadian rhythm [104-108] and whether the animal is nocturnal [105, 109] or diurnal [106]. Consistency regarding instrumentation, time of day, method of restraint (including sedation / general anaesthesia) and head/body position is of utmost importance when measuring IOP [40].

Intraocular pressure has been demonstrated to be increased in the early morning and decreased in the afternoon / evening in humans [110-112], nonhuman primates [113, 114], and dogs [106-108]. Kida *et al.* (2006) reported the peak IOP in humans was at 05:30AM and the trough IOP was at 09:30PM [111]. IOP and CCT are positively correlated with both parameters displaying a similar diurnal variation [107, 111, 112, 115].

Human IOP was increased when measured in the supine (dorsal recumbency) position, compared to when measured in both sitting and standing positions [85]. The postulated mechanisms for this difference include increases in episcleral venous pressure, compressive forces on the globe by congested orbital contents, and when congestion of the uveal tract causes increases in ocular blood volume [116, 117]. Wu *et al.* (2006) identified various patient factors that were associated with increased IOP, including systemic disease (hypertension and diabetes), lifestyle factors (current alcohol use and smoking), signalment factors (female gender, darker complexion, and higher body mass) and a family history of glaucoma [118].

Various sedative and anaesthetic drugs can influence IOP by altering the rate of aqueous humor production or outflow and/or by the extent of relaxation of the extraocular and eyelid muscles [119]. Aside from ketamine [25, 103, 120], all agents commonly used to induce general anaesthesia in veterinary medicine lowers the IOP [121]. The increased IOP observed in veterinary patients anaesthetised with ketamine is as a result of increased extraocular muscle tone [103]. However, no significant effect on IOP was observed when ketamine was combined with xylazine in cynomolgus macaques [122] and cats [101], when ketamine was combined with dexmedetomidine in capuchin monkeys [123], or when ketamine was combined with diazepam in lions [103]. In humans receiving ketamine, no clinically relevant IOP elevation has been observed [124]. Tiletamine-zolazepam (Zoletil®) has no significant effect on IOP in both dogs [125] and cats [120]. Tiletamine is a dissociative agent similar to ketamine but it has minimal effect on the contraction of the extraocular muscles [120]. Anaesthesia with pentothal sodium decreases the IOP of chimpanzees [29].

1.2.1.2 Keratometry

The cornea-air interface is responsible for the majority of the refractive power of the eye. Keratometry measures the corneal refractive power (in diopters (D)) from the corneal radius of curvature (in mm), which assumes the cornea to be a spherocylinder [126, 127]. When one considers the curvature of the cornea, one may (incorrectly) assume that the cornea is perfectly spherical, like a soccer ball. However, the reality is that many human patients have some degree of astigmatism, where the corneal surface is shaped more like a rugby ball, i.e. where one of the corneal axes or meridians is steeper (and thus has a shorter radius of curvature) than the other. Here we have to determine the amount of cylinder power if we want to determine the corneal astigmatism, since a difference in power across the cornea (opposite meridians) results in astigmatism [36].
Obtaining these measurements with an auto-refract keratometer is a non-invasive procedure whereby the instrument shines a well-lit target on the corneal surface, the cornea acting as a convex mirror, then produces a virtual image of the target which the instrument then uses to predict the corneal radius of curvature [127]. To determine mean corneal radius of curvature (mm) and mean corneal refractive power (D), two values R1 and R2 are averaged. R1 represents the maximum radius of curvature (i.e. the "flattest" curve) and the lowest power meridian. R2 represents the minimum radius of curvature (i.e. the "steepest" curve) and the highest power meridian.

For the original prediction of intraocular lens (IOL) power for the horse, the corneal curvature was calculated by manually determining the radius of the cornea using B-mode ultrasonography images [36]. Corneal power (K) is considered the second most important factor (after axial globe length) for IOL power determination. Changes in K readings alter the IOL power in a ratio of nearly 1:1 [128]. Later studies measured equine corneal curvature using keratography and reported a different (higher) mean corneal curvature in the horse [37, 129]. Recently, a study by Kawasaki et al. (2020) established keratometric reference values for popular dog breeds in Japan using an automatic handheld keratometer [130]. The authors reported considerable interbreed variation, which did not correlate with bodyweight [130].

In a recent study, possible measurement errors were identified as a major limitation of performing automatic hand-held keratometry on veterinary species [130]. The authors of this work excluded readings from individuals were the difference in R1R2avg between right and left eyes was greater than 4.5% [130]. This 4.5% cut-off value was based on a preliminary study of intra-operator variability conducted by the same authors [130].

1.2.1.3 Slit Lamp Biomicroscopy

Slit lamp biomicrocscope is the instrument of choice for examining the anterior segment of the eye, from the eyelids and adnexa, to the conjuncitva, cornea, sclera, anterior chamber, iris, lens and anterior face of the vitreous. In veterinary medicine, a portable slit lamp is commonly used whereas in physician-based

ophthalmology, a table-mounted slit-lamp is generally preferred (except in paediatric and debilitated patients where a portable slit-lamp may be indicated). The instrument combines magnification with a bright focused light source and offers a choice of diffuse or slit light beams. During examination, the light beam is generally angled at 20 to 45 degrees from the axis of the microscope. For the Keeler Classic Portable Slit Lamp (Keeler Ltd., Winsor, UK) the magnification can be adjusted between 10 and 16 times, the focal distance is 7 to 10 cm, and fine focus is achieved by moving either towards or away from the eye. A diffuse beam is used to assess the eyelids and adnexa, cornea and iris and is helpful to identify gross pathology. The slit beam (a narrow, focused beam of light) creates an optical section and gives the examiner an appreciation of the variable depth of potential lesions and relative distances between the various intraocular structures. The techniques of direct and retro-illumination are both utilised when performing slit lamp biomicroscopy. Direct illumination refers to when the structure being observed is illuminated by the light source itself, whereas retro-illumination refers to using light reflected from neighbouring structures to indirectly illuminate the structure of interest [40].

1.2.1.4 Pachymetry

Pachymetry refers to measurement of the thickness of the cornea. Various devices, utilising different technologies, are available to measure central corneal thickness (CCT) *in vivo*. Contact methods include ultrasound pachymetry, high frequency ultrasound and ultrasound biomicroscopy (UBM) [131-133]. Non-contact methods include specular and confocal microscopy, optical biometry with a Scheimpflug camera (Oculus Pentacam-HR®, Oculus, Inc. Arlington, WA), optical coherence tomography (OCT), optical low-coherence reflectometry, and slit-scanning optical pachymetry [40, 134]. Ultrasound pachymetry (UP) is the most commonly used technique to measure CCT in both veterinary and physician-based ophthalmology, owing to its repeatability, practicality, portability and affordability [134-138]. Confocal microscopy and OCT are also now considered the diagnostic standard in human ophthalmology [139-141].

Ultrasonic pachymetry is equivalent to an A-mode ultrasound in that it uses ultrasound waves reflected from interfaces of differing refractive indices – in the case of the cornea, those interfaces are the epithelial and endothelial surfaces respectively [40, 136]. The difference between reflections is then calculated based on the corneal ultrasound velocity (reported to range from 1550 to 1639 m/s in humans) [142-144]. Since different species have different corneal velocities, conversion factors are useful when calculating measurements in veterinary medicine [40]. In the dog, ultrasonic pachymetry set at the standard velocity of 1636 m/s was observed to consistently overestimate CCT compared to OCT [145].

Central corneal thickness is an important parameter in the diagnosing of ocular diseases. Clinically, these measurements can be used to help guide surgical planning and to monitor disease progression and response to treatment [135, 145]. In physician-based ophthalmology, CCT is an important parameter in the assessment of

any potential glaucoma patient, having been identified as a significant risk factor for progression of ocular hypertension in primary open-angle glaucoma [134, 146, 147].

A number of patient factors are known to influence CCT including; the state of corneal hydration / dehydration [40], taking repeated measurements [40], age (decreased CCT with age) [94, 134], diurnal variations (decreased CCT in the afternoon/evening compared to the morning) [107, 108, 111, 112, 148, 149], and in human patients; body position (recumbency increases CCT) [40], ethnicity, sex, glaucoma medications and glaucoma subtype [134]. Central corneal thickness has been found to be positively correlated with IOP in humans and animals [93, 108, 111, 112, 148-153], since estimated IOP values (via applanation and rebound tonometry), depend on biomechanical properties of the cornea and corneal surface conditions including CCT [154, 155], corneal curvature [153, 155] and precorneal tear film [156]. Park *et al*. (2011) demonstrated that, in the canine cornea, for every 100 µm increase in CCT, there was an elevation of 2 mmHg in IOP measured by the TonoVet® [93], while another study reported an elevation of only 0.8 mmHg for every 100 µm increase in CCT [108] and a further studies showed no influence of CCT on IOP measurements in canines [94] and penguins [66].

Mean CCT has been determined for a number of animals including gorillas [11], rhesus macaques [146, 157], cynomolgus macaques[54], capuchin monkeys [30], dogs [93, 94, 108, 133, 135, 136, 145, 158, 159], cats [137, 160], horses [132, 161-163], camels [164], llamas and alpacas [165], deer [61], capybaras [166], guinea pigs (167), chickens [168], penguins [66, 67] and koi fish [169].

1.2.1.5 Ocular Ultrasonography, Biometry and Calculation of Intraocular Lens Power

Ocular ultrasonography has become an important technique for exploring the globe and orbit [170] and is often the first imaging modality used in ocular and orbit assessment due its non-invasiveness, the ease of access and its real-time, rapid and reliable nature [171]. Ultrasonography of the globe can be achieved either with general purpose machines (using a 7.5 - 10 MHz small footprint high frequency transducer) or with dedicated "ophthalmology only" scanners, that allow for zonal speed error correction and A-mode scanning [171]. Ocular ultrasonography is indicated in a clinical setting in cases of suspected orbital disease, ocular trauma, intraocular or orbital foreign bodies and neoplasia, and whenever ocular opacity is hindering a full ophthalmic examination, including corneal oedema or marked keratitis, hyphema, hypopyon, cataract and vitreal opacity [172].

In A-mode (Amplitude modulation) ultrasonography, returning echoes are displayed in a graph-like one-dimensional manner where changes in amplitude (vertical spikes) from baseline are plotted against time. A-

mode allows for more accurate and objective measurement of intraocular dimensions and of the size of any intraocular lesions [173].

B-mode (Brightness modulation) ultrasonography reveals topographical information of intraocular structures and any ocular lesions, as the returning echoes are displayed two-dimensionally, forming an image that resembles a histological 'slice' [173]. Using B-mode together with A-mode can be useful to obtain on-incidence measurements since the observer can ensure the correct positioning of the probe along the optical axis, such that the posterior wall of the globe and reflections of the cornea, anterior lens capsule and posterior lens capsule are all perpendicular [129]. The B-mode image can also be used to visualise which A-mode amplitude corresponds to which intraocular structure [38]. B-mode ultrasonography is most commonly used in veterinary ophthalmology, with a standard 10 - 14 MHz transducer and a focal range of 3-4 cm [173].

Ocular ultrasonography is typically performed on the awake domestic animal after instillation of topical anaesthesia. The eyelids are held open manually and the transducer is applied gently to the corneal surface coupled with acoustic gel [174, 175]. It is also possible to scan through the eyelids, although this technique creates artefacts, adds to the level of penetration required by the transducer and thus does not yield the best visualisation of the posterior segment. However, this becomes the preferred technique in cases of corneal injury, ocular trauma or post intraocular surgery since the eyelids provide protection to the corneal surface [173]. Axial sections are generally used and different axial sections can be imaged depending on the clock-hour position of the probe marker [170]. Two axial scanning planes are generally used – a vertical section (where the probe marker is located at the 12 o´clock position) and a horizontal section (where the probe marker is located at the 3 o´clock position for the right eye and at the 9 o´clock position for the left eye) [176]. In order to obtain optimal images, adjustment of the gain setting is important. As a general rule, the lower the gain, the better the image resolution [170].

The cornea appears as a convex hyperechoic line. The anterior chamber is anechoic and delineated posteriorly by the hyperechoic iris. The pupil appears as a translucent disruption of iris continuity. In humans, both the anterior and posterior lens capsules are often not apparent [171] while in the majority of animal species these structures are clearly imaged. The body of the lens is anechoic and the posterior margin of the lens (posterior lens capsule) is observed as a concave hyperechoic line, that due to its variable spacial relationship with the ultrasonic beam, is only partially visible. The vitreous humour is homogenously anechoic and comprises more than two thirds of the total globe volume. The posterior wall of the globe is hyperechoic and the retina-choroid-sclera complex appears as a single echoic curved line [170, 171, 177].

High frequency ultrasound (10 - 38 MHz) and ultrasound biomicroscopy (40 - 100 MHz) are imaging modalities that are becoming increasingly popular in veterinary ophthalmology [178]. These imaging modalities allow for very detailed examination of the most superficial ocular structures, with a resolution 5 - 10 times

greater than conventional ultrasonography but with a penetration of only 4 - 5 mm. Detailed imaging of the iridiocorneal angle, ciliary body and cleft, iris, anterior chamber, cornea and sclera is possible and is clinically useful for assessment of the iridiocorneal angle and ciliary cleft in glaucoma [176, 179], assessing the depth of corneal sequestra in cats and differentiating between iris melanoma and melanosis [176].

Biometry is the measurement of intraocular and orbital structural dimensions. These measurements can be obtained using contact ultrasound ocular biometry (A-mode and/or B-mode ultrasonography) or non-contact optical biometry (laser partial coherence interferometry and low-coherence optical reflectometry) [126, 127]. In A-mode, time (sound velocity within different tissues) is converted into distance in order to obtain the biometric globe measurements [170]. A-mode biometry is still considered the gold standard for axial globe length and anterior chamber depth measurement [127], although B-mode biometry has also proved reliable [180, 181]. While some studies have observed decreased values of axial globe length, lens thickness and posterior segment depth measurements obtained with B-mode as compared to A-mode ultrasonography [182], other studies have failed to show a significant difference in these ocular biometric measurements regardless of whether A-mode or B-mode was utilised [129, 180, 183].

A complete set of measurements should include: axial eye globe length, anterior chamber depth, lens thickness and vitreous chamber / posterior segment depth [23, 170, 184]. These intraocular distance measurements are calculated by determining the travel time of an ultrasonic wave and multiplying it by velocity of that wave [185]. The ultrasound velocity through ocular tissues has been established for humans [186, 187] and several animals including dogs [188, 189], pigs [189], rabbits [189], camels [164, 190] and horses [185]. Obtaining baseline data for the chimpanzee will be of important clinical value for establishing lens implant size, IOL power prediction, and estimating prosthetic globe size following enucleation [170], as well as being of diagnostic importance for clinical ultrasonography (as ocular pathology may result in derangements of ocular measurements). Ocular biometric measurements have been determined for several species including dogs [158, 180, 188], cats [35], rabbits [191], ferrets [102], horses [36, 37, 132], camels [182, 192], bovines [193], goats [194], caimans [181], and elephants [195].

For patients undergoing cataract surgery by phacoemulsification, the goal of the procedure is to restore vision. The quality of this post-operative vision can be affected if the patient is left aphakic (without a lens), since the lens contributes substantially to the optical power of the eye [36]. An aphakic patient will invariably be hyperopic (farsighted), since light entering the eyes of these patients will be focussed beyond the retina [36]. In these eyes, no object in space is sharply imaged on the retina and the degree of defocus worsens as objects are moved closer to the patient´s eye [37]. This degree of defocus has been shown to correlate directly with a decrease in visual acuity in dogs and humans [196]. Intraocular lens implantation can overcome these challenges but correctly deciding on the appropriate IOL to implant is a vital step towards achieving emmetropia (normal refractive condition of the eye). Clinically, this decision-making is approached differently

in veterinary and physician-based ophthalmology. In veterinary ophthalmology, pre-established power predictions for IOLs are used. Thus far, these dioptic powers have been predicted for the dog [34], cat [35], horse [36, 37], rabbit [197], tiger [39] and bald eagle [38]. In physician-based ophthalmology, the IOL power prediction is carried out for each individual patient [198]. As veterinary ophthalmology becomes more advanced, perhaps we will ultimately predict the IOL power for each individual patient undergoing cataract surgery in the future, but this requires expensive specialist equipment (A-mode ultrasonography and keratometry). Therefore, determining the standard lens power for each species is of considerable importance and has far-reaching clinical application to allow veterinary ophthalmologists to achieve as near to emmetropia as possible in our phacoemulsification patients [38].

The refractive power of the eye depends on: 1.) the power of the cornea (related to cornea curvature) and lens, (2.) the position of the lens (related to anterior chamber depth and lens thickness) and 3.) the length of the eye (axial globe length) [126]. These values are obtained via keratometry and ocular biometry respectively. Recall that the corneal-air interface provides the majority of refractive power for the eye (approximately 40 diopters of refraction in humans, while the lens makes up the last approximately 20 diopters). With regards to eye size (axial globe length), the shorter the eye, the more hyperopic ("farsighted") it is, this results in light entering the eye to be focused beyond the globe. In order to focus light on the retina, a more powerful lens will be needed compared to a larger (myopic) globe, since the refractive power of the eye needs to be increased.

IOL power is predicted using theoretical formulae. The Retzlaff [199] and Brinkhorst [200] formulae have been used to predict IOL power in humans [199], dogs [34], cats [35], horses [36, 37, 201], rabbits [197], tigers [39] and the bald eagle [38]. The latter study made additional use of the Colenbrander and Fyodorov formulae [202, 203]. Third generation formulae (Hoffer Q, Holladay and SRK/T) are becoming popular in physician-based ophthalmology but require extra variables and mathematical constants that are not directly applicable to veterinary species, thus making these formulae inappropriate for veterinary patients [37, 126, 127].

The Retzlaff and Brinkhorst formulae require the estimation of the post-operative anterior chamber depth (PACD). Two methods have been described in the veterinary literature for determining this value, the first being to perform A-mode biometry on individuals that have already undergone phacoemulsification and IOL implantation [38]. Meister *et al*. (2018) made use of the formula PACD = (ACD) / 0.73, taken from a previous study that had determined mean preoperative-to-postoperative ACD ratio to be 0.73 for equine eyes, based on pre- and post-operative biometry [37, 204]. Kuhn *et al.* (2015) were in a similar position with not having suitable post-operative phacoemulsification patients with IOL implants, but did describe measuring from cornea to the location of the capsular bag in aphakic patients [38].

The second approach is to predict PACD from pre-operative A-mode-measured anterior chamber depth (ACD) and crystalline lens thickness (CLT), such that PACD = ACD + ½ CLT [35, 36, 38]. Further, as one cannot

predict the actual postoperative position of the intracapsular IOL, two values for PACD (2 mm anterior or 2 mm posterior to the central lens position) are applied to the formulae in order to compensate for the effect of lens position on the refractive power of an IOL to achieve emmetropia [36].

More recently in physician-based ophthalmology, Martinez-Enriquez *et al*. (2018) proposed a new formula to preoperatively estimate the postoperative intraocular lens position using measurements of the crystalline lens obtained using optical coherence tomography (OCT) imaging [205]. The authors observed that this method produced lower estimation errors than current state-of-the-art methods and propose this to be a new generation of IOL power calculation formulae [205].

1.2.2 Ocular pathology and ophthalmic parameters in non-human primates

Our current body of knowledge regarding ophthalmic pathology, parameters and vision in great apes and in the chimpanzee in particular is lacking. In a comprehensive review article from Lowenstine, *et al*. (2016) concerning comparative pathology of aging apes, ophthalmologic pathology was identified as an area requiring further investigation [12].

In 1971, Schmidt reported on spontaneous ophthalmic lesions in over 100 nonhuman primates [206]. The study included macaque monkeys, and baboons, as well as chimpanzees. Despite being the smallest group examined, chimpanzees had the highest number of ocular lesions. Schmidt reported congenital lesions to be the most prevalent, with 35 chimpanzees displaying physiologic cupping of the optic nerve. Coloboma of the retina and choroid was seen in a single individual, as were cataracts. Ten chimpanzees had superficial abrasions to the cornea. Lesions of undetermined aetiology included retinal detachment in one chimpanzee and myopia in seven chimpanzees [206].

Hoffman *et al.* (2007) published the first documented case of ocular coccidioidomycosis in a captive 12-year-old female chimpanzee [207]. Gemensky Metzler *et al.* (2016) reported chronic keratopathy, suspected to be solar / UV-induced keratitis, in 16 captive chimpanzees in Kenya [208]. The first (and only) report of suspected presbyopia (farsightedness) in a wild elderly chimpanzee was published in 2010 [209].

Recently, Sigmund *et al.* (2020) described ophthalmic findings in ten captive anaesthetised chimpazees at a zoo in the USA [210]. All chimpanzees examined had diffusely pigmented bulbar conjunctiva, a finding noted across all nonhuman primates, with humans being the only primate species to maintain a nonpigmented conjunctiva [210]. All geriatric animals had dense continuous circumferential perilimbal white corneal stromal deposits bilaterally that the authors presumed to be lipid deposition, an age-related change that resembled a human condition called arcus senilis or arcus lipoides [211]. Nuclear sclerosis was observed in the three oldest chimpanzees, with the oldest male having a lens with a brunescent hue. One male had unilateral corneal

stromal diffuse dystrophic mineralization presumed to be secondary to trauma. One female with a history of epiphora had conjunctival follicles and was diagnosed with allegic conjunctivitis. One female had a bilateral physiologic cupping of the optic nerve. The authors also described mean pupil diameter after induction and at varying time-points post pharmacological dilation and reported a protocol to successfully dilate the pupil in order to facilitate fundoscopy (tropicamide 1% (Akorn, Lake Forest, IL, USA) every five minutes for four applications) [210].

Knapp *et al*. (2007) described the comparative ocular anatomy of the western lowland gorilla, concluding that their eyes showed great similarity to the human eye [212]. The retinal anatomy and presence of a macula are commonalities between humans and nonhuman primates [213]. A single case of suspected macular degeneration has been reported in a female western lowland gorilla [214]. There has also been a case report published on malignant hypertension and retinopathy in this species [215]. Nonhuman primates also suffer from ocular disease and the findings in 218 grey mouse lemurs have been described, with the authors reporting a high incidence of acquired, slowly progressive, bilateral cataracts in more than 50% of the study population over 7 years-old [216].

There are several reports of cataract surgery (phacoemulsification) being performed in great apes, the first being published in 2004 where bilateral phacoemulsification with IOL implantation was performed on two captive western lowland gorillas [10]. In both cases, the authors (medical ophthalmologists) had predicted the IOL power for each eye of each individual gorilla, by performing A-scan biometry and keratometry and then applying these values to the SRK2 formula. Both gorillas had developed complete mature cataracts at a young age (18 and 17 months respectively), though the one gorilla was affected unilaterally due to blunt trauma to the head, while the other was affected bilaterally by presumed hereditary cataracts. In the case of the gorilla that was affected unilaterally, cataract surgery was only performed when he was 7 years-old, when he developed an immature cataract in the contralateral eye and began experiencing visual deficits. Post-surgery this gorilla remained poorly visual in the eye with the long-standing mature cataract due to amblyopia (decreased vision due to abnormal visual development), but had good vision in the contra-lateral eye. The second gorilla (with mature bilateral cataracts) underwent cataract surgery at an early age to avoid amblyopia and had good vision after surgery but developed posterior capsular opacities that required Nd:YAG laser capsulotomy two years later [10].

The first bilateral cataract surgery to be performed on an adult western lowland gorilla in Europe in 2001 was reported by Warwick *et al*. (2017) The operation was staged with right and left eyes being operated on separate occasions (as is typical practice in medical ophthalmology). Pre-operative biometric measurements were used to guide intraocular lens strength selection, using the SRK/T formula. Pre-operative electroretinography was performed using a rapid protocol ERG, where comparison with human reference values indicated normal retinal function. A three-piece foldable silicone lens implant was inserted into the

capsular bag post phacoemulsification (17 diopter IOL in the right eye and a 16 diopter IOL in the left eye). A good visual outcome was achieved and no sign of posterior capsule opacification had been observed up to 16 years post-operatively [33]. What was a notable difference between this case and other reports of cataract surgeries performed in great apes was that the larger 3.2 mm corneal incision was purposely not sutured to minimalise irritation. Cataract surgery in this gorilla appeared to be well tolerated and she was seen to touch her eye on a single occasion following the first operation and no post-operative complications were observed [33]. Previous publications of cataract surgery in great apes reported the larger corneal incision being sutured to protect against eye-rubbing [10].

Bilateral phacoemulsification has been performed on a captive 14-year-old female orang-utan where no IOL was implanted but the importance of pre-operative B-mode ultrasonography (to rule out retinal detachment) and electroretinography (to assess retinal function) was discussed [32].

Leiva *et. al.* (2012) reviewed phacoemulsification in non-human primates and described cataract surgery performed on one 29-year-old female chimpanzee as well as a gorilla, an orang-utan, a chacma baboon and a pygmy marmoset [31]. A-scan biometry and keratometry to predict IOL power was only performed in the gorilla. All the primates in this case series had intraocular lenses implanted, with the exception of the pygmy marmoset. Primates were identified as good candidates for IOL implantation post-phacoemulsification since good vision in these animals is paramount given their complex social interactions that involve social eye contact and gesturing. The authors commented on the need for studies predicting the IOL power for the various primate species, since in veterinary medicine, the use of a pre-established IOL power for a particular species is the convention. B-mode ultrasonography and ERG was performed pre-operatively in all primates, as well as an ophthalmic examination including tonometry, slit lamp biomicroscopy and indirect ophthalmoscopy. Primates have shallower anterior chambers and smaller flatter lenses compared to other domestic animals. Cataract surgery was highly successful and associated with good visual outcomes in primates. Post-surgery, the subjects underwent positive behavioural changes, becoming more active and social and regained their place in the social hierarchy [31].

There is a paucity of published baseline ocular data for the chimpanzee in the English literature. In 1964 Young and Farrer reported on refractive characteristics and intraocular pressure in 43 laboratory chimpanzees at the colony of Hollman Air Force Base in New Mexico [29]. These were predominantly young animals (ranging from 2 - 8 years) that were refracted and had their intraocular pressure measured with a Schiotz tonometer under general anaesthesia (Pentothal Sodium). Mean intraocular pressure was 16.2 ± 3.98 mmHg for both eyes and mean refractive error was -0.61 diopters (OD -0.58 D, OS -0.65 D) [29]. To assess the effects of anaesthesia on these parameters, 22 chimpanzees were refracted and 16 had their intraocular pressure measured without general anaesthesia. The intraocular pressure was significantly lower in anaesthetised (16.2 ± 3.98 mmHg) compared to non-anaesthetised animals (18.4 ± 4.75 mmHg), whereas

there were not significant differences in terms of refractive values [29]. The authors compared the refractive error results with those of 455 human children aged 4 - 11 years-old (OD +0.33 D and OS +0.35 D) [217] and seven monkeys (*Macaca nemestrina)* aged 1.5 - 4 years-old (OD -0.96 and OS-0.96) [218] and found the humans were more on the plus (hyperopic) side and the chimpanzees and monkeys more on the minus (myopic) side [29]. Both the monkeys and chimpanzees had been kept in laboratory cages and pens with restricted visual space and not been allowed freedom of movement. Female chimpanzees were also more myopic than male chimpanzees [29]. Myopic eyes also have a lower intraocular pressure than hyperopic eyes [29].

More recently, Milnes *et al*. (2020) conducted an opportunistic study during health examinations at a chimpanzee sanctuary in Zambia, and measured IOP and tear production in 27 and 24 chimpanzees respectively [52]. Body position significantly affect IOP readings (obtained using rebound tonometry), and in chimpanzees that were positioned in lateral recumbency for tonometric readings, the IOP in the dependant (lower / downward-facing) eye (24.77 ± 4.49 mmHg) was consistently higher that the IOP in the non-dependant (upper / upward-facing) eye (22.27 ± 4.65 mmHg) [52]. Due to this finding, IOP was subsequently measured in a subset of the population with the chimpanzees held in an upright position and mean IOP was reported at 18.74 ± 3.01 mmHg, which was similar to that obtained in non-anaesthetised chimpanzees in the Young and Farrer study [29, 52].

Mean IOP using predominantly (n=7) applanation tonometry (Tono-Pen AVIA VET, Reichert Inc., NY, USA) and rebound tonometry (n=3) was 14 ± 4.2 mmHg for ten anaesthetised captive chimpanzees, where the authors combined the values obtained from the different tonometers [210]. In the three individuals where rebound tonometry was used, higher IOP readings were recorded compared to the other seven individuals. The authors were unable to draw any statistical conclusions regarding tonometry methods due to the low sample size [210].

In 2005, Liang *et al.* recorded baseline data for the western lowland gorilla, based on 5 captive anaesthetised individuals (four males and one female, two adolescents and three adults). Mean intraocular pressure, using Schiotz tonometry was recorded as 12.0 ± 4.3 mmHg. Ocular biometry measurements obtained using A- and B-mode ultrasonography included axial globe length, lens thickness and anterior chamber depth. Mean corneal curvature and mean central corneal thickness were also determined. The findings showed important similarities between gorilla and human eyes with the major difference being the larger corneal diameter and deeper anterior chamber of gorillas in contrast to humans. Liang *et al.* (2005) also commented on the importance of individual prediction of IOL power prior to performing cataract surgery in these great apes, given the apparent intraspecies variability [11].

De Faber *et al.* (2004) and Warwick *et al.* (2017) also reported on ocular biometric data (using handheld keratometry and A-scan ultrasonography) for their individual gorilla cases undergoing cataract surgery [10, 33]. A large study on nonhuman primate ocular growth was conducted by Augusteyn *et al.* (2016) involving measurement of ex vivo globes of 98 hamadryas baboons, 551 cynomolgus macaques, and 112 rhesus macaques, ranging in age from 23 - 360 months. Globe and lens growth were noted to differ to that of humans in a number of ways [219]. Growth of the nonhuman primate globe continues throughout life, whereas the human globe stops growing at around 1 year-old [220]. Nonhuman primate lens growth is monophasic, whereas human lens growth is biphasic. With increasing age, the nonhuman primate lens diameter increases but the thickness decreases and the lens becomes progressively thinner and flatter. In contrast, the human lens becomes increasingly thicker and rounder with age [219].

A study comparing orbital morphology of humans and apes found that humans have morphology favouring lateral vision [221]. Both humans and apes have front-facing orbits that allow for an overlap of monocular visual fields but conversely limits the extent of lateral vision. Humans are able to compensate for this using eye motion to expand their lateral visual fields [221]. Human skulls were compared with skulls from chimpanzees and bonobos, orangutans, gorillas and gibbons. The orbital width/height ratio and two orbital angles (representing orbital convergence and rearward position of the orbital margin) were calculated. Humans and gibbons have orbits which were less convergent than those of chimpanzees, bonobos, orangutans and gorillas [221]. Further, the human orbit displays a uniquely rearward temporal orbital margin, which avoids visual obstruction and promotes lateral visual field expansion though eye motion. It is postulated that this morphological evolution came about through adaptation to bipedal posture and open-country habitat [221].

Reference values for selected ophthalmic diagnostic tests (including tonometry, pachymetry and ocular biometry) have been reported for the rhesus [14, 53, 146, 157] and cynomolgus [54] macaques, and the capuchin monkey [30]. Using ultrasonic pachymetry, the central corneal thickness of the adult capuchin monkey (0.46 ± 0.03 mm) [30] was measured to be similar to that of humans (0.467 ± 0.040 mm) [222]. Monkeys have similar ocular anatomy and visual function to humans and thus are good candidates for ocular pathology studies [14]. Rhesus macaques are used as nonhuman primate models of experimental glaucoma, where ocular hypertension is induced either directly through anterior chamber cannulation or using Argon laser burns to scar the trabecular meshwork in the drainage angle, to decrease aqueous outflow [14].

In a recent article, McAllister *et al.* (2018) reported that, when compared to intracameral manometry, the TonoVet® rebound tonometer consistently overestimated IOP at all anterior chamber settings [14], a finding that was partially consistent with an earlier study in this same species which showed an overestimation of IOP to occur at low manometric IOP values but that the instrument underestimated IOP at high manometric IOP values [53]. In contrast, Elsmo et al. (2011) showed a non-significant tendency for the TonoVet® rebound

tonometer to consistently underestimate manometric IOP in cynomolgus macaques and they recommended use of a conversion equation to provide a more accurate estimate of the true IOP in this species [54].

1.3. OBJECTIVES AND BENEFITS

1.3.1 Objectives

The objectives of this study are:

1.) To describe the ocular pathology in a group of 33 captive chimpanzees.
2.) To determine the mean intraocular pressure in the anaesthetised chimpanzee, utilising two different rebound tonometers.
3.) To ascertain the mean corneal curvature in the chimpanzee, utilising an automatic handheld keratometer.
4.) To determine the mean central corneal thickness in the chimpanzee utilising ultrasonic pachymetry.
5.) To establish the ocular biometric measurements in the chimpanzee, utilising A- and B-mode ultrasonography.
6.) To calculate the intraocular lens power for this species, employing theoretical formulae.

1.3.2 Benefits

- Reporting on ocular pathology in a group of captive chimpanzees will serve as an important reference for veterinarians conducting clinical examinations on these animals.
- Establishing reference values for intraocular pressure in the chimpanzee will assist veterinarians in diagnosing and treating glaucoma in this species.
- Establishing reference values for corneal curvature, corneal thickness and ocular biometry can aid in the diagnosis and treatment of ocular disease in chimpanzees.
- Calculating the intraocular lens power for the chimpanzee will assist ophthalmologists performing cataract surgery, to select the most appropriate intraocular lens for this species.

CHAPTER 2. MATERIALS AND METHODS

2.1 MODEL, EXPERIMENTAL DESIGN AND JUSTIFICATION

This was a live animal model utilising 33 anaesthetised chimpanzees (*Pan troglodytes*) of varying age and gender, which were enrolled into this prospective, descriptive / observational cross-sectional geographic population study. The animals were anaesthetised for the purposes of veterinary health evaluations and/or other veterinary procedures at the Jane Goodall Institute (JGI) of South Africa's Chimp Eden (Fig. 2.1). The data for this study was collected opportunistically and no chimpanzees were anaesthetised for the sole purpose of this study.

Chimp Eden is located outside Mbombela (previously Nelspruit) in Mpumalanga, a province in eastern South Africa, bordering Swaziland and Mozambique. It is the only chimpanzee sanctuary in the country and is a member of the Pan African Sanctuary Alliance (PASA). It provides a permanent home to rescued chimpanzees that have survived the bush meat trade, been orphaned or traded in the illegal pet market. There are currently 33 chimpanzees at the sanctuary. The chimpanzees are kept semi-wild, in large outdoor enclosures, in three different "family groups" and exhibit normal social interactions and behavioural patterns (Figs. 2.2 & 2.3).

Figure 2.1. Entrance to the Chimp Eden facility, belonging to the Jane Goddall Institute South Africa.

Figure 2.2. Night rooms at the Chimp Eden facility, for chimpanzee Groups 1 & 2. Chimpanzee Group 1 enclosure in the foreground.

Figure 2.3. Group 2 chimpanzee enclosure, at the Chimp Eden facility in Mbombela, South Africa.

2.2 EXPERIMENTAL PROCEDURE

2.2.1 General anaesthesia of the chimpanzee for health examination

The chimpanzees were immobilised one at a time in their night rooms by specialist wildlife veterinarian Dr Katja Koeppel, who was responsible for the general anaesthesia from immobilisation, monitoring, maintenance, reversal and recovery of the chimpanzee. For the biannual health examinations at Chimp Eden, the chimpanzees were pre-medicated with 15mg oral midazolam (Dormicum® 7.5mg, Roche Products (Pty) Ltd., 24 Fricker Road, Illovo, Sandton, 2196). A combination of medetomidine (Domitor® 1mg/ml, Zoetis South Africa (Pty) Ltd., 85 Bute Lane, Sandton, 2196) at 0.03mg/kg and tiletamine-zolazepam (Zoletil® 100mg/ml, Virbac South Africa (Pty) Ltd., 38 Landmarks Avenue, Samrand Business Park, Centurion 0157) at 1.2mg/kg was administered intramuscularly via remote injection (Pneudart 1cc ¾ needle with gel collar from Excalibur carbon dioxide-powered rifle) or occasionally hand injection.

The chimpanzees received top-up boluses (1mg/kg) of ketamine (AnaKetV® 100mg/ml, Bayer South Africa (Pty) Ltd., 27 Wrench Road, Isando 1600) during transportation (intramuscularly) and maintenance (intravenously) if their plane of anaesthesia was inadequate. They were carried on canvass stretchers to the nearby examination room. Upon arrival in the examination room, after being weighed, the chimpanzee was place on an examination table, intubated and thereafter maintained on isoflurane (Isofor®, Safeline Pharmaceuticals (Pty) Ltd., 4845 Rugby Street, Weltevreden Park 1715). Once the health examination was complete, the chimpanzees were transported back to the night room. Here they were placed in the recovery position and the sedation was reversed with atipamezole (Antisedan® 5mg/ml, Zoetis South Africa (Pty) Ltd., 85 Bute Lane, Sandton, 2196) (at 5x the original medetomidine dose) intramuscularly and monitored until extubation. (See Appendix 2 for the Chimp Eden Veterinary Anaesthetic Record data collection sheet.)

While the detailed ophthalmic examination (see details below) was being carried out, the patient was simultaneously undergoing other procedures as part of the health examination, including echocardiography, hormone implantation and, where applicable, pelvic ultrasonography or vasectomy procedures. (See Appendix 3 for the Chimp Eden Health Check and Assessment data collection sheets.)

2.2.2 Ophthalmic examination and selected diagnostic tests

The ophthalmic examination was performed solely by myself. The examinations and measurements were taken between 07h00 and 17h00. The following procedures were done, in order from first approach to the anaesthetised chimpanzee, to ensure a thorough ophthalmic examination:

1. Cursory ophthalmic examination (of the orbit, eyelids, conjunctiva, cornea, sclera and anterior chamber) for obvious pathology.

2. Determination of the intraocular pressure using two different rebound tonometers: the TonoVet® and the Icare PRO®. Care was taken to avoid pressure on the globe and jugular veins.
   For the measurement using the TonoVet®, measurements were obtained using both the "d" and "P" settings on the instrument. The chimpanzee was placed in either right or left lateral recumbency (depending on which cephalic vein was being used by the wildlife veterinarian to simultaneously place an intravenous catheter), as the instrument must be held upright / perpendicular to the ground (Fig. 2.4).
   The Icare PRO® allows for accurate measurement in the supine / dorsally recumbent body position (Fig. 2.5). A set of measurements was obtained for both the laterally recumbent as well as dorsally recumbent body positions (Figs. 2.6 and 2.7).
   For both instruments, the probe was positioned 3-7 mm from the corneal surface, directed at the central cornea, and the measurements were taken before any ointment was placed in the eyes, since the reading is affected by ocular surface tension.

3. Mydriasis was accomplished by instilling one drop of tropicamide (Mydriacyl® 1% ophthalmic solution, Novartis, Alcon Laboratories, South Africa) into each eye. IOP was measured prior to application of tropicamide in order to rule out glaucoma (contra-indication for pharmacological mydriasis). Tropicamide is widely and routinely used for diagnostic purposes as complete mydriasis is necessary for a thorough examination of the lens and peripheral fundus. Tropicamide is the preferred diagnostic mydriatic due to its rapid onset (10-20 minutes) and short duration. Side effects include photosensitivity and blurred vision (for up to 6 hours). All chimpanzees receiving tropicamide were recovered and kept overnight indoors in darkened "night rooms".

4. Keratometry (measurement of corneal curvature) using a hand-held auto-refract keratometer (Retinomax K Plus-3, Righton Ophthalmic Instruments, Tokyo, Japan) and/or the Nidek Handy Ref-K handheld refractometer/keratometer (Nidek Co.Ltd., Tokyo, Japan). These measurements were obtained generally with the chimpanzee in dorsal recumbency but occasionally also in sternal recumbency (as a result of the opportunistic nature of this study and dependant on what other

concurrent necessary procedures were being performed simultaneously or what body positioning was required for those procedures).

The instrument was calibrated (with the use of the manufacturer´s calibration cylinder) at the beginning of each day. The measurements were obtained according to the manufacturer's instructions, moving the instrument towards the eye until the images appeared sharp on the instrument´s display and a beeping tone confirmed a completed measurement.

The instrument measures curvature of the central cornea (generally 3 mm to 4 mm diameter according to the size and shape of the mire ring image reflected on the anterior corneal surface). The instrument automatically takes multiple readings consecutively. R1 (minor meridian) and R2 (major meridian) measurements, as well as the mean of the two meridians, are recorded in millimetres.

A Williams-type eyelid speculum was used to keep the eyelids open while measurements were being obtained (Fig. 2.8).

5. Slit lamp biomicroscopy, using the Keeler Classic Portable Slit Lamp Biomicroscope (Keeler Ltd, Winsor, UK) to evaluate the globe and adnexa from the extraocular structures to the cornea, anterior chamber, iris, lens, and anterior face of the vitreous (Fig. 2.9).

   Initially, a diffuse beam was used to survey the globe for eyelid and adnexal, corneal, anterior chamber, lens and posterior segment pathology, after which a focal slit beam was used to better evaluate the cornea, iris and lens, to assess the anterior chamber depth, and to detect aqueous flare. Techniques of both direct and retroillumination were employed.

6. Indirect Ophthalmoscopy, using the Vantage Plus LED Indirect Ophthalmoscope (Keeler Ltd, Windsor, UK) and a Volk 2.2 Pan-retinal BIO lens (Volk Optical Inc., Ohio, USA) (Fig. 2.10). This method allows for a larger field of view of the fundus.

7. Fundus photography was performed, using the Smartscope PRO (Optomed Oy, Finland) (Fig. 2.11) to evaluate and image the retina.

8. Fluorescein staining using a paper strip impregnated with sodium fluorescein (Haag-Streit AG, Koeniz, Switzerland) and evaluation with cobalt blue light of the portable slit lamp biomicroscope in order to assess the integrity of the corneal epithelium.

9. Ultrasonic pachymetry (measurement of central corneal thickness) using the 10 MHz pachymeter probe of the Accutome 4Sight® (Accutome Inc., Pennsylvania, USA). The probe was placed on the axial cornea, with the speed of sound in the cornea present at 1640 m/s. This study made use of UP to measure CCT in chimpanzees, using the preset on the machine for a human corneal ultrasound

velocity of 1640 m/s, since the corneal ultrasound velocity has not been determined for the chimpanzee.

10. Ocular ultrasonography for biometry and posterior segment pathology.

A-mode ultrasonography was performed using the 10 MHz A-scan probe of the Accutome 4Sight® (Accutome Inc., Pennsylvania, USA) to obtain accurate biometric measurements (including axial globe length, anterior chamber depth, lens thickness and posterior segment / vitreous chamber depth). The probe was used in the contact mode, applied directly to the axial cornea, with the default eye type selected as "phakic". As optimal ultrasound velocities have not been determined for the chimpanzee eye, this study used the ultrasound velocity established for physician-based ophthalmology [223]. Ultrasound velocities were set at 1532 m/s for the anterior chamber and vitreous body, and at 1641 m/s for the crystalline lens.

A William´s-type eyelid speculum was used to retract the eyelids (Fig. 2.12).

B-mode ultrasonography was performed, using the 12-15 MHz B-scan probe of the Accutome 4Sight® (Accutome Inc., Pennsylvannia, USA) (Fig. 2.13) or the Sonosite M-Turbo with 13-6 MHz HFL38x linear transducer (FUGIFILM SonoSite Inc., Washington, USA) (Fig. 2.14) via a trans-corneal approach. Coupling gel (methylcellulose) was used to decrease reverberation artefacts as a result of air being otherwise trapped between the transducer and surface of the cornea. The transducer was applied perpendicularly to the surface of the central cornea, ensuring optimal contact but avoiding corneal indentation. It is important to achieve optimal positioning in order to obtain an image from which reliable biometric measurements may be taken. Optimal positioning was confirmed when the image appeared symmetrical, the posterior wall of the globe could be clearly seen and the reflections of the four major landmarks (cornea, anterior lens capsule, posterior lens capsule, and retinal surface) were perpendicular along the eye globe axis. Both vertical (12 o´clock) and horizontal (9 and 3 o´clock) axial scans were performed for each eye.

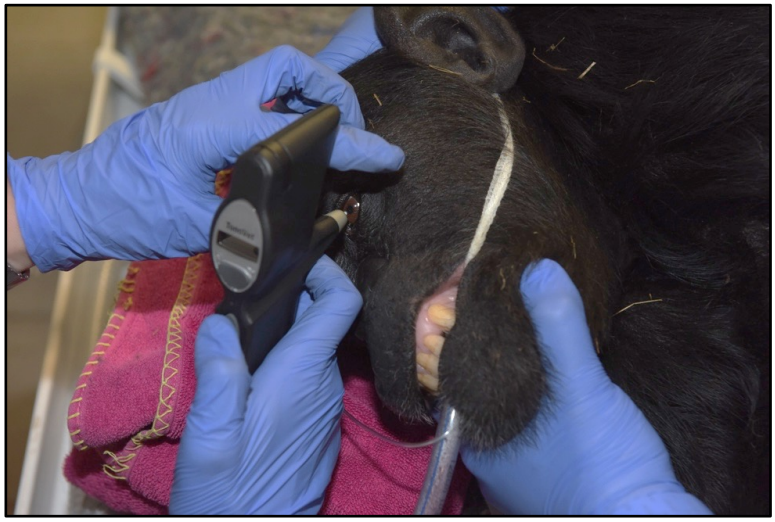

Figure 2.4. Tonometry being performed on the left eye of an anaesthetised chimpanzee in right lateral recumbency, using the TonoVet® rebound tonometer.

Figure 2.5. Tonometry being performed on the right eye of an anaesthetised chimpanzee in dorsal recumbency (supine position), using the Icare PRO rebound tonometer.

Figure 2.6. An anaesthetised chimpanzee at Chimp Eden in right lateral recumbency for ophthalmic and echocardiography evaluations.

Figure 2.7. An anaesthetised chimpanzee at Chimp Eden in dorsal recumbency (supine postion) for ophthalmic evaluations. The green fluorescein stain can be seen on the left eye.

Figure 2.8. Keratometry being performed on the right eye of an anaesthetised chimpanzee in dorsal recumbency, using the Retinomax K Plus-3 handheld keratometer. A Williams-type eyelid speculum was used to retract the eyelids.

Figure 2.9. Slit-lamp biomicroscopic examination of the left eye of an anaesthetised chimpanzee in dorsal recumbency, using the diffuse light beam on the Keeler Classic Portable Slit-lamp biomicroscope.

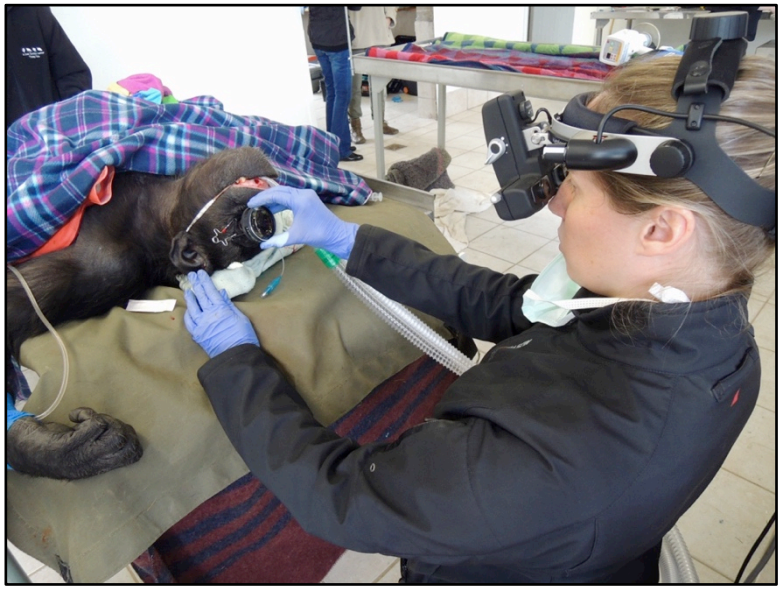

Figure 2.10. Binocular indirect ophthalmoscopy being performed on the left eye of an anaesthetised chimpanzee in dorsal recumbency, using the Keeler Vantage Plus LED Indirect Ophthalmoscope and a Volk 2.2 Pan-retinal BIO lens. A Williams-type eyelid speculum was used to retract the eyelids.

Figure 2.11. Fundus imaging being performed on the right eye of an anaesthetised chimpanzee in sternal recumbency, using the Smartscope PRO ophthalmic camera. A Williams-type eyelid speculum (not visible here) was used to retract the eyelids.

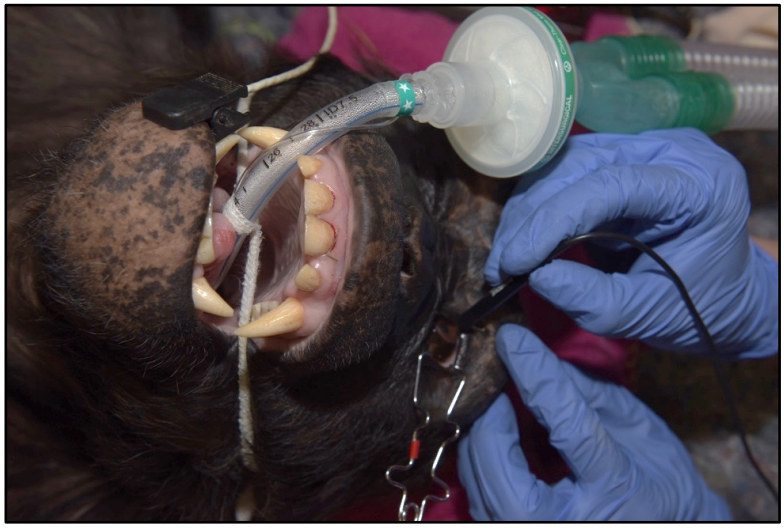

Figure 2.12. A-mode ultrasongraphy of the left eye of an anaesthetised chimpanzee in dorsal recumbency, using the 10 MHz A-scan probe of the Accutome 4Sight®. A trans-corneal approach is used. A Williams-type eyelid speculum was used to retract the eyelids.

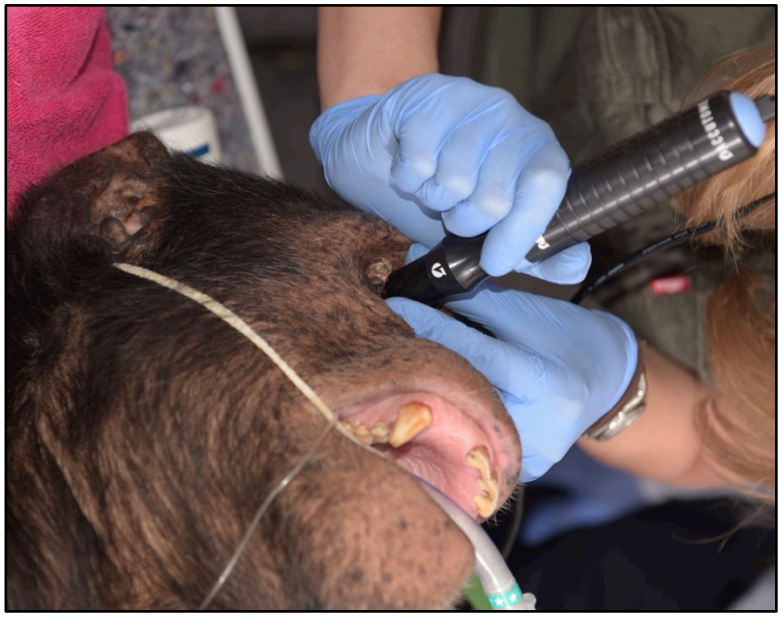

Figure 2.13. B-mode ultrasongraphy of the right eye of an anaesthetised chimpanzee in dorsal recumbency, using the 12-15 MHz B-scan probe of the Accutome 4Sight®. A trans-corneal approach was used.

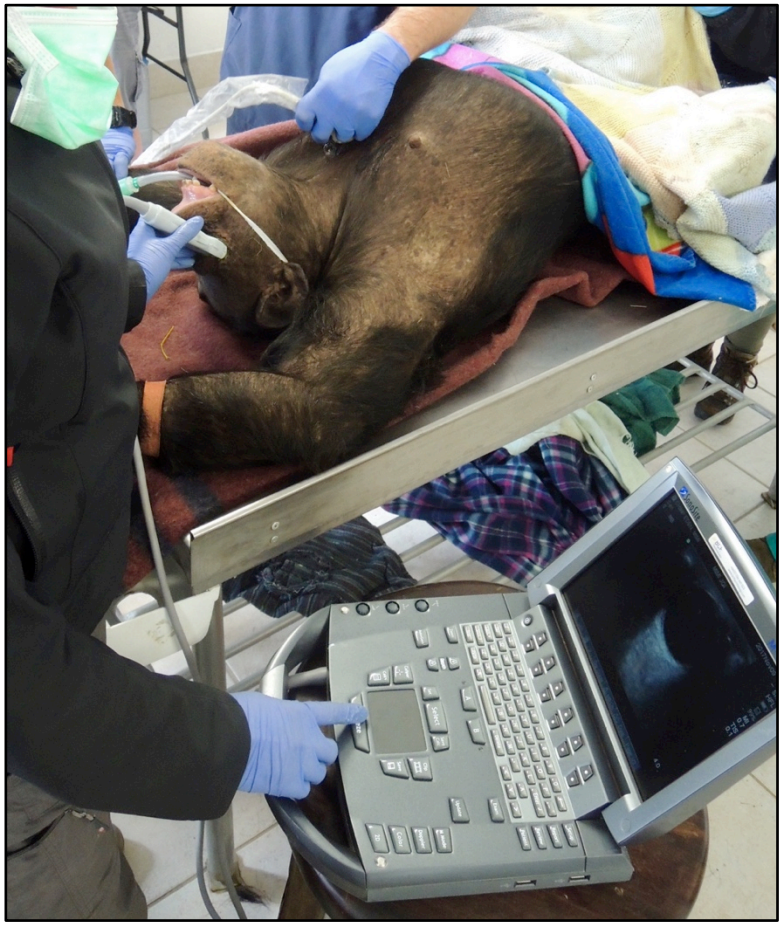

Figure 2.14. B-mode ultrasonography of the right eye of an anaesthetised chimpanzee in dorsal recumbency, using a 13-6 MHz HFL38x linear transducer and the Sonosite M-Turbo portable ultrasound. A horizontal (3 o´clock) axial scan is being performed, using a trans-corneal approach. This examination was performed at the same time as the echocardiography.

2.3 DATA COLLECTION

The ophthalmic data collected was recorded on a data collection sheet developed for this purpose (Addendum 1).

2.3.1 Patient side data capture for each eye:

1. Extra-ocular, corneal, anterior chamber, lens, posterior segment and retinal pathology were all drawn on the eye diagram, if present.

2. Intraocular pressure: The measurement was repeated three times for the Icare PRO® (Icare Oy, Finland) and three times for two different settings (Dog/Cat and P settings) on the TonoVet® (Icare Oy, Finland). The TonoVet® readings, the time of the readings and the side the animal was lying on was recorded. The non-dependant eye was always measured first. Icare PRO® readings were obtained with the chimpanzee in both lateral and dorsal recumbency.

3. Mydriatic used or not.

4. Keratometry was performed with the use of a handheld auto-refract keratometer where after the values were automatically printed by the on-board printer and were attached to the data collection sheet. Corneal astigmatism and horizontal and vertical corneal radii of curvature in the central corneal region were obtained for each eye (Fig. 2.15).

5. Slit-lamp biomicroscopy examination findings was recorded on the eye diagram together with short comments.

6. Fundus / retinal images were obtained using an Optomed Smartscope PRO (Optomed Oy, Finland), and they were stored on the on-board memory. All images were downloaded on a computer and stored with all the data of this project.

7. Fluorescein staining was performed and the results recorded on the record sheet.

8. Pachymetry readings were obtained and recorded on the Accutome 4Sight® (Accutome Inc., Pennsylvannia, USA) on-board memory, memory stick and primary investigator's computer. A series of 10 measurements was taken for each eye and the mean central corneal thickness and standard deviation calculated by the Accutome 4Sight® were recorded on the data collection sheet.

9. A-mode biometric measurements (including axial globe length, anterior chamber depth, lens thickness and posterior segment depth) were recorded on the Accutome 4Sight® (Accutome Inc., Pennsylvania, USA) on-board memory, memory stick and primary investigator's computer.

10. B-mode ultrasound images were recorded on either the Accutome 4Sight® (Accutome Inc., Pennsylvania, USA) or the Sonosite M-Turbo (FUGIFILM SonoSite Inc., Washington, USA) on-board memory, memory stick and primary investigator's computer for further evaluation.

2.3.2 Office data collection:

1. Keratometry measurements obtained using the hand-held auto-refract keratometer (Retinomax K Plus-3, Righton Ophthalmic Instruments, Tokyo, Japan) and/or the Nidek Handy Ref-K handheld refractometer/keratometer (Nidek Co.Ltd., Tokyo, Japan) were subject to specific inclusion criteria, based on the recent publication by Kawasaki *et al.* (2020) [130]. Readings from individuals where the difference in R1R2avg between right and left eyes was greater than 4.5% were excluded since the authors concluded that such a variation represents intra-operator variability [130].

2. The central corneal thickness measurements obtained by the pachymetry probe on the Accutome 4Sight® (Accutome Inc., Pennsylvania, USA) were printed out and attached to the data collection sheet (Fig. 2.16).

3. The biometric measurements automatically calculated by the A-mode function on Accutome 4Sight® (Accutome Inc., Pennsylvania, USA), including: axial globe length (AGL), anterior chamber depth (ACD), crystalline lens thickness (CLT) / lens depth (LD) and posterior segment depth (PSD) / vitreal chamber depth (VCD), were printed out and attached to the data collection sheet (Fig. 2.17).

4. . Biometric measurements were also done manually on the saved B-mode ultrasound images using ImageJ (U.S. National Institutes of Health, Bethesda, Maryland, USA) a Java-based image processing program. The following biometric measurements were determined (were possible) for each suitable globe ultrasonograph: Axial eye globe length (AGL), anterior chamber depth (ACD), crystalline lens thickness (CLT) / lens depth (LD) and posterior segment depth (PSD) / vitreous chamber depth (VCD). All measurements were recoded on the chimpanzee's data collection sheet (Fig. 2.18).

5. Copies of the veterinary anaesthetic record, health and assessment data collection sheets were obtained for each individual from JGI Chimp Eden (Addenda 2 & 3).

6. Calculation of IOL power: Binkhorst and Retzlaff theoretical formulae were used to calculate the IOL power (in diopters) for each chimpanzee which had a full set of keratometric and biometric measurements (obtained with either A-mode and/or manually measured on B-mode ultrasonography).

Binkhorst theoretical formula [200]:

$$Pe = \frac{1336\ (4r - L)}{(L-C)\ (4r-C)}$$

Pe is the predicted IOL power in diopters (D), *r* is the averaged corneal radius in mm, *L* is the axial globe length (AGL) in mm, and *C* is the expected postoperative anterior chamber depth (PACD) in mm.

Retzlaf theoretical formula [199]:

$$Pe = \frac{N}{L-C} - \frac{NK}{N-KC}$$

Pe is the predicted IOL power in diopters (D), *N* is the refractive index of the aqueous and vitreous (1.336), *L* is the axial globe length (AGL) in m, *C* is the postoperative anterior chamber depth (PACD) in m, and *K* is the averaged corneal curvature in D.

In both cases, PACD was predicted from pre-operative A-mode(or B-mode)-measured anterior chamber depth (ACD) and crystalline lens thickness (CLT), such that:

PACD = ACD + ½ CLT.

Further, as one cannot predict the actual postoperative position of the intracapsular IOL, two values for PACD (2 mm anterior or 2 mm posterior to the central lens position) were applied to the formulae in order to compensate for the effect of lens position on the refractive power of an IOL to achieve emmetropia [36].

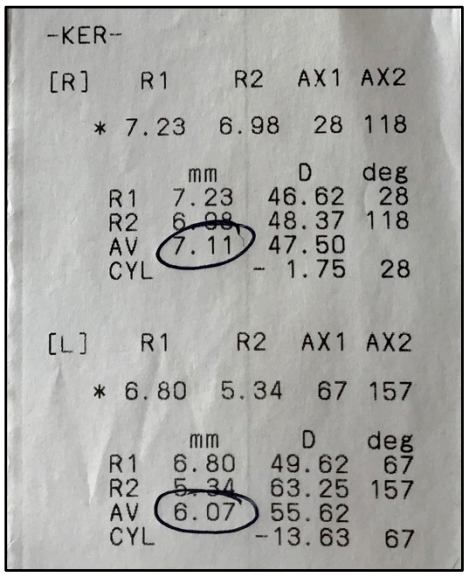

Figure 2.15. A printout of the corneal curvature measurements of an adult chimpanzee using the Retinomax K Plus-3 handheld keratometer.

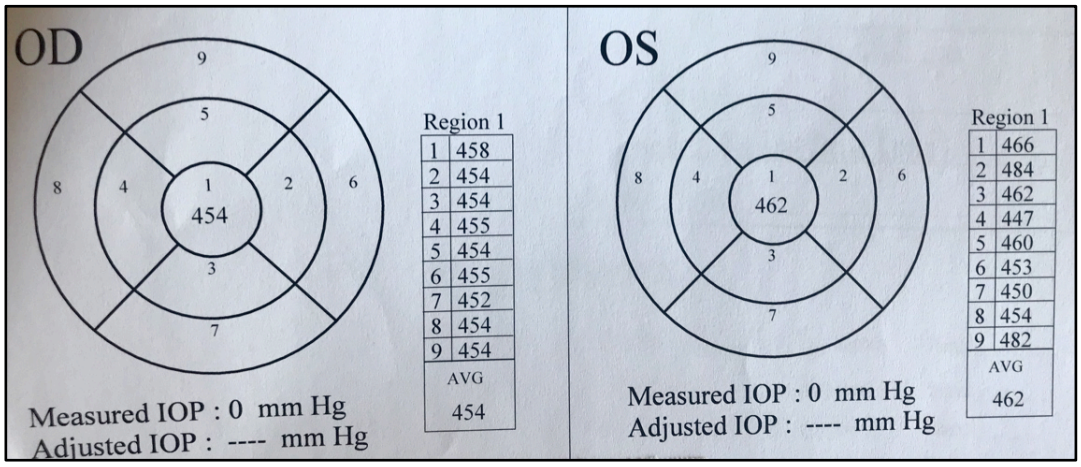

Figure 2.16. Central corneal thickness measurements of an adult chimpanzee, generated on a printout of the Accutome 4Sight® ultrasonic pachymeter.

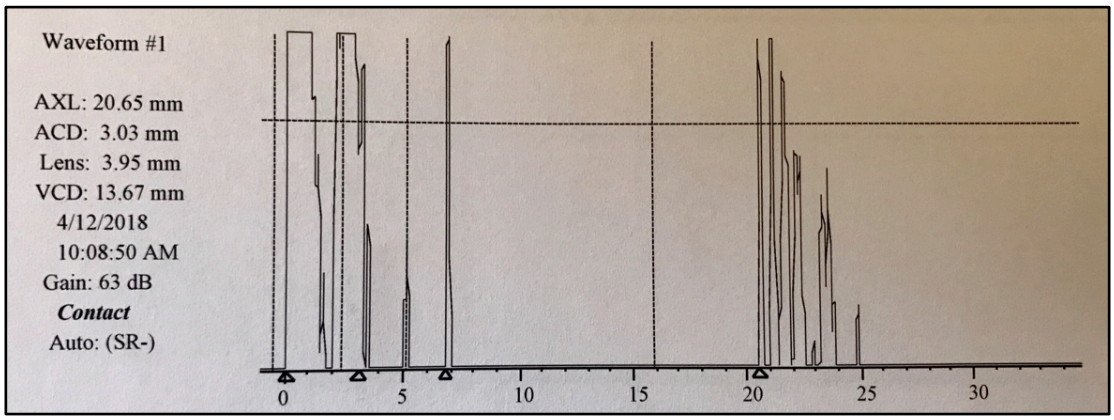

Figure 2.17. A printout of the ocular biometry of an adult chimpanzee with A-mode ultrasonography, using the Accutome 4Sight®. AXL – Axial globe length. ACD – Anterior chamber depth. VCD – Vitreous chamber depth.

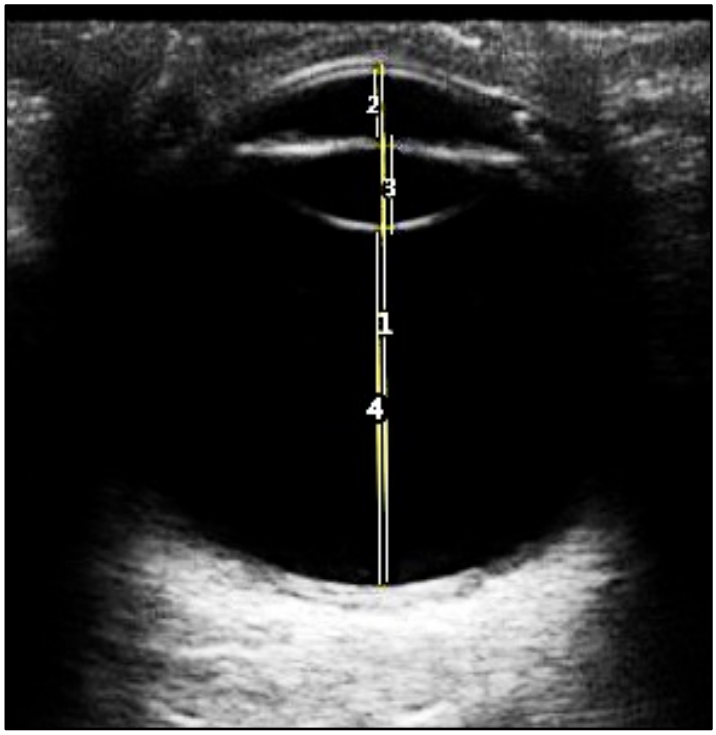

Figure 2.18. Ocular biometry of an adult chimpanzee with B-mode ultrasonography, using the Sonosite M-Turbo portable ultrasound and HFL38x 13-6 MHz linear transducer, where measurements have been performed manually on the saved ultrasonograph with ImageJ. 1 – Axial globe length (AGL). 2-Anterior chamber depth (ACD). 3- Crystalline lens thickness (CLT). 4 – posterior segment depth (PSD) / vitreous chamber depth (VCD).

2.4 DATA ANALYSIS

All data was recorded in Excel spreadsheets. The data was analysed using JMP® Pro Version 15 (SAS Institute Inc., Cary, NC, 1989-2019). Histograms of all data were visually inspected and the data was tested for normality using the Anderson-Darling test. For the keratometry data, an ordinary least squares regression model was used to evaluate the relationship between the measurements and model effects including age, sex and body weight. Wilcoxon signed-rank tests were used to compare keratometry measurements between the right and left eyes. The tonometry data was log transformed and analysed using a least squares repeated measures factor analysis, with age, sex, instrument, instrument setting and body position as factors. For the biometry data, an ordinary least squares regression model was used to evaluate the effects of age, sex, weight, scan and mode on each of the measurements. Wilcoxon signed-rank tests was used to compare the pachymetry measurements of the left versus right eyes. All statistical tests were 2-tailed and significance was defined as p-value < 0.05 in all cases. The data were reported as means ± standard deviation (SD).

2.5 ETHICAL CONSIDERATIONS

Ethics clearance for this research was obtained from the University of Pretoria Animal Ethics Committee (V089-18) and Research Ethics Committee (REC088-18) on 30 October 2018 and 5 November 2018 respectively.

The study was performed on chimpanzees already undergoing immobilisation for veterinary health examinations and involves only non-invasive and rapid ophthalmic examination techniques. The data was collected opportunistically and no animal was specifically anaesthetised for the sole purpose of this study.

CHAPTER 3. RESULTS

Mean age of the 33 chimpanzees in this study was 18.55 ± 12.12 years (median 15 years, range two to 73-years-old). There were 20 females (20/33: 60.6%) with a mean age of 21.8 ± 7.06 years (median 15 years) and 13 males (13/33; 39.4%) with a mean age of 16.4 ± 17.48 years (median 15 years).

Table 3.1. List of ophthalmic diagnostic procedures performed with corresponding number of chimpanzees and total number of eyes.

Diagnostic Procedure	No. of chimpanzees	No. of eyes
Slit-lamp biomicroscopy	33	66
Fluorescein staining	32	64
B-mode ultrasonography	20	40
Indirect ophthalmoscopy	4	8
Pharmacologically dilated	4	8
Tonometry (TonoVet)	33	66
Tonometry (Icare PRO)	8	16
Keratometry	22	44
Pachymetry	11	21
A-mode ultrasonography	11	22
IOL power calculation	10	16

All 33 chimpanzees underwent slit-lamp examination by the primary investigator, which facilitated assessment of the globe from the eyelids and adnexa, conjunctiva, cornea, anterior chamber, iris and lens. Examination of the posterior segment (vitreous body and retina) was conducted via B-scan ocular ultrasonography, which was performed bilaterally on 20 chimpanzees (13 chimpanzees with the SonoSite M-Turbo with 13-6 MHz HFL38x linear transducer, nine chimpanzees with the 12-15 MHz B-scan probe of the Accutome 4Sight®, and four chimpanzees with both instruments on separate occasions). While indirect ophthalmoscopy and fundus photography (Fig. 3.1) was accomplished in only four individuals. Three individuals that had previously been identified to have ocular pathology were pharmacologically dilated to facilitate a more thorough investigation (including electroretinography in one case).

3.1 OCULAR FINDINGS

Table 3.2. Pathological ocular findings with corresponding number of chimpanzees and total number of eyes.

Pathological Ocular Finding	No. of chimpanzees	No. of eyes
Blepharospasm	1	1
Eyelid oedema	1	1
Conjunctival hyperaemia	1	1
Chemosis	1	1
Perilimbal white stromal deposits	13	26
Corneal erosion	1	1
Senile corneal degeneration	1	2
Iris hypoplasia	1	2
Dyscoria	3	3
Cataract	2	2
Pseudophakia	1	1
Nuclear sclerosis	1	2
Vitreal degeneration	4	5

3.1.1 Eyelids and adnexa

A 23-year-old castrated male chimpanzee was seen with acute unilateral blepharospasm and eyelid oedema after sustaining blunt trauma to the left eye and periocular tissues from a fellow chimpanzee on the day of examination.

3.1.2 Conjunctiva

Dense, limbal, conjunctival melanosis was observed bilaterally in all chimpanzees (Figs. 3.2A & B and 3.3). The bulbar conjunctiva was diffusely pigmented to varying degrees in all chimpanzees (Figs. 3.2A & B and 3.3). The same castrated male chimpanzee that sustained blunt trauma to the left eye, also had marked conjunctival hyperaemia, mild chemosis and laceration of the dorsal palpebral conjunctiva.

3.1.3 Cornea

Continuous circumferential perilimbal white corneal stromal deposits (Fig. 3.3) of varying density were observed bilaterally in 13 chimpanzees (six males and seven females). The average and median age of chimpanzees with this finding was 23.18 years and 16 years respectively, with an age range of 11 - 73 years. A 23-year-old female chimpanzee was seen with a focal superficial corneal erosion of the right ventral cornea that was fluorescein positive. It was suspected that the erosion was acute and secondary to immobilisation as there was no corneal neovascularisation or cellular infiltrate noted on slit-lamp biomicroscopy. All the other 31 chimpanzees (64 eyes) evaluated, were fluorescein negative. A 73-year-old male chimpanzee displayed a focal crystalline stromal opacity of the ventral paraxial cornea (in a crescent-like shape from 4-8 o´clock). No vascularisation was associated with the opacity and the cornea was fluorescein negative. Senile corneal degeneration was suspected.

3.1.4 Anterior chamber and iris

Bilateral and unilateral focal and multifocal iridal melanosis (Fig. 3.2 A & B), appeared to be a common finding and was noted in seven chimpanzees (bilaterally in four and unilaterally in three individuals). All these discreet areas of iridal hyperpigmentation were flat on slit-lamp biomicroscopy and not associated with dyscoria. The melanosis was noted as an incidental finding. A 13-year-old female chimpanzee was presented with bilateral iris hypoplasia on transillumination (Fig. 3.4). On slit-lamp biomicroscopy, there was considerable variation in the width of the iris circumferentially, with the peripheral iris appearing to bulge anteriorly and the central / peri-pupillary iris appearing to recede posteriorly resulting in a deeper anterior chamber axially. This chimpanzee had a history of photophobia, appeared to be more sensitive to glare, and was known by the Chimp Eden staff to shade her eyes in bright sunlight. Dyscoria was observed unilaterally in three male chimpanzees, in two cases the dyscoria was due to posterior synechiae secondary to historic lens-induced uveitis, and in one case the dyscoria was due to an entrapped haptic of an anteriorally luxated intraocular lens. The latter case also displayed diffuse iris hyperpigmentation. No aqueous flare was detected in any individuals.

3.1.5 Lens

Cataract was observed unilaterally in a 34-year-old male and an immature cataract in a 26-year-old male (Fig. 3.3) in their left and right eyes respectively. In both cases, the cataracts were suspected to be secondary to blunt force trauma (due to the history, unilateral presentation and the associated posterior segment pathology). Both cases showed evidence of previous lens-induced uveitis (posterior synechiae and pigment dispersion on the anterior lens capsule). A unilateral pseudophakic 12-year-old male chimpanzee was presented with a history of dorso-lateral strabismus in the right eye. This chimpanzee had reportedly undergone cataract surgery in the right eye nine years previously, although no medical records regarding this surgery were available. Upon examination of the right eye, the intraocular lens (IOL) was displaced anteriorly and occupying the anterior chamber, aside from the ventrally positioned haptic that was posterior to the iris and causing dyscoria of the ventral pupillary margin (Fig. 3.5 A & B). Pigment dispersion was noted on the surface of the IOL. Marked nuclear sclerosis was noted bilaterally in a 73-year-old male chimpanzee. This chimpanzee was subsequently pharmacologically dilated and indirect ophthalmoscopy of the fundus was possible and not hampered by the lenticular changes.

3.1.6 Posterior segment

The findings discussed here are all based on B-mode ultrasonography findings (as opposed to ophthalmoscopy), which was performed in 20 chimpanzees (40 eyes). Both adult male chimpanzees that presented with unilateral mature cataracts had mild and severe ipsilateral vitreal degeneration respectively. One of these individuals, the 34-year-old male, had concurrent ipsilateral retinal detachment (Fig. 3.6). Electroretinography was performed on the 26-year-old male to determine if he would be a suitable candidate

for cataract surgery. Despite no retinal detachment being evident on ocular ultrasonography (Fig. 3.7), an extinguished electroretinogram (Fig. 3.8) was observed in the cataractous eye. Marked vitreal degeneration was observed in the right eye of the 12-year-old pseudophakic chimpanzee, consistent with previous intraocular surgery (Fig. 3.9). Mild to moderate bilateral suspected age-related vitreal degeneration was observed in a 73-year-old male chimpanzee.

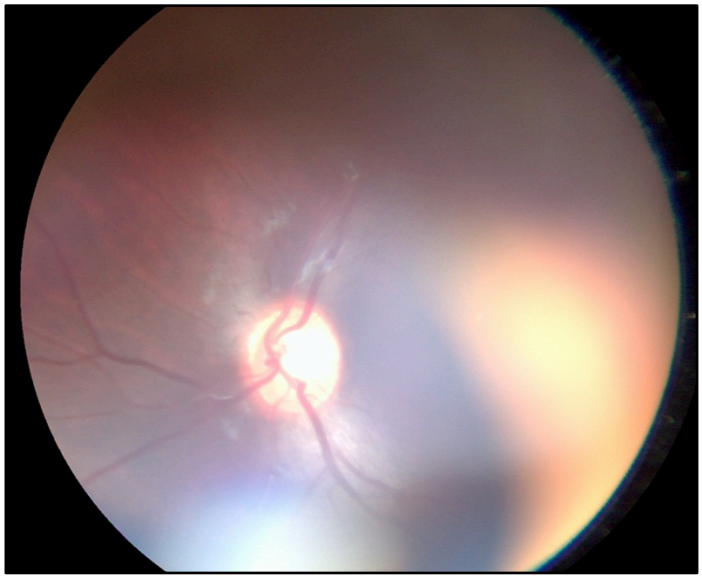

Figure 3.1. Fundus photograph (obtained with the Smartscope PRO ophthalmic camera) of an anaesthetised chimpanzee showing the normal fundic appearance.

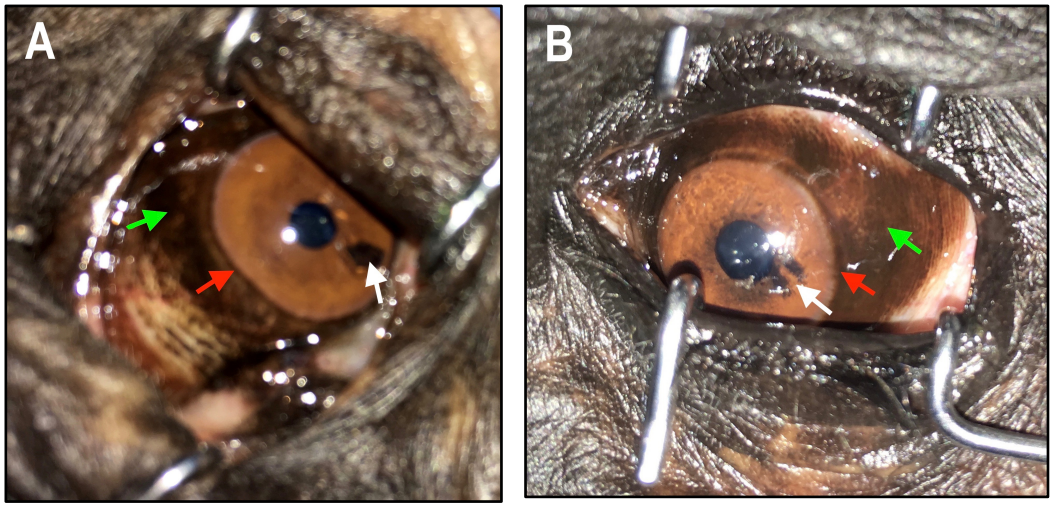

Figure 3.2 A & B. Focal (A) and multifocal (B) iridal melanosis (white arrow) in two chimpanzees. These discreet areas of iridal hyperpigmentation were flat on slit-lamp biomicroscopy and not associated with dyscoria. Dense, limbal, conjunctival melanosis (red arrow) was observed bilaterally in all chimpanzees examined. The bulbar conjunctiva was pigmented (green arrow) in all chimpanzees.

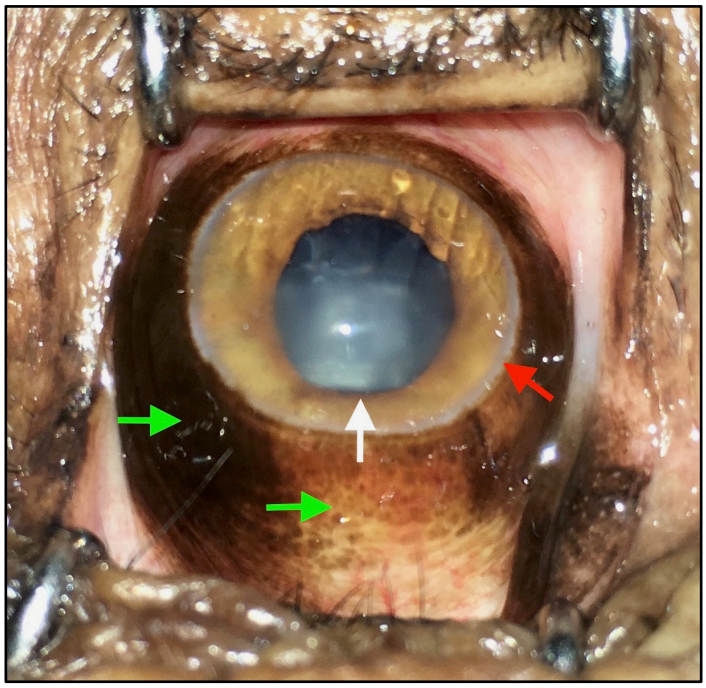

Figure 3.3. An immature cataract in the right eye of a 26-year-old male chimpanzee, presumed secondary to blunt force trauma. Posterior synechiae (white arrow) were evident, causing dyscoria of the ventral pupillary margin. Perilimbal white deposits (red arrow) and darkly to lightly pigmented bulbar conjunctiva (green arrows) can be observed.

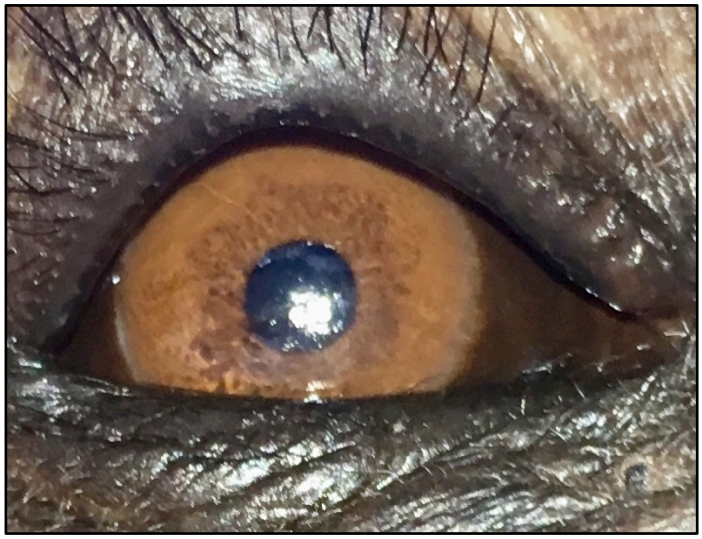

Figure 3.4. Iris hypoplasia in the right eye of a 13-year-old female chimpanzee. On slit-lamp biomicroscopy, there was considerable variation in the width of the iris circumferentially, with the peripheral iris appearing to bulge anteriorly and the central / peri-pupillary iris appearing to recede posteriorly resulting in a deeper anterior chamber axially.

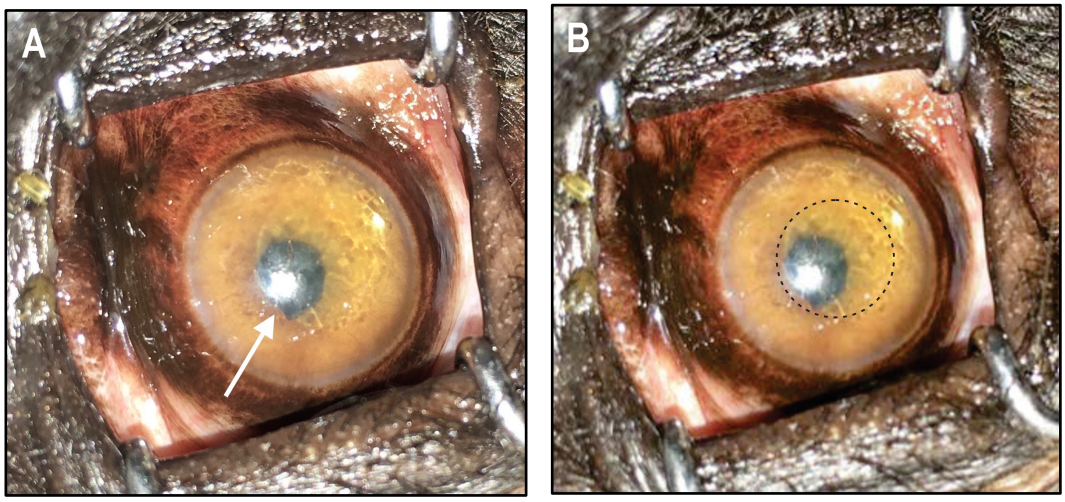

Figure 3.5 A & B. Anterior displacement of an intraocular lens (IOL) in the right eye of a unilateral pseudophakic 12-year-old male chimpanzee. The IOL can be observed in the anterior chamber in B (edges of IOL delineated by black dotted line). The ventrally positioned haptic (not visible here) was posterior to the iris, causing dyscoria of the ventral pupillary margin (white arrow).

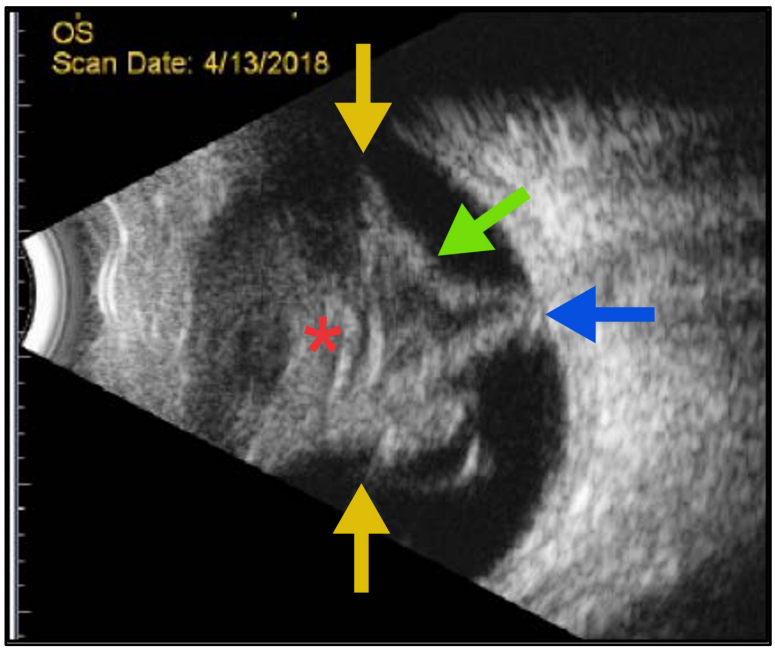

Figure 3.6. B-mode ultrasonograph of the left eye of a 34-year-old male chimpanzee with mature cataract (red asterix) and retinal detachment (green arrow). The retina has a typical "gull wing" appearance where it remains attached at the optic nerve posteriorly (blue arrow) and the ora serrata anteriorly and equatorially (yellow arrows).

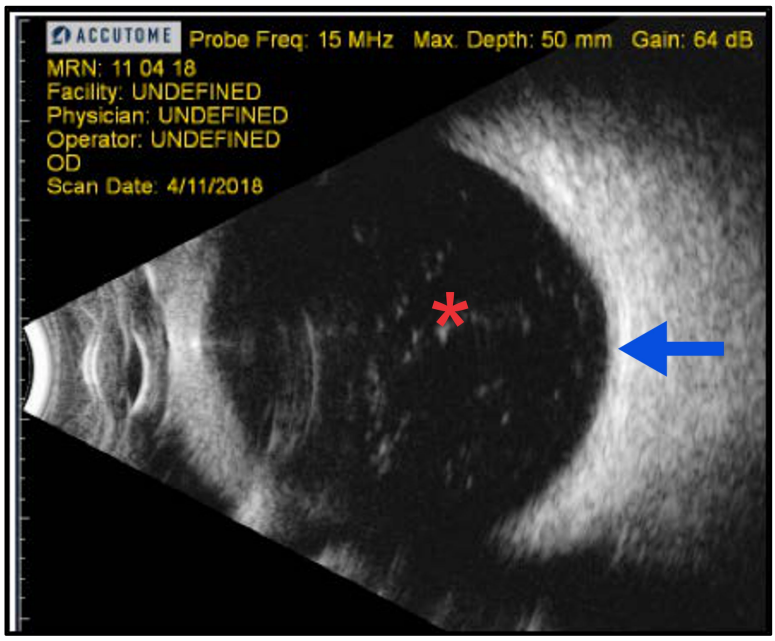

Figure 3.7. B-mode ultrasonograph of the right eye of a 26-year-old male chimpanzee with immature cataract (not readily visible here) and mild to moderate vitreal degeneration (red asterix), but no discernible retinal detachment. The intact retina / choroid / scleral interface is delineated with the blue arrow.

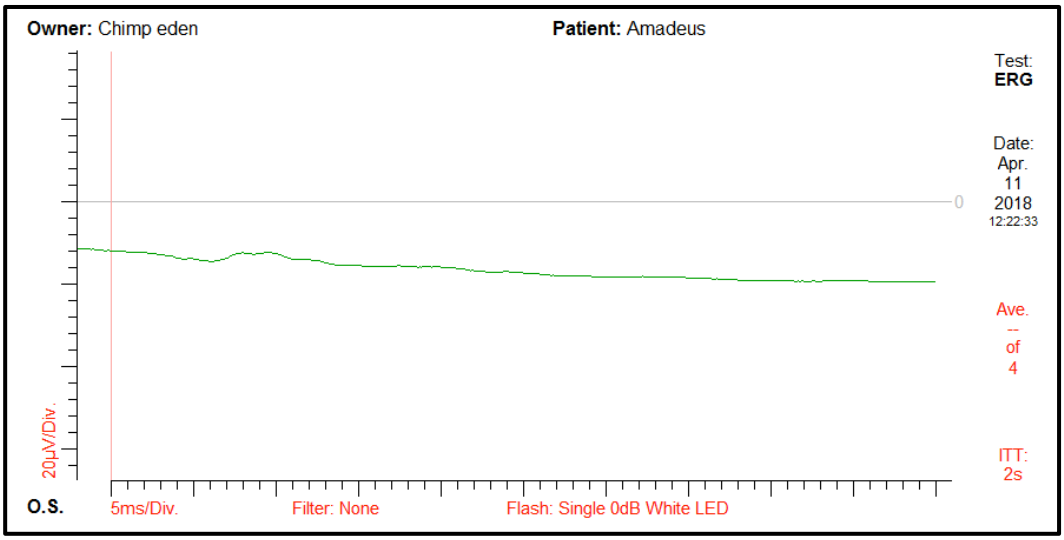

Figure 3.8. Extinguished ("flat line") electroretinogram of the right eye of a 26-year-old male chimpanzee with mature cataract and mild to moderate vitreal degeneration but no discernible retinal detachment on B-mode ultrasonography.

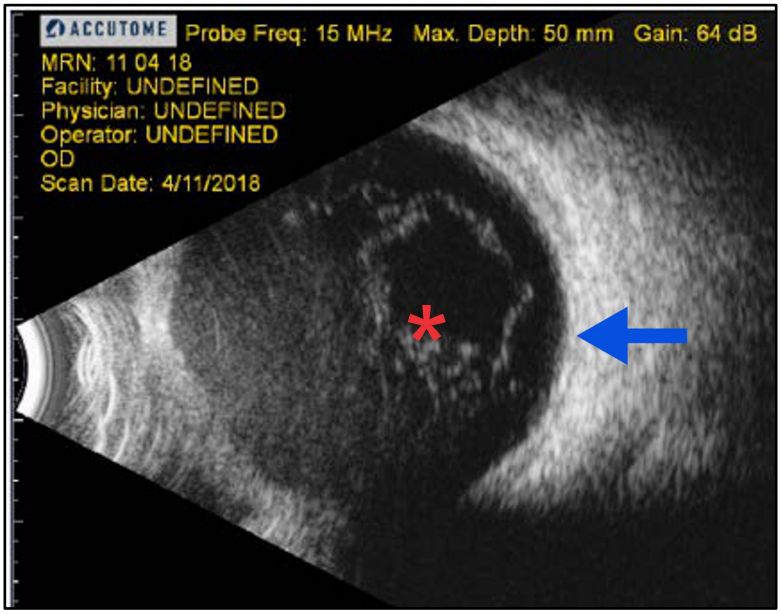

Figure 3.9. B-mode ultrasonograph of the right eye of a 12-year-old pseudophakic chimpanzee, with marked vitreal degeneration (red asterix) consistent with previous intraocular surgery. The intact retina / choroid / scleral interface is delineated with the blue arrow.

3.2. INTRAOCULAR PRESSURE

The tonometric values for right and left eyes utilizing the TonoVet® (on two different manufacturer settings) and the Icare PRO® (in two different recumbencies) are shown in Table 3.3. Mean IOP was 14.34 ± 4.03 mmHg with the TonoVet® on the "P" setting, 22.59 ± 5.34 mmHg with the TonoVet® on the "d" setting and 13.32 ± 3.60 mmHg with the Icare PRO® in dorsal recumbency.

Table 3.3. Mean tonometric values (in mmHg) for right and left eye in 33 captive chimpanzees (*Pan troglodytes*), utilizing the TonoVet® in lateral recumbency on different manufacturer settings and in eight captive chimapzees utilizing the Icare PRO in lateral and dorsal recumbency.

Tonometer and setting / recumbency	IOP right eye	IOP left eye
TonoVet®		
"P" setting	14.69 ± 3.79	13.99 ± 4.33
"d" setting	23.03 ± 4.99	22.15 ± 5.78
Icare PRO®		
Lateral	16.73 ± 3.17	14.33 ± 2.90
Dorsal	13.79 ± 3.73	12.85 ± 3.50

There was no difference noted in IOP obtained with the TonoVet® for age and weight, for either eye, and no difference between left and right eyes. Using a least squares repeated measures regression analysis, a significant difference (P= 0.0173) was identified between males and females, with males having a consistently lower IOP than females, regardless of the setting used (Fig. 3.10). IOP measurements taken on the "P" setting

differed significantly from those taken on the “d” setting (P < 0.0001) in both left and right eyes, with the IOP consistently higher when measured on the “d” setting (Fig. 3.10).

There was no difference noted in IOP obtained with the Icare PRO® for age and weight, for either eye. Using a Wilcoxon signed rank test, a difference was identified between left and right eyes for measurements taken in right lateral recumbency (P= 0.0078), where the right eye (dependant globe / “down” eye) consistently measured higher than the left eye (“up” eye) (Fig. 3.11). A significant difference (P= 0.0173) was identified between males and females, with males having a consistently lower IOP than females, regardless of the recumbency. Recumbency influenced the small subset (n=8) of IOP measurements taken with the Icare PRO® with a difference between dorsal and lateral recumbency (P= 0.0072).

IOP measurements obtained with the Icare PRO® (regardless of the patient´s recumbency) and those obtained with the TonoVet® on the “P” setting did not differ significantly (Fig. 3.10). Further, IOP measurements obtained with the TonoVet® on the “P” setting in lateral recumbency did not differ from those measurements obtained with the Icare PRO in dorsal recumbency (Figure 3.12).

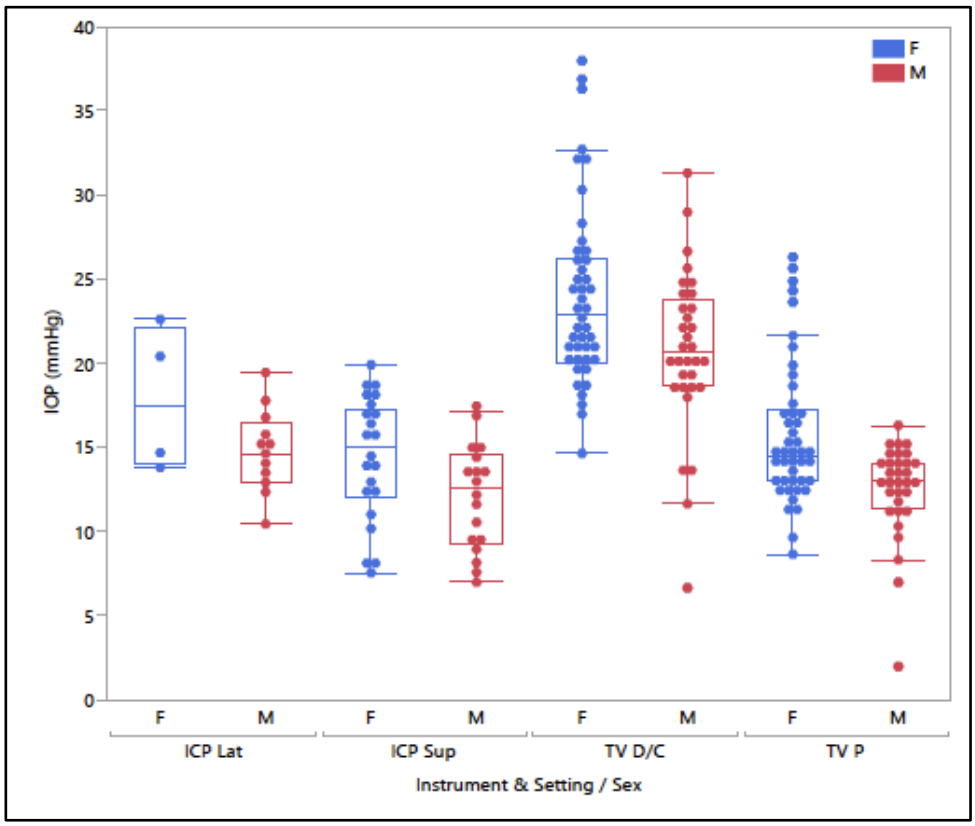

Figures 3.10. Box and whisker plot illustrating the influence of sex, instrument and instrument setting on the intraocular pressure measurement in 33 chimpanzees. Males had consistently lower IOPs than females, regardless of the instrument and instrument setting used. IOP was consistently higher using the TonoVet® on the “d” setting whereas similar values were recorded with the Icare PRO® (regardless of what recumbecy the patient was in) and the TonoVet® on the “P” setting.

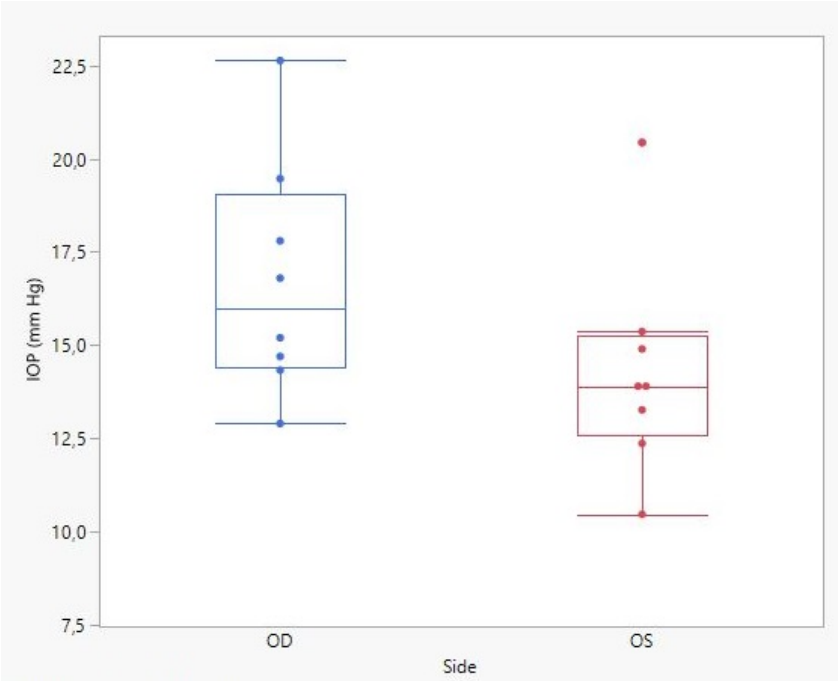

Figure 3.11 Box and whisker plot illustrating the difference between right and left eyes for those IOP measurements obtained with the Icare PRO® in right lateral recumbency. The IOP in the right eye (dependant globe / "down" eye) was consitently higher than in the left eye ("up" eye).

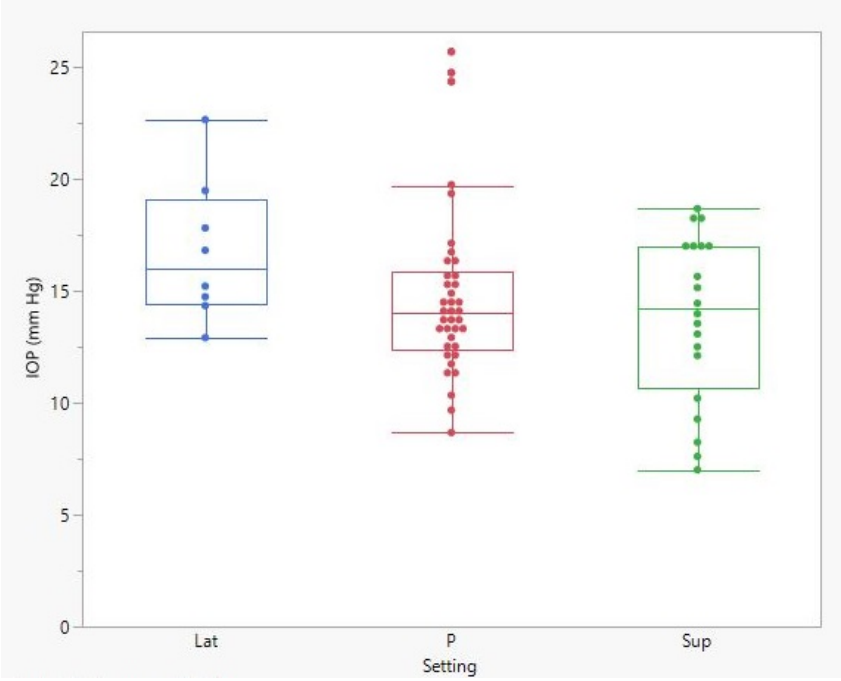

Figures 3.12 Box Whisker plot illustrating the influence of recumbency, where IOP measurements in the right eye obtained with the Icare PRO® in dorsal recumbency (green) differed from those taken with the same instrument in lateral recumbency (red). IOP measurements with the TonoVet® on the "P" setting (obtained in lateral recumbency) (blue) did not differ from those taken with the Icare PRO® with the patient in dorsal recumbency (green).

3.3. KERATOMETRY

Keratometry was performed on 22 chimpanzees (44 eyes). Analysis was then performed on those measurements that fulfilled the previously outlined inclusion criteria (i.e. those where the difference in mean corneal radius (R1R2avg) between eyes was less than 4.5%). Seven chimpanzees did not fulfil this criteria and so analysis was performed on those measurements obtained from the remaining 15 chimpanzees (30 eyes).

Measurements for the horizontal radius / minor meridian (R1) and vertical radius / major meridian (R2) of curvature in the central corneal region (in millimetres) were obtained for both eyes of each chimpanzee and used to calculate the horizontal (K1) and vertical (K2) corneal curvature / refractive power (in diopters). Using these measurements, the average corneal astigmatism was determined (represented as R1-R2 and K1-K2). The mean values ± SD for keratometry in the chimpanzee eye are shown in Table 3.4.

Table 3.4. Mean keratometric values ± SD of 15 captive chimpanzees (*Pan troglodytes*).

Keratometric parameter (unit)	Mean	± SD
R1 (mm)	7.33	0.50
R2 (mm)	6.53	0.48
R1R2avg (mm)	6.93	0.37
Corneal astigmatism (mm)	0.86	0.66
K1 (D)	46.22	3.12
K2 (D)	52.22	3.90
K1K2avg (D)	48.90	2.61
Corneal astigmatism (D)	6.00	4.49

R1, horizontal corneal radius; R2, vertical corneal radius; R1R2avg, average corneal radius; K1, horizontal corneal curvature; K2, vertical corneal curvature; K1K2avg, mean corneal curvature

The mean horizontal corneal radius (R1) was consistently larger than the vertical corneal radius (R2), illustrating an astigmatic corneal curvature, where one axis / meridian of the cornea is steeper than the other. In the case of the chimpanzee, the cornea appears to be flatter horizontally than vertically. No correlation was found between corneal curvature and age, weight or sex. There was no positive correlation between corneal curvature and axial globe length.

3.4. CENTRAL CORNEAL THICKNESS

The mean central corneal thickness (CCT) was 0.45 ± 0.04 mm. No significant CCT differences were determined between right and left eyes and there was no influence of weight, sex or age on the measurements. No correlation was found between intraocular pressure (IOP) and CCT, for either eye (Figure 3.13 A & B).

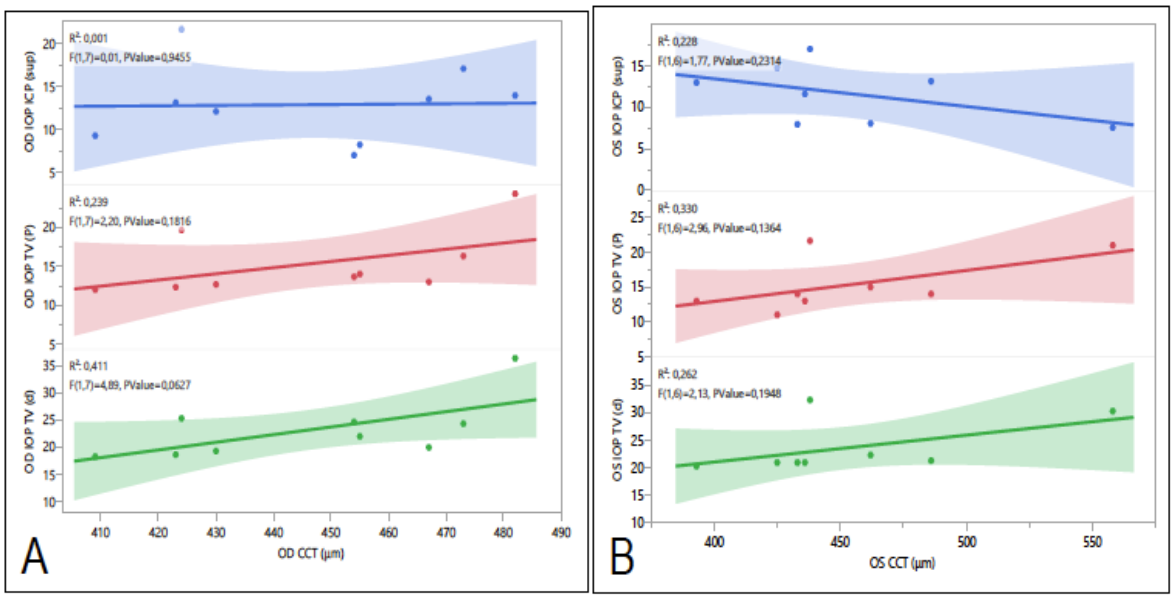

Figure 3.13 A & B. Scatter plots, linear regression lines and 95% confidence intervals for right (A) and left (B) eyes illustrating no correlation between central corneal thickness and intraocular pressure (for the TonoVet® on the "P" and "d" setting and the Icare PRO®).

3.5. BIOMETRY

The mean A-scan biometric measurements for axial globe length (AGL), anterior chamber depth (ACD), crystalline lens thickness (LT) and posterior segment depth (PSD) are summarised in Table 3.5 below. There was no significant difference between right and left eyes and no influence of sex, age or weight on the measurements.

Table 3.5. Mean A-scan ocular biometric measurements for 11 captive chimpanzees (*Pan troglodytes*). Values for right and left eyes have been combined, since there was no statistical difference between eyes.

Biometric measurement	Mean (mm)	± SD (mm)
Axial globe length	21.41	0.76
Anterior chamber depth	3.63	0.47
Lens thickness	3.81	0.68
Posterior segment depth	13.98	1.00

B-scan biometry was performed on 13 chimpanzees. The measurements were performed in two scanning planes, horizontal (9 and 3 o´clock) and vertical (12 o´clock) planes. Using an ordinary least squares regression model, there was no difference identified in measurements regardless of the scanning plane utilized (Fig. 3.14).

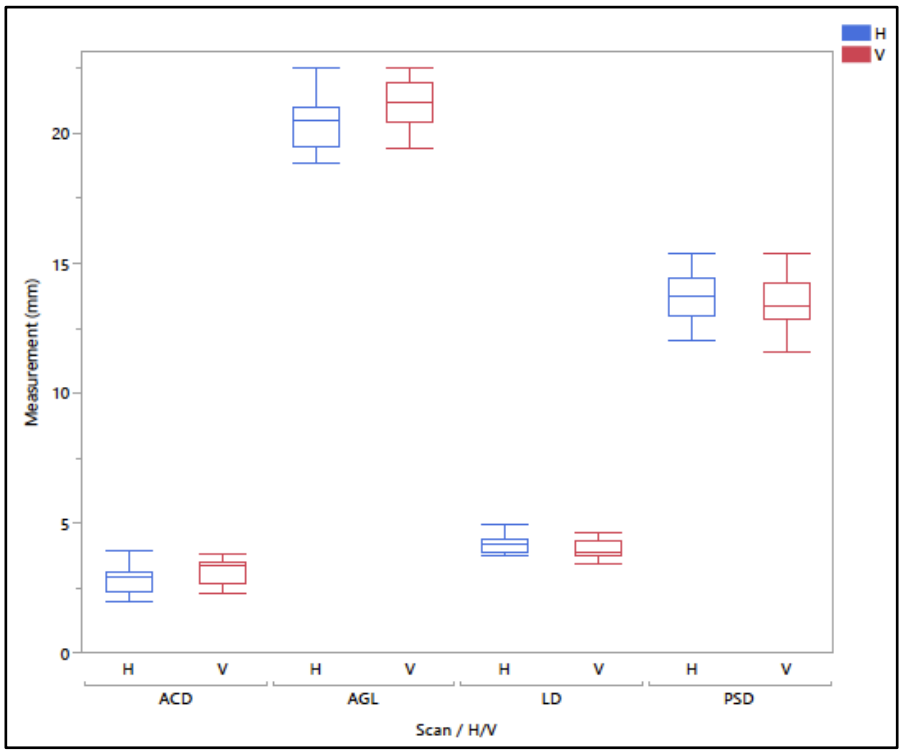

Figures 3.14. Box and whisker plot of the B-mode ultrasonography ocular biometric measurements obtained using two different scanning planes, horizontal (H) and vertical (V). ACD: Anterior chamber depth, AGL: Axial globe length, LD: Lens depth, PSD: Posterior segment depth.

3.6 INTRAOCULAR LENS POWER CALCULATION

Intraocular lens power was calculated for 16 healthy eyes (10 chimpanzees) where required biometric (axial globe length and crystalline lens thickness) and keratometric (corneal curvature "K" in diopters and radius of corneal curvature "r" in millimetres) measurements were available. Eyes which had full sets of measurements but where ocular pathology had been identified (two adult males with unilateral mature cataracts and one adult male which was unilaterally pseudophakic) were excluded from the calculations. The Binkhorst and Retzlaff theoretical formulae were used to calculated the required intraocular lens (IOL) power to approximate emmetropia, and were performed for each of the 16 eyes and then averaged to give an overall mean IOL dioptric strength (± SD) for this species. Predicted post-operative anterior chamber depth (PACD) was calculated as the ACD plus 50% of the lens thickness. To account for variable terminal IOL positions and evaluate the effect of post-operative IOL position on refraction, additional calculations using PACD -2mm and +2mm were performed. IOL power calculations are summarised in Table 3.6.

Table 3.6. Mean calculated intraocular lens power for the chimpanzee, using Retzlaff and Binkhorst theoretical formulae, at different predicted postoperative anterior chamber depths (PACD).

	Retzlaff theoretical formula (diopters ± SD)	**Binkhorst theoretical formula (diopters ± SD)**
***PACD**	21.86 ± 5.73	22.81 ± 5.79
***PACD -2mm**	17.71 ± 4.59	18.51 ± 4.65
***PACD +2mm**	27.67 ± 7.36	28.83 ± 7.43

* Predicted post-operative anterior chamber depth = anterior chamber depth plus 50% of lens thickness

CHAPTER 4. DISCUSSION

4.1 OCULAR FINDINGS

In a recent comprehensive comparative pathology review on aging great apes (including chimpanzees), ophthalmological pathology was identified by the authors as an area needing further investigation [12]. The biggest survey reporting on ophthalmic lesions in non-human primates to date was published almost five decades ago, and included results from 35 laboratory chimpanzees [206]. In contrast to our findings, the most common ocular lesion observed in the 1971 study was traumatic corneal abrasion (10/35 chimpazees) [206], while only a single corneal abrasion was identified in our study. Although similar in numbers of chimpanzees examined, the 1971 study´s mean population age was 9.5-years-old [206], whereas the mean age of our study population was double that at 18.55-years-old but with a large standard deviation of 12.12-years-old. This large deviation is owing to our population having one very young individual (two-year-old) and reportedly the oldest living captive chimpanzee in the world (at an estimated 73-years-old). Further, while details of the environment in which these laboratory chimpanzees were kept was not detailed in the 1971 publication, if these laboratory chimpanzees were kept separately, restricted in small cages, with minimal environmental enrichment, they may have spent more time up against the bars of their cages, possibly fighting or reaching through the bars, increasing the risk for corneal trauma. Self-trauma due to stress, the inabilty to exhibit normal behaviour, and a lack of social interaction and mental stimulation may have also been a contributing factor in the eitiology of traumatic corneal abrasions. The chimpanzees in our study were kept semi-wild in large outdoor enclosures within “family groups” with the freedom to express natural behaviour and were only restricted in smaller indoor encloures at night.

Continuous circumferential perilimbal white corneal stromal deposits of varying density were observed bilaterally in 13 chimpanzees. A recent study first described this observation in chimpanzees, classifying the white deposits as “lipid” since it resembled a condition in humans called *arcus senilis* or *arcus lipoides* [210]. *Arcus senilis* (AS) refers to a lipid deposit in the peripheral cornea of humans that is typically asymptomatic [211]. Sigmund *et al.* (2020) identified these corneal deposits in seven of the ten chimpanzees in their study group and decided it was likely an age-related change, since the mean age of their population was 31-years-old and the average lifespan for a chimpanzee in captivity is approximately 25 years for males and 34 years for females [12, 210]. Our study does not show this to be necessarily simply an age-related change in chimpanzees. Eight of the 13 chimpazees with this finding were under 20 years of age (including three 11-year-olds), while five chimpanzees over 20 years of age (including a 30-year-old male) did not display this finding. Human males are over-represented in AS compared to females. In our study group, 46% of male chimpanzees were affected while 35% of females were affected. Smoking is a known risk factor for AS in humans [211]. Interestingly, four of the five chimpanzees that were known active smokers prior to their rescue

and rehabilitation, displayed these corneal deposits. Familiar hypercholesterolemia is a potential cause of AS in humans but no chimpanzees in our study had raised cholesterol. Systemic hypertension is another known risk factor for AS but concious blood pressure monitoring could not be perfromed in these animals.

Bilateral senile corneal degeneration was suspected in a 73-year-old male chimpazee in our study. The only reports on corneal pathology in chimpazees include corneal abrasions in ten laboratory chimpazees in the USA [206], one chimpanzees with unilateral diffuse dystrophic corneal stromal mineralisation and fibrosis [210], and chronic suspected solar / UV-induced keratitis in 16 captive chimpanzees in Kenya [224]. Since the affected chimpanzee in our study did not present with ocular discomfort or visual deficits, keratectomy and histopathology was not indicated and thus a definitive diagnosis was not made. The presumed aetiology was based on the clinical appearance, bilaterally symmetrical nature, absence of vascularisation and signalment of the patient.

In decreasing order of incidence, this study showed vitreal degeneration (four chimpanzees), dyscoria (three chimpanzees) and cataracts (two chimpanzees) to be the most common pathologies in this group of captive chimpanzees. The 1971 study reported cataracts in one chimpanzee but did mention the aetiology nor did they specify whether these cataracts were bilateral or unilateral [206]. Cataracts were not an uncommon finding in aging great apes, including chimpanzees, orangutans and gorillas [12]. Despite being most often age-related, cataracts were reported in young gorillas and orangutans [10, 31, 32]. Leiva et al. reported of a 29-year-old chimpanzee with a unilateral mature cortical cataract [31], a similar age and presentation to the two affected individuals in our study. The cataracts identified in this study are likely traumatic in nature based on history of ocular injury after a fight with a fellow chimpanzee, their unilateral presentation, and accompanying retinal detachment in one case, and lack of retinal function in another case. One pseudophakic chimpanzee that had previously undergone cataract surgery was also originally presented with a unilateral cataract with a history of ocular injury post fight. All these three chimpazees were males and it appears that males are more likely to sustain serious vision-threatening ocular trauma as a result of intra-species aggression, likely due to social hierachy disputes. Dyscoria secondary to uveitis caused by ocular coccidiomycosis was reported in a 12-year-old female chimpanzee [207]. We report on three cases of dyscoria (this study). Two of these were caused by posterior synechiae that developed secondary to lens-induced uveitis from suspected traumatic cataracts. The dyscoria in the third case was caused by an entraped haptic from a subluxated intraocular lens post cataract surgery.

A 73-year-old male chimpazee presented with marked bilateral nuclear sclerosis. Nuclear sclerosis is a normal age-related change of the mammalian lens where the central nucleus portion becomes increasingly dense [225]. Nuclear sclerosis has been reported in three geriatric captive chimpanzees (of ages 35, 40 and 42 years) with the oldest male (40-years-old) exhibiting a brunescent hue to his lenses [210].

This study confirmed retinal detachment in association with a cataract in one individual (via B-mode ultrasonography), and suspected this finding in a second individual (based on electroretinography recordings). Both these male chimpanzees had historically sustained injury to their globes and had presumed traumatic cataracts. The retinal detachments were thus presumed to be traumatic in origin (blunt-force trauma) or secondary to phacolytic uveitis (lens-induced uveitis) from cataract formation. Retinal detachment has previously been reported in one chimpanzee (not associated with cataract) where ophthalmoscopy was possible, although the authors did not speculate as to the aetiology of the cataract [206]. Ophthalmoscopy was only successfully achieved in four chimpanzees in our study, as animals were not routinely pharmacologically dilated. B-mode ultrasonography was thus the modality used to assess the posterior segment in this study. Both animals with presumed retinal detachment had marked cataractous lenticular changes which precluded ophthamoloscopy. While the one case had obvious retinal detachment evident on B-mode ultrasonography, the other case had no discernable retinal detachment and the only appreciable posterior segment abnormality was a mild to moderate vitreal degeneration. The suspected retinal detachment diagnosis in this individual was based on extinguished electroretinography recordings which were carried out to assess whether this individual would be a suitable candidate for cataract surgery. A loss of retinal function could be expected in cases of retinal detachment, glaucoma and uveitis / chorioretinitis. It is possible that the retina could have detached at the time of trauma and later reattached as concomminant intraocular inflammation resolved. Bilateral retinal detachment has been reported in a 34-year-old female western lowland gorilla secondary to malignant hypertension [215].

Incidental observations in our study included dense limbal conjunctival and iridal melanosis. The limbal melanosis has previously been described in gorillas [11] but the author is not aware of any mention in the literature regarding iridal melanosis in other great apes. All chimpanzees examined had lightly to darkly pigmentated bulbar conjunctiva. This same finding was observed by Sigmund *et al.* (2020) and indeed has been noted in all nonhuman primate species, humans being the only primate species to display a nonpigmented conjunctiva [210].

A further incidental finding was that of mild bilateral iridal hypoplasia in a 13-year-old female chimpanzee. Hypoplasia is a congenital underdevelopment of an organ or tissue that may be induced by decreased neural crest induction or migration, while a coloboma represents a defect due to an absence of tissue as a result of a failure of induction of cellular development [226]. Mild iridal hypoplasia generally has no major clinical relevance, except that in this chimpanzee, her keepers had noted that she was more sensitive to bright light, exhibiting mild photophobia, for which no other pathological ocular finding (for example uveitis) was identified.

The major limitation of the ophthalmic examination in this study was that fundoscopy was not consistently performed, largely due to miosis and globe rotation. The chimpanzees were not routinely pharmacologically dilated due to time constraints and the concern that previously dilated individuals had suffered from

intraspecies aggression during recovery from general anaesthesia. The ophthalmic examinations in this study were performed opportunistically but I would recommend that if assessing a chimpanzee specifically for ocular pathology, pharmacological dilation, to prevent miosis, and avoidance of isoflurane anaesthesia, to prevent globe rotation, would be preferable. Alpha-2 adrenergic agonists (such as medetomidine used in this study) can cause marked miosis. Sigmund *et al.* (2020) reported a protocol which provided adequate mydriasis for evaluation of the fundus in all cases [210]. Four applications of tropicamide 1% every 5 minutes was recommended. Further, these authors found normal eye positon was maintained using a sedation protocol of ketamine, midazolam and dexmedetomidine [210].

4.2. INTRAOCULAR PRESSURE

Mean intraocular pressure (IOP) measurement obtained in this study (n= 33), using the TonoVet® on the "d" setting with the anaesthetised chimpanzee in lateral recumbency is similar to that reported by Milnes *et al.* (2020) in the non-dependant eye of the anaesthetised chimpanzee (n= 21) in lateral recumbency taken with the same instrument, on the same setting [52]. Sigmund *et al.* (2020) reported a mean IOP of 14 ± 4.2 mmHg in 10 anaesthetised chimpanzees in dorsal recumbency, although two different modalities were used to obtain these readings (seven with applanation tonometry, three with rebound tonometry) [210]. The three cases were rebound tonometry was used had higher IOP readings. Their mean IOP with predominantly applanation tonometry is similar to the mean IOP measurements obtained in this study with the TonoVet on the "P" setting (14.34 ± 4.03 mmHg) and the Icare PRO (13.32 ± 3.60 mmHg). The findings of the Milnes, *et al*. (2020) study and the Sigmund *et al.* (2020) study were not published at the time of the primary investigator conducting this study.

While Milnes et al. (2020) determined body position to be an important consideration and noted that in lateral recumbency, the dependant eye recorded a consistently higher IOP [52], the statistical analysis of the IOP measurements obtained in our study did not support this finding. This trend of lateral recumbency increasing pressure in the dependant eye was only noted in our study using the Icare PRO® rebound tonometer, however, this instrument was only used in eight chimpanzees in lateral recumbency. Milnes *et al*. (2020) proposed changes in episcleral venous pressure in the dependant eye as the likely cause [52]. Systemic blood pressure, head position and pressure on the neck can all affect episcleral venous pressure and in turn cause increases in the dependant eye of the patient in lateral recumbency [117]. While in both this study and the one by Milnes *et al*. (2020) the chimpanzees were positioned in lateral recumbency, differences in the head position and angle of the neck could account for the described differences. For IOP measurement in lateral recumbency the chimpanzees in our study had a rolled-up towel placed under their head to keep their neck straight.

This study describes an influence of sex on IOP measurement, with male chimpanzees having consistently lower IOP than female chimpanzees. Young and Farrer (1964) reported no sex difference in IOP in 43 chimpanzees [29], while the effect of sex was not explored in the study by Milnes *et al.* (2020) [52]. In humans, IOP in females tends to be higher than in males [227, 228]. There are a number of hypotheses to explain this gender-related difference in IOP [100]. Anatomical differences in the female globe (shorter axial length and steeper corneas) have been proposed to lead to increased IOP in females compared to males [227]. Systemic hypertension has also been proposed as a cause of this gender-related difference [228]. The most prevailing hypothesis however is that the gender-related IOP differences are as a result of fluctuations in levels of sex hormones [100]. Administration of progesterone decreases IOP [229]. IOP decreases during pregnancy due to increased outflow of aqueous humor from the eye [230, 231]. Excess progesterone during pregnancy is thought to block the ocular hypertensive effect of endogenous corticosteroids [230]. A study evaluating the influence of hormone therapy (oestrogen-only and oestrogen-progesterone therapy) on IOP in postmenopausal women, showed mean IOP in the hormone therapy group to be significantly lower than in the group not receiving hormone therapy. Furthermore, there was no difference in the mean IOP between women taking combined (oestrogen-progesterone) versus oestrogen-only therapy [232].

Inter-species differences exist in regards to the effect of progesterone on IOP [100]. While progesterone decreases IOP in the human, it increases IOP in the rabbit [233-235], lion [100] and domestic cat [101]. In 1998, Ofri *et a*l. reported higher IOP in male lions than in females. They postulated that the fluctuations in the level of sex-hormones were likely the cause [103]. In 1999, the same group had the opportunity to reassess the same animals (once they were sexually mature) and on this occasion tested levels of progesterone, oestrogen and testosterone [100]. In this second study, elevated progesterone was associated with increased IOP in luteal female lionesses compared to males and immature females, while oestrogen and testosterone had no effect on IOP [100]. The same group later explored the effect of reproductive status on IOP in domestic cats and found that female cats in oestrus had significantly higher IOP than female cats not in oestrus and that progesterone concentrations significantly affected IOP in pregnant cats [101].

The female chimpanzees in our study population had long-acting subdermal contraceptive implants (Implanon™), since Chimp Eden is a non-breeding rescue and rehabilitation facility. These implants contains the synthetic progestogen, etonogestrel. Etonogestrel exerts its contraceptive action by down-regulating the gonadotropin releasing hormone (GnRH) surge centre, which in turns prevents luteinising hormone (LH) surge and ovulation. Having this continuous progestogen secretion seems to be a plausible explanation as to why the female chimpanzees in our study had consistently higher IOP than the males. Measurement of sex hormones was beyond the scope of this study but this should be considered in future studies on chimpanzees.

This study demonstrated a definite effect of instrument and instrument setting on measured IOP. Thus far, IOP for the chimpanzee has only been reported using the Schiotz tonometer [29], the Tono-Pen AVIA VET applanation tonometer [210] and the TonoVet® rebound tonometer on the "d" setting [52]. The IOP for the chimpanzee using the Icare PRO® is reported for the first time in this study. The Icare PRO® is a rebound tonometer calibrated for humans with the major advantage of being able to measure IOP in supine (dorsally recumbent) patients, which is typically how chimpanzees are positioned under anaesthesia. Despite the instrument not being calibrated for the chimpanzee, the primary investigator postulates that since these primates share >98% of their DNA with humans [3] and are man's closest living relative, this instrument may give an accurate IOP reading in this species.

We further report on the IOP using the "P" setting of the TonoVet® . This setting is adjusted human calibration that is not tested for animal use and is used for servicing the instrument [236]. Since the TonoVet® is only calibrated for dogs, cat and horses, when used on other species, the common approach is to use the setting closest to the eye size of the patient. Again, due to the close similarity of chimpanzees and humans, the primary investigator decided to use the "P" setting of the TonoVet® and compare it to the Icare PRO® readings and "d" setting TonoVet® readings. As anticipated, "P" setting values were close to Icare PRO® readings, while "d" setting readings were different (and higher). The only way to definitively prove which instrument and setting yields the most representative IOP reading for this species would be to perform manometry on the chimpanzee globe. Manometry is an invasive technique and was not ethically justifiable in the live animals in our study. Further, we did not have any deceased animals for us to perform manometry on enucleated globes. Based on the findings in this study, the primary investigator would recommend the use of the Icare PRO® on chimpanzees, since the instrument allows for the measurement of IOP in dorsally recumbent patients. The use of the "P" setting can also be recommended using a Tonovet and is suspected to give a more accurate reading than the "d" setting.

General anaesthesia is known to affect IOP readings, since sedative and anaesthetic drugs can influence IOP by altering the rate of aqueous humor production or outflow and/or by the extent of relaxation of the extraocular and eyelid muscles [119]. Aside from ketamine [25, 103, 120], all agents commonly used to induce general anaesthesia in veterinary medicine lower IOP [121]. Tiletamine-zolazepam (Zoletil®) have no significant effect on IOP in both dogs [125] and cats [120]. Although Milnes et al. (2020) did anaesthetise their study population with two different anaesthetic protocols (tiletamine-zolazepam combined with medetomidine and tiletamine-zolazepam alone), their small sample size precluded statistical analysis [52]. Young and Farrer (1964) did describe lower IOP readings in anaesthetised chimpanzees (16.2 ± 3.98 mmHg) compared to awake chimpanzees (18.4 ± 4.75 mmHg), however it is difficult to draw comparisons with this study since the anaesthetic agent used was pentothal sodium, the IOP was measured with a Schiotz tonometer, and the animals were all young laboratory chimpanzees [29]. Since chimpanzees need to be anaesthetised to conduct

ophthalmic examinations, the primary investigator believes that the tonometry values obtained in this study will serve as useful reference values in the clinical setting.

A limitation of this study with respect to IOP measurement was that the IOP readings were taken throughout the day, due to the opportunistic nature of this study. The effect of circadian rhythm on IOP has been well described in the literature and the primary investigator is aware of the importance of consistency in terms of time of day when recording IOP [104-108]. Intraocular pressure is increased in the early morning and decreased in the afternoon or evening in humans [110-112] and nonhuman primates [113, 114] . Central corneal thickness is positively correlated with IOP, displaying a similar diurnal variation [107, 111, 112, 115].

4.3. KERATOMETRY

The mean keratometry reading in the chimpanzee (48.9 ± 2.61 D) was higher than that of both gorillas (44.38 ± 1.64 D) [11] and humans (43 D) [237]. No positive correlation was found between age and corneal radii, as reported in horses [129, 161]. Weight and sex also did not influence the keratometry reading in this study. There was no correlation between corneal curvature and axial globe length, as described in humans and horses. [238] [37]

Corneal astigmatism in the subset of the population examined (n= 15) was marked at 6.00 ± 4.49 D. However, this degree of astigmatism does not represent the true picture as astigmatism determined with keratometry is derived only from measurements of the central (3-4 mm in diameter) anterior corneal curvature and does not take into account the effects of the posterior corneal curvature, lens and axial globe length [130]. This is a limitation inherent to keratometers. In physician-based ophthalmology the posterior corneal curvature partially compensates for anterior corneal astigmatism, thereby reducing total corneal astigmatism [239].

Another limitation of the keratometer is that it is not able to evaluate irregular astigmatism because it assumes the cornea has a symmetrically spherical shape [130]. While the keratometer only measures major and minor meridans at right angles to one another [130], the astigmatism may affect an axis which is not orientated perpendicularly.

Despite keratometry being performed on 22 chimpanzees (44 eyes), the statistical analysis was only performed on a subset of these measurements, in an attempt to address intra-operator variability (as previously outlined in our exclusion criteria in Chapter 3). In a recent study, possible measurement errors were identified as a major limitation of performing automatic hand-held keratometry on veterinary species [130]. Readings from individuals were the difference in R1R2avg between right and left eyes was greater than 4.5% were excluded [130]. This 4.5% cut-off value was based on a preliminary study of intra-operator variability conducted by the same authors [130]. The same approach was followed when deciding the inclusion criteria for

keratometry measurements in this study, and resulted in the measurements of seven chimpanzees not being included in the statistical analysis, which made our sample size small.

Inaccurate readings and measurement failure can result from distortion of the mire rings reflected on the corneal surface. Since the instrument is hand-held, an unsteady hand of the operator can result in this distortion. Despite the subjects in this study being immobilised under general anaesthesia, the prominent supraorbital crest made it challenging in many cases and impossible in certain individuals to position the instrument close enough to the cornea and at the correct angle to achieve an accurate reading. Dorsal rotation of the globes made it difficult to assess the eyes and may have also contributed to the inaccurate readings.

To address the discussed limitations inherent to keratometers, future studies should consider using more sophisticated imaging modalities, such as corneal topographers (photokeratoscopy) and anterior segment optic coherence tomography [130]. There are some studies in the veterinary literature reporting keratometric values obtained using the Pentacam® HR topographer (rotating Scheimflug camera) in dogs [240], cats [241] and rabbits [242].

4.4 CENTRAL CORNEAL THICKNESS

This study is the first to report central corneal thickness (CCT) in the chimpanzee. There was no influence of age on CCT, contrary to reports in humans [134] and dogs [94]. Weight or sex did not affect the measurements and no difference found between right and left eyes. No relationship was found between central corneal thickness and intraocular pressure in this study, similar to findings reported in canines [94] and penguins [66].

CCT in the chimpanzee (0.45 ± 0.04 mm) is most similar to that of capuchin monkeys (0.46 ± 0.03 mm) [30], gorillas (0.49 ± 0.05 mm) [11], humans (0.52 mm) [243] and cynomolgus macaques (0.38 ± 0.02) [54]. It has an important influence on tonometry since estimated IOP values obtained with rebound tonometry depend on the biomechanical properties of the cornea [154, 155], and this close similarity of chimpanzee CCT to that of humans suggests that a tonometer calibrated for humans would be appropriate to use on chimpanzees. In contrast, the CCT of the dog (0.56 ± 0.01 mm) [136] and cat (0.58 ± 0.6 mm) [137] are considerably thicker. This would explain why an instrument calibrated to work on a thicker cornea ("d" seting on the TonoVet) would yield an elevated value when used on a thinner cornea.

There are limitations in this study pertaining to CCT measurement. Pachymetry was only performed on 11 chimpanzees due to limited availability of the loaned Accutome 4Sight® unit. It is possible that relationships between CCT and age or IOP may have been detected with a larger sample size. In this study, pachymetry was performed in dorsal recumbency for the sake of expediency, which has been shown to increase CCT in

humans [40]. A further limitation was lack of consistency in terms of time of day when pachymetry was performed, due to the opportunistic nature of this study. The primary investigator acknowledges that diurnal variations (decreased CCT in the afternoon/evening compared to the morning) have been described in the literature *[107, 108, 111, 112, 148, 149]*.

4.5. OCULAR ULTRASONOGRAPHY & BIOMETRY

This study is the first to report the ocular biometry of the chimpanzee. Axial globe length (AGL) in the chimpanzee (21.41 ± 0.76 mm) is less than that of both gorillas (22.75 ± 0.71 mm) [11] and humans (23.6 mm) [244-246]. A seven-year-old western lowland gorilla that underwent A-scan ultrasonography prior to cataract surgery had a reported AGL very similar to our average chimpanzee AGL, of 21.0 mm [10]. Anterior chamber depth (ACD) in the chimpanzee (3.63 ± 0.47 mm) is shallower than that of the gorilla (4.00 ± 0.26 mm) [11] but both have deeper ACD's compared to humans humans (3.24 ± 0.44 mm) [244]. Finally, the crystalline lens thickness in the chimpanzee (3.81 ± 0.68 mm) is less than both the gorilla (4.23 ± 0.34 mm) [11] and the human (4.63 mm) [244, 247]. Establishing this baseline data for the chimpanzee is of important clinical value in order to determine lens implant size, intraocular lens power prediction, and estimating prosthetic globe size following enucleation [170]. It is also of diagnostic importance for clinical ultrasonography as ocular pathology may result in derangements of ocular measurements.

Biometric measurements obtained with A- and B-scan ultrasonography correlated well with each other in our study, similar correlations have been reported for dogs[180], horses[129] and caiman[181]. This is an important finding since A-scan ultrasonography is less readily available in veterinary medicine than B-scan ultrasonography. In this study however, A-scan ultrasonography proved invaluable for establishing the standard biometric measurements for the chimpanzee globe, as not all measurements were always achievable with B-scan ultrasonography. Axial globe length and anterior chamber depth were readily measured on B-scan ultrasonography, in both horizontal and vertical scanning planes. It was the primary investigators experience however, that the thin posterior lens capsule was more often than not, not visualised on B-scan ultrasonography. This precluded measurement of the crystalline lens thickness and posterior segment depth in many individuals and appeared to be more often the case in the horizontal scanning plane than in the vertical scanning plane. In some instances, neither the anterior nor the posterior lens capsule was imaged on B-scan ultrasonography. This may have been a result of the scanning plane being altered from trans-corneal to partially trans-scleral when the globes were partially rotated as an effect of the general anaesthesia. Scanning in the trans-scleral plane avoids the lens and provides a higher resolution of the ocular fundus [170].

Two major limitations exist in this study regarding ocular biometry of the chimpazee. Firstly, only 11 chimpanzees underwent A-scan ultrasonography. This small sample size was due to the availability of the

loaned Accutome 4Sight® unit. Secondly, since optimal ultrasound velocities in chimpanzee eyes have not been reported, this study used the ultrasound velocity established in physician-based ophthalmology [186, 223] and the default setting on the Accutome 4Sight® unit. A future study could establish the optimal ultrasound velocity of the lens and vitreous in chimpanzees, as has been determined in veterinary ophthalmology for the dog [188, 189], horse [185], camel [164, 190], pig [189] and rabbit [189]. While no interspecies difference in the aqueous or vitreous has been noted thus far, ultrasound velocity of the lens has shown considerable variability between species [185]. Ultrasound velocity of the lens will affect the measurement of lens thickness, an important measurement used in the Retzlaff and Binkhorst theoretical formulae to determine intraocular lens power [185].

4.6 INTRAOCULAR LENS POWER

The need for IOL in chimpanzees have been mentioned before[31]. Although we are seeking to report a single dioptric strength for the chimpanzee, it is still recommended to perform these power calculations for each individual where possible, if the required equipment (A-scan ultrasonography and keratometry) is available, since intraspecies variability has been reported in the gorilla [11].

This study is the first to report the calculated IOL lens power for the chimpanzee, using the Retzlaff (21.86 ± 5.73 D) and Binkorst theoretical formulae (22.81 ± 5.79 D). This suggests that an IOL of approximately 22.0 D would be a good choice to approximate emmetropia in the chimpanzee. The only report in the English literature that the author is aware of where an IOL was placed post phacoemulsification in a chimpanzee, was by Levia *et al.* (2012) where a +19.0 D non-foldable polymethylmethacrylate (PMMA) (6mm optic) lens was implanted into a 29-year-old female chimpanzee [31]. Ultrasound biometry and keratometry was not performed in this animal. The chimpanzee was reported to have a good visual outcome (with a follow-up time of 108 months) but was not refracted post-operatively [31].

The same authors reported on bilateral phacoemulsification in a gorilla where ocular biometry and keratometry was performed. A +19.0 D foldable acrylic (6mm optic) IOL was inserted in the right eye and a + 20.0 D foldable acrylic (6mm optic) IOL was inserted in the left eye, although details with regards to what theoretical formula was used to calculate these lens powers was not included in the manuscript [31]. In a different study, two captive-born western lowland gorillas underwent bilateral phacoemulsification where pre-operative A-scan biometry and keratometry were performed and IOL power for each individual animal was determined using the SRK2 formula [10]. The 7-year-old male gorilla had his right eye operated first and the surgeons deliberately selected a lens that they estimated would leave this juvenile animal slightly (+1.5 D) hyperopic as they anticipated a myopic shift as the animal grew and the axial length of the eye enlarged [10]. However, post-operative retinoscopy revealed a hyperopia of +3.0 D [10]. As a result of this outcome, the +24.0 D IOL was selected for the left eye to aim for emmetropia [10]. A 17-month-old male gorilla had +23.0 D and +25.0 D IOLs implanted in his right and left eyes respectively and the authors reported a good visual

outcome, although no post-operative refraction was reported for this second animal [10]. In yet another study bilateral phacoemulsification with IOL implant was reported in a 6-year-old male orang-utan where a +21.5 D foldable acrylic (6mm optic) IOL was implanted bilaterally [31]. This animal did not have pre-operative ultrasound biometry and keratometry performed, nor was he refracted post-operatively [32]. The authors reported a good visual outcome in this animal [32].

The estimation of predicted post-operative anterior chamber depth (PACD) has a marked effect on the Retzlaff and Binkhorst theoretical formulae and must be recognised as a limitation of this study. If we take into account the possible effect of the terminal IOL position, the powers for the chimpanzee range from 18.0 – 28.0 D. The estimation of predicated post-operative anterior chamber depth (PACD) accounts for this large deviation. This study followed the same approach to PACD as has been most commonly reported in the veterinary literature, reporting the dioptric strength for the Retzlaff and Binkhorst theoretical formulae using a PACD of +2mm and -2mm [35, 36, 39]. Perhaps a better approach to estimating PACD for future studies would be to determine the mean preoperative-to-postoperative ACD ratio for the chimpanzee, as was determined for the horse [204].

Four studies that have explored IOL power for the horse differed significantly from each other, the earlier studies reporting an IOL strength of approximately 30.0 D to achieve emmetropia [36, 201] and the later studies confirming that an 18.0 D IOL was the most appropriate to achieve emmetropia in this species [37, 204]. This difference could be attributed, in part, to the different PACD that were used in the power calculations, since the first study estimated the PACD as was done in our study (i.e. PACD = ACD + 50% LT), while a later study determined the specific preoperative-to-postoperative ACD ratio for the horse [204] and the most recent study used this ratio in their power calculations [37]. In our study, we were not able to determine the mean preoperative-to-postoperative ACD ratio for the chimpanzee, as we did not have suitable pseudophakic individuals in our population that we could compare pre- and post-operative A-scan biometry. We did have one pseudophakic individual in our study population, but he was not an appropriate candidate to assess for this purpose since his intraocular lens had luxated anteriorly into the anterior chamber. Kuhn et al. (2015) were in a similar position with not having suitable post-operative phacoemulsification patients with IOL implants, but did describe measuring from cornea to the location of the capsular bag in aphakic patients [38]. Unfortunately, this was also not a viable approach in our study, since we had no aphakic individuals. Further studies evaluating pseudophakic refraction and determination of actual PACD in the chimpanzee are required.

A further limitation was the use of older IOL formulae and the equipment used to obtain the biometric measurements. While A-scan contact ultrasound ocular biometry and automated keratometry (as used in this study) has been considered the gold standard for decades, several noncontact optical-based devices generate more accurate results [126, 127, 248-250]. Due to the very nature of the technique, contact applanation biometry invariably leads to errors in measurement of axial globe length and anterior chamber depth due to

indentation of the cornea by the probe and thus shallowing of the anterior chamber [126, 127]. The use of these measurements typically leads to an underestimation of the IOL power [126]. For this reason, immersion biometry is preferred over contact applanation biometry [245]. Newer contact-free optical biometry technologies overcome the limitation of contact biometry and are gaining traction in physician-based ophthalmology. The optical biometry technologies that should be considered for future studies include laser partial coherence interferometry (PCI), low-coherence optical reflectometry (LCOR), slit-scanning videokeratography, Scheimflug imaging and anterior segment optical coherence tomography [126].

The primary investigator used the Retzlaff and Binkhorst theoretical formulae based on precedent in the veterinary literature [35-39]. Third generation formulae (Hoffer Q, Holladay and SRK/T) popularly used in physician-based ophthalmology are two variable formulae that differ mainly in the manner they calculate terminal IOL position [126]. The Haigis-L formula is deemed more accurate than the third generation formulae and does not require corneal curvature measurements, however, it uses three IOL and surgeon-specific constants which are derived by regression analysis based on surgeon-specific data of a large number of cases, and thus not a feasible option for this study [126]. Indeed this is a constantly evolving field in physician-based ophthalmology, and recently a new formula to preoperatively estimate the postoperative IOL position using measurements of the crystalline lens obtained using optical coherence tomography (OCT) imaging has been shown to produce lower estimation errors than current state-of-the-art methods [205].

CHAPTER 5: CONCLUSIONS

Clinical and diagnostic parameters described in this study will serve as a reference for veterinarians and will aid in the diagnosis of ocular disease in chimpanzees. Reference values for intraocular pressure, corneal curvature, central corneal thickness and ocular biometry have been reported under typical field conditions and commonly used general anaesthetic protocols for chimpanzees.

Traumatic cataract, vitreal degeneration and retinal detachment were important vision-threatening clinical findings reported in this group of 33 captive chimpazees. Clinical findings differed from those previously reported in laboratory chimpanzees and are thus a valid contribution to the literature.

The determination of the intraocular lens power for the chimpanzee will enable ophthalmologists performing cataract surgery to select the most appropriate intraocular lens for this species, although further studies evaluating pseudophakic refraction and determination of actual postoperative anterior chamber depth are required.

REFERENCES

1. Groves CP. Primate Taxonomy. Washington: DC: Smithsonian Institution Press; 2001.
2. Consortium CSaA. Initial sequence of the chimpanzee genome and comparison with the human genome. Nature. 2005;437(7055):69-87.
3. Initial sequence of the chimpanzee genome and comparison with the human genome. Nature. 2005;437(7055):69-87.
4. IUCN. The IUCN Red List of Threatened Species 2017 [Available from: http://www.iucnredlist.org.
5. Hof JS, V. . Apes Like Us: Portraits of a Kinship. Mannheim: Panorama2010.
6. de Manuel M, Kuhlwilm M, Frandsen P, Sousa VC, Desai T, Prado-Martinez J, et al. Chimpanzee genomic diversity reveals ancient admixture with bonobos. Science (New York, NY). 2016;354(6311):477-81.
7. Groves CP. In: Wilson DER, D.M. , editor. Mammal Species of the World: A Taxonomic and Geographic Reference. 3rd ed. Baltimore: Johns Hopkins University Press; 2005. p. 183.
8. Funkhouser JA, Mayhew JA, Mulcahy JB. Social network and dominance hierarchy analyses at Chimpanzee Sanctuary Northwest. PLoS One. 2018;13(2):e0191898.
9. Goodall J. The Chimpanzees of Gombe: Patterns of Behavior: The Belknap Press of Harvard University Press; 1986.
10. de Faber JT, Pameijer JH, Schaftenaar W. Cataract surgery with foldable intraocular lens implants in captive lowland gorillas (Gorilla gorilla gorilla). Journal of zoo and wildlife medicine : official publication of the American Association of Zoo Veterinarians. 2004;35(4):520-4.
11. Liang D, Alvarado TP, Oral D, Vargas JM, Denena MM, McCulley JP. Ophthalmic examination of the captive western lowland gorilla (Gorilla gorilla gorilla). Journal of zoo and wildlife medicine : official publication of the American Association of Zoo Veterinarians. 2005;36(3):430-3.
12. Lowenstine LJ, McManamon R, Terio KA. Comparative Pathology of Aging Great Apes: Bonobos, Chimpanzees, Gorillas, and Orangutans. Veterinary pathology. 2016;53(2):250-76.
13. Quigley HA. Number of people with glaucoma worldwide. Br J Ophthalmol. 1996;80(5):389-93.
14. McAllister F, Harwerth R, Patel N. Assessing the True Intraocular Pressure in the Non-human Primate. Optom Vis Sci. 2018;95(2):113-9.
15. Miller PE. The glaucomas. In: Maggs DJM, P.E.; Ofri, R., editor. Slatter´s Fundamentals of Veterinary Ophthalmology. 5th ed. Missouri: Elsevier Saunders; 2013. p. 247-71.
16. Leske MC. The epidemiology of open-angle glaucoma: a review. Am J Epidemiol. 1983;118(2):166-91.
17. Gordon MO, Beiser JA, Brandt JD, Heuer DK, Higginbotham EJ, Johnson CA, et al. The Ocular Hypertension Treatment Study: baseline factors that predict the onset of primary open-angle glaucoma. Arch Ophthalmol. 2002;120(6):714-20; discussion 829-30.
18. Anderson DR, Normal Tension Glaucoma S. Collaborative normal tension glaucoma study. Current opinion in ophthalmology. 2003;14(2):86-90.

19. Leske MC, Heijl A, Hyman L, Bengtsson B, Komaroff E. Factors for progression and glaucoma treatment: the Early Manifest Glaucoma Trial. Current opinion in ophthalmology. 2004;15(2):102-6.

20. Ofri R, Horowitz IH, Raz D, Shvartsman E, Kass PH. Intraocular pressure and tear production in five herbivorous wildlife species. The Veterinary record. 2002;151(9):265-8.

21. van der Woerdt A, Gilger BC, Wilkie DA, Strauch SM. Effect of auriculopalpebral nerve block and intravenous administration of xylazine on intraocular pressure and corneal thickness in horses. Am J Vet Res. 1995;56(2):155-8.

22. McClure JR, Jr., Gelatt KN, Gum GG, Manning JP. The effect of parenteral acepromazine and xylazine on intraocular pressure in the horse. Veterinary medicine, small animal clinician : VM, SAC. 1976;71(12):1727-30.

23. Bapodra P, Wolfe BA. Baseline assessment of ophthalmic parameters in the greater one-horned rhinoceros (Rhinoceros unicornis). Journal of zoo and wildlife medicine : official publication of the American Association of Zoo Veterinarians. 2014;45(4):859-65.

24. Smith PJ, Gum GG, Whitley RD, Samuelson DA, Brooks DE, Garcia-Sanchez GA. Tonometric and tonographic studies in the normal pony eye. Equine veterinary journal Supplement. 1990(10):36-8.

25. Hofmeister EH, Mosunic CB, Torres BT, Ralph AG, Moore PA, Read MR. Effects of ketamine, diazepam, and their combination on intraocular pressures in clinically normal dogs. American journal of veterinary research. 2006;67(7):1136-9.

26. Ghaffari MS, Rezaei MA, Mirani AH, Khorami N. The effects of ketamine-midazolam anesthesia on intraocular pressure in clinically normal dogs. Veterinary ophthalmology. 2010;13(2):91-3.

27. Wallin-Hakanson N, Wallin-Hakanson B. The effects of topical tropicamide and systemic medetomidine, followed by atipamezole reversal, on pupil size and intraocular pressure in normal dogs. Veterinary ophthalmology. 2001;4(1):3-6.

28. Hofmeister EH, Weinstein WL, Burger D, Brainard BM, Accola PJ, Moore PA. Effects of graded doses of propofol for anesthesia induction on cardiovascular parameters and intraocular pressures in normal dogs. Vet Anaesth Analg. 2009;36(5):442-8.

29. Young FAF, D.N. Refractive Characteristics of Chimpanzees. American Journal of Optometry and Archives of American Academy of Optometry. 1964:81-91.

30. Montiani-Ferreira F, Shaw G, Mattos BC, Russ HH, Vilani RG. Reference values for selected ophthalmic diagnostic tests of the capuchin monkey (Cebus apella). Veterinary ophthalmology. 2008;11(3):197-201.

31. Leiva M, Pena T, Bayon A, de Leon M, Morales I. Phacoemulsification considerations in nonhuman primates. Journal of medical primatology. 2012;41(5):317-24.

32. Montiani-Ferreira F, Lima L, Bacellar M, D'Otaviano Vilani RG, Fedullo JD, Lange RR. Bilateral phacoemulsification in an orangutan (Pongo pygmaeus). Veterinary ophthalmology. 2010;13 Suppl:91-9.

33. Warwick A, Redrobe S, Lotery A, Watts J. Bilateral cataract surgery with intraocular lens implant in a captive western lowland gorilla. Journal of medical primatology. 2017;46(5):252-5.

34. Gaiddon J, Rosolen SG, Steru L, Cook CS, Peiffer R, Jr. Use of biometry and keratometry for determining optimal power for intraocular lens implants in dogs. American journal of veterinary research. 1991;52(5):781-3.

35. Gilger BC, Davidson MG, Howard PB. Keratometry, ultrasonic biometry, and prediction of intraocular lens power in the feline eye. American journal of veterinary research. 1998;59(2):131-4.

36. McMullen RJ, Jr., Gilger BC. Keratometry, biometry and prediction of intraocular lens power in the equine eye. Veterinary ophthalmology. 2006;9(5):357-60.

37. Meister U, Görig C, Murphy CJ, Haan H, Ohnesorge B, Boevé MH. Intraocular lens power calculation for the equine eye. BMC Vet Res. 2018;14(1):123-.

38. Kuhn SE, Hendrix DV, Jones MP, Ward DA, Baine KH, Franklin SR. Biometry, keratometry, and calculation of intraocular lens power for the bald eagle (Haliaeetus leucocephalus). Veterinary ophthalmology. 2015;18 Suppl 1:106-12.

39. Owens CDM, T.M.; Boorstein, J.; Wynn, E.R.; Weihozkiy, A.; Stine, J.M.; McMullen Jr, R.J. . Keratometry, biometry and prediction of intraocular lens power in the tiger (Panthera tigris). ACVO 49th Annual Conference; Minneapolis2018.

40. Featherstone HJ, Heinrich CL. Ophthalmic Examination and Diagnostics Part 1: The Eye Examination and Diagnostic Procedures. In: Gelatt KN, Gilger BC, Kern TJ, editors. Veterinary ophthalmology. 5th ed. Ames: Wiley-Blackwell; 2013. p. 300-50.

41. Friedenwald JS. Tonometer calibration; an attempt to remove discrepancies found in the 1954 calibration scale for Schiotz tonometers. Transactions - American Academy of Ophthalmology and Otolaryngology American Academy of Ophthalmology and Otolaryngology. 1957;61(1):108-22.

42. Wang W-H, Millar JC, Pang I-H, Wax MB, Clark AF. Noninvasive measurement of rodent intraocular pressure with a rebound tonometer. Investigative ophthalmology & visual science. 2005;46(12):4617-21.

43. Kontiola A. A new electromechanical method for measuring intraocular pressure. Doc Ophthalmol. 1996;93(3):265-76.

44. Kontiola AI. A new induction-based impact method for measuring intraocular pressure. Acta Ophthalmol Scand. 2000;78(2):142-5.

45. Kontiola AI, Goldblum D, Mittag T, Danias J. The induction/impact tonometer: a new instrument to measure intraocular pressure in the rat. Exp Eye Res. 2001;73(6):781-5.

46. Knollinger AM, La Croix NC, Barrett PM, Miller PE. Evaluation of a rebound tonometer for measuring intraocular pressure in dogs and horses. Journal of the American Veterinary Medical Association. 2005;227(2):244-8.

47. Takenaka J, Mochizuki H, Kunihara E, Tanaka J, Kiuchi Y. Intraocular pressure measurement using rebound tonometer for deviated angles and positions in human eyes. Current eye research. 2012;37(2):109-14.

48. Rusanen E, Florin M, Hassig M, Spiess BM. Evaluation of a rebound tonometer (Tonovet) in clinically normal cat eyes. Veterinary ophthalmology. 2010;13(1):31-6.

49. Lobler M, Rehmer A, Guthoff R, Martin H, Sternberg K, Stachs O. Suitability and calibration of a rebound tonometer to measure IOP in rabbit and pig eyes. Veterinary ophthalmology. 2011;14(1):66-8.

50. Abraham LM, Epasinghe NC, Selva D, Casson R. Comparison of the ICare rebound tonometer with the Goldmann applanation tonometer by experienced and inexperienced tonometrists. Eye (Lond). 2008;22(4):503-6.

51. Filippopoulos T, Matsubara A, Danias J, Huang W, Dobberfuhl A, Ren L, et al. Predictability and limitations of non-invasive murine tonometry: comparison of two devices. Experimental eye research. 2006;83(1):194-201.

52. Milnes ELC, T.; Feltrer, Y.; Drane, A.L.; Howatson, G.; Shave, R.E.; Curry, B.A.; Tremblay, J.C.; Williams, D.L. The effects of medetomidine and body postion on tear production and intraocular pressure in anesthetized chimpanzees (Pan troglodytes). Journal of Zoo and Wildlife Medicine. 2020.

53. Yu W, Cao G, Qiu J, Liu X, Ma J, Li N, et al. Evaluation of monkey intraocular pressure by rebound tonometer. Mol Vis. 2009;15:2196-201.

54. Elsmo EJ, Kiland JA, Kaufman PL, McLellan GJ. Evaluation of rebound tonometry in non-human primates. Exp Eye Res. 2011;92(4):268-73.

55. Görig C, Coenen RTI, Stades FC, Djajadiningrat-Laanen SC, Boevé MH. Comparison of the use of new handheld tonometers and established applanation tonometers in dogs. American journal of veterinary research. 2006;67(1):134-44.

56. Leiva M, Naranjo C, Pena MT. Comparison of the rebound tonometer (ICare) to the applanation tonometer (Tonopen XL) in normotensive dogs. Veterinary ophthalmology. 2006;9(1):17-21.

57. McLellan GJ, Kemmerling JP, Kiland JA. Validation of the TonoVet® rebound tonometer in normal and glaucomatous cats. Veterinary ophthalmology. 2013;16(2):111-8.

58. Broadwater JJ, Schorling JJ, Herring IP, Pickett JP. Ophthalmic examination findings in adult pygmy goats (Capra hicus). Veterinary ophthalmology. 2007;10(5):269-73.

59. Pereira FQ, Bercht BS, Soares MG, da Mota MG, Pigatto JA. Comparison of a rebound and an applanation tonometer for measuring intraocular pressure in normal rabbits. Veterinary ophthalmology. 2011;14(5):321-6.

60. Kim CY, Kuehn MH, Anderson MG, Kwon YH. Intraocular pressure measurement in mice: a comparison between Goldmann and rebound tonometry. Eye (London, England). 2007;21(9):1202-9.

61. Villar T, Pascoli AL, Klein A, Chacaltana FC, Capistrano E, Shipley CF, et al. Tear production, intraocular pressure, and central corneal thickness in white-tailed deer (Odocoileus virginianus). Veterinary ophthalmology. 2020;23(1):123-8.

62. Rajaei SM, Mood MA, Sadjadi R, Azizi F. Intraocular Pressure, Tear Production, and Ocular Echobiometry in Guinea Pigs (Cavia porcellus). J Am Assoc Lab Anim Sci. 2016;55(4):475-9.

63. Di Y, Luo X-M, Qiao T, Lu N. Intraocular pressure with rebound tonometry and effects of topical intraocular pressure reducing medications in guinea pigs. Int J Ophthalmol. 2017;10(2):186-90.

64. Somma AT, Coimbra CM, Lange RR, Moore BA, Montiani-Ferreira F. Reference values for selected ophthalmic diagnostic tests in two species of microchiroptera bats (Artibeus lituratus and Anoura caudifer). Veterinary ophthalmology. 2020;23(1):61-6.

65. Schuster EJ, Strueve J, Fehr MJ, Mathes KA. Measurement of intraocular pressure in healthy unanesthetized inland bearded dragons (Pogona vitticeps). American journal of veterinary research. 2015;76(6):494-9.

66. Gonzalez-Alonso-Alegre EM, Martinez-Nevado E, Caro-Vadillo A, Rodriguez-Alvaro A. Central corneal thickness and intraocular pressure in captive black-footed penguins (Spheniscus dermersus). Veterinary ophthalmology. 2015;18(s1):94-7.

67. Mercado JA, Wirtu G, Beaufrere H, Lydick D. Intraocular pressure in captive black-footed penguins (Spheniscus demevsus) measured by rebound tonometry. J Avian Med Surg. 2010;24(2):138-41.

68. Harris MC, Schorling JJ, Herring IP, Elvinger F, Bright PR, Pickett JP. Ophthalmic examination findings in a colony of Screech owls (Megascops asio). Veterinary ophthalmology. 2008;11(3):186-92.

69. Jeong MB, Kim YJ, Yi NY, Park SA, Kim WT, Kim SE, et al. Comparison of the rebound tonometer (TonoVet) with the applanation tonometer (TonoPen XL) in normal Eurasian Eagle owls (Bubo bubo). Veterinary ophthalmology. 2007;10(6):376-9.

70. Labelle AL, Whittington JK, Breaux CB, Labelle P, Mitchell MA, Zarfoss MK, et al. Clinical utility of a complete diagnostic protocol for the ocular evaluation of free-living raptors. Veterinary ophthalmology. 2012;15(1):5-17.

71. Reuter A, Muller K, Arndt G, Eule JC. Accuracy and reproducibility of the TonoVet rebound tonometer in birds of prey. Veterinary ophthalmology. 2010;13 Suppl:80-5.

72. Jeong M-B, Kim Y-J, Yi N-Y, Park S-A, Kim W-T, Kim S-E, et al. Comparison of the rebound tonometer (TonoVet) with the applanation tonometer (TonoPen XL) in normal Eurasian Eagle owls (Bubo bubo). Veterinary ophthalmology. 2007;10(6):376-9.

73. Reuter A, Müller K, Arndt G, Eule JC. Accuracy and reproducibility of the TonoVet rebound tonometer in birds of prey. Veterinary ophthalmology. 2010;13 Suppl:80-5.

74. Wills S, Pinard C, Nykamp S, Beaufrère H. OPHTHALMIC REFERENCE VALUES AND LESIONS IN TWO CAPTIVE POPULATIONS OF NORTHERN OWLS: GREAT GREY OWLS (STRIX NEBULOSA) AND SNOWY OWLS (BUBO SCANDIACUS). Journal of zoo and wildlife medicine : official publication of the American Association of Zoo Veterinarians. 2016;47(1):244-55.

75. Muller K, Mauler DA, Eule JC. Reference values for selected ophthalmic diagnostic tests and clinical characteristics of chinchilla eyes (Chinchilla lanigera). Veterinary ophthalmology. 2010;13 Suppl:29-34.

76. Klein HE, Krohne SG, Moore GE, Mohamed AS, Stiles J. Effect of eyelid manipulation and manual jugular compression on intraocular pressure measurement in dogs. Journal of the American Veterinary Medical Association. 2011;238(10):1292-5.

77. Pauli AM, Bentley E, Diehl KA, Miller PE. Effects of the application of neck pressure by a collar or harness on intraocular pressure in dogs. J Am Anim Hosp Assoc. 2006;42(3):207-11.

78. Broadwater JJ, Schorling JJ, Herring IP, Elvinger F. Effect of body position on intraocular pressure in dogs without glaucoma. American journal of veterinary research. 2008;69(4):527-30.

79. de Oliveira JK, Montiani-Ferreira F, Williams DL. The influence of the tonometer position on canine intraocular pressure measurements using the Tonovet(®) rebound tonometer. Open Vet J. 2018;8(1):68-76.

80. Komaromy AM, Garg CD, Ying GS, Liu C. Effect of head position on intraocular pressure in horses. American journal of veterinary research. 2006;67(7):1232-5.

81. Blackwood SE, Plummer CE, Crumley W, Mackay EO, Brooks DE, Barrie KP. Ocular parameters in a captive colony of fruit bats. Veterinary ophthalmology. 2010;13 Suppl:72-9.

82. Chittick B, Harms C. Intraocular pressure of juvenile loggerhead sea turtles (Caretta caretta) held in different positions. The Veterinary record. 2001;149(19):587-9.

83. Klein A, Shemesh G, Loewenstein A, Kurtz S. Intraocular pressure measurements in relation to head position and through soft contact lenses: comparison of three portable instruments. Ophthalmic surgery, lasers & imaging : the official journal of the International Society for Imaging in the Eye. 2011;42(1):64-71.

84. Aihara M, Lindsey JD, Weinreb RN. Twenty-four-hour pattern of mouse intraocular pressure. Exp Eye Res. 2003;77(6):681-6.

85. Galin MA, Mc IJ, Magruder GB. Influence of position on intraocular pressure. Am J Ophthalmol. 1963;55:720-3.

86. Park YW, Jeong MB, Kim TH, Ahn JS, Ahn JT, Park SA, et al. Effect of central corneal thickness on intraocular pressure with the rebound tonometer and the applanation tonometer in normal dogs. Veterinary ophthalmology. 2011;14(3):169-73.

87. Chui W-s, Lam A, Chen D, Chiu R. The influence of corneal properties on rebound tonometry. Ophthalmology. 2008;115(1):80-4.

88. Kalesnykas G, Uusitalo H. Comparison of simultaneous readings of intraocular pressure in rabbits using Perkins handheld, Tono-Pen XL, and TonoVet tonometers. Graefe's archive for clinical and experimental ophthalmology = Albrecht von Graefes Archiv fur klinische und experimentelle Ophthalmologie. 2007;245(5):761-2.

89. Martinez-de-la-Casa JM, Garcia-Feijoo J, Vico E, Fernandez-Vidal A, Benitez del Castillo JM, Wasfi M, et al. Effect of corneal thickness on dynamic contour, rebound, and goldmann tonometry. Ophthalmology. 2006;113(12):2156-62.

90. Poostchi A, Mitchell R, Nicholas S, Purdie G, Wells A. The iCare rebound tonometer: comparisons with Goldmann tonometry, and influence of central corneal thickness. Clinical & experimental ophthalmology. 2009;37(7):687-91.

91. Bhan A, Browning AC, Shah S, Hamilton R, Dave D, Dua HS. Effect of corneal thickness on intraocular pressure measurements with the pneumotonometer, Goldmann applanation tonometer, and Tono-Pen. Invest Ophthalmol Vis Sci. 2002;43(5):1389-92.

92. Rao A, Kumar M, Prakash B, Varshney G. Relationship of central corneal thickness and intraocular pressure by iCare rebound tonometer. Journal of glaucoma. 2014;23(6):380-4.

93. Park Y-W, Jeong M-B, Kim T-H, Ahn J-S, Ahn J-T, Park S-A, et al. Effect of central corneal thickness on intraocular pressure with the rebound tonometer and the applanation tonometer in normal dogs. Veterinary ophthalmology. 2011;14(3):169-73.

94. Kato K. Comparison of two handheld applanation tonometers and the association of central corneal thickness, age, and intraocular pressure in normal and diseased canine eyes. Veterinary ophthalmology. 2014;17(6):417-25.

95. Gelatt KN, MacKay EO. Distribution of intraocular pressure in dogs. Veterinary ophthalmology. 1998;1(2-3):109-14.

96. Mughannam AJ, Cook CS, Fritz CL. Change in intraocular pressure during maturation in Labrador Retriever dogs. Veterinary ophthalmology. 2004;7(2):87-9.

97. Kroll MM, Miller PE, Rodan I. Intraocular pressure measurements obtained as part of a comprehensive geriatric health examination from cats seven years of age or older. Journal of the American Veterinary Medical Association. 2001;219(10):1406-10.

98. Ofri R, Steinmetz A, Thielebein J, Horowitz IH, Oechtering G, Kass PH. Factors affecting intraocular pressure in lions. Vet J. 2008;177(1):124-9.

99. Marzok MA, El-Khodery SA. Intraocular pressure in clinically normal dromedary camels (Camelus dromedarius). American journal of veterinary research. 2015;76(2):149-54.

100. Ofri R, Shore LS, Kass PH, Horowitz IH. The effect of elevated progesterone levels on intraocular pressure in lions (Panthera leo). Res Vet Sci. 1999;67(2):121-3.

101. Ofri R, Shub N, Galin Z, Shemesh M, Shore LS. Effect of reproductive status on intraocular pressure in cats. American journal of veterinary research. 2002;63(2):159-62.

102. Hernandez-Guerra AM, Rodilla V, Lopez-Murcia MM. Ocular biometry in the adult anesthetized ferret (Mustela putorius furo). Veterinary ophthalmology. 2007;10(1):50-2.

103. Ofri R, Horowitz I, Jacobson S, Kass PH. The effects of anesthesia and gender on intraocular pressure in lions (Panthera leo). Journal of zoo and wildlife medicine : official publication of the American Association of Zoo Veterinarians. 1998;29(3):307-10.

104. Bertolucci C, Giudice E, Fazio F, Piccione G. Circadian intraocular pressure rhythms in athletic horses under different lighting regime. Chronobiology international. 2009;26(2):348-58.

105. Del Sole MJ, Sande PH, Bernades JM, Aba MA, Rosenstein RE. Circadian rhythm of intraocular pressure in cats. Veterinary ophthalmology. 2007;10(3):155-61.

106. Giannetto C, Piccione G, Giudice E. Daytime profile of the intraocular pressure and tear production in normal dog. Veterinary ophthalmology. 2009;12(5):302-5.

107. Martin-Suarez E, Molleda C, Tardon R, Galan A, Gallardo J, Molleda J. Diurnal variations of central corneal thickness and intraocular pressure in dogs from 8:00 am to 8:00 pm. Can Vet J. 2014;55(4):361-5.

108. Garzón-Ariza A, Guisado A, Galán A, Martín-Suárez E. Diurnal variations in intraocular pressure and central corneal thickness and the correlation between these factors in dogs. Veterinary ophthalmology. 2018;21(5):464-70.

109. Rowland JM, Potter DE, Reiter RJ. Circadian rhythm in intraocular pressure: a rabbit model. Current eye research. 1981;1(3):169-73.

110. Shiose Y. Intraocular pressure: new perspectives. Survey of ophthalmology. 1990;34(6):413-35.

111. Kida T, Liu JH, Weinreb RN. Effect of 24-hour corneal biomechanical changes on intraocular pressure measurement. Invest Ophthalmol Vis Sci. 2006;47(10):4422-6.

112. Kotecha A, Crabb DP, Spratt A, Garway-Heath DF. The relationship between diurnal variations in intraocular pressure measurements and central corneal thickness and corneal hysteresis. Invest Ophthalmol Vis Sci. 2009;50(9):4229-36.

113. Komaromy AM, Brooks DE, Kubilis PS, Dawson WW, Sapp HL, Jr., Nelson G, et al. Diurnal intraocular pressure curves in healthy rhesus macaques (Macaca mulatta) and rhesus macaques with normotensive and hypertensive primary open-angle glaucoma. Journal of glaucoma. 1998;7(2):128-31.

114. Madigan MC, Gillard-Crewther S, Kiely PM, Crewther DP, Brennan NA, Efron N, et al. Corneal thickness changes following sleep and overnight contact lens wear in the primate (Macaca fascicularis). Current eye research. 1987;6(6):809-15.

115. Garzón-Ariza A, Guisado A, Galán A, Martín-Suárez E. Diurnal variations in intraocular pressure and central corneal thickness and the correlation between these factors in dogs. Veterinary ophthalmology. 2018;21(5):464-70.

116. Weinreb RN, Cook J, Friberg TR. Effect of inverted body position on intraocular pressure. Am J Ophthalmol. 1984;98(6):784-7.

117. Linder BJ, Trick GL, Wolf ML. Altering body position affects intraocular pressure and visual function. Invest Ophthalmol Vis Sci. 1988;29(10):1492-7.

118. Wu SY, Nemesure B, Hennis A, Leske MC, Barbados Eye Studies G. Nine-year changes in intraocular pressure: the Barbados Eye Studies. Arch Ophthalmol. 2006;124(11):1631-6.

119. Cunningham AJ, Barry P. Intraocular pressure--physiology and implications for anaesthetic management. Can Anaesth Soc J. 1986;33(2):195-208.

120. Hahnenberger RW. Influence of various anesthetic drugs on the intraocular pressure of cats. Albrecht Von Graefes Arch Klin Exp Ophthalmol. 1976;199(2):179-86.

121. Murphy DF. Anesthesia and intraocular pressure. Anesth Analg. 1985;64(5):520-30.

122. Erickson-Lamy KA, Kaufman PL, McDermott ML, France NK. Comparative anesthetic effects on aqueous humor dynamics in the cynomolgus monkey. Arch Ophthalmol. 1984;102(12):1815-20.

123. Raposo AC, Ofri R, Schaffer DP, Gomes Júnior DC, Libório FA, Martins Filho EF, et al. Evaluation of ophthalmic and hemodynamic parameters in capuchin monkeys (Sapajus sp.) submitted to dissociative anesthetic protocols. Journal of medical primatology. 2015;44(6):381-9.

124. Wadia S, Bhola R, Lorenz D, Padmanabhan P, Gross J, Stevenson M. Ketamine and intraocular pressure in children. Annals of emergency medicine. 2014;64(4):385-8.e1.

125. Jang M, Park S, Son WG, Jo SM, Hwang H, Seo K, et al. Effect of tiletamine-zolazepam on the intraocular pressure of the dog. Veterinary ophthalmology. 2015;18(6):481-4.

126. Lee AC, Qazi MA, Pepose JS. Biometry and intraocular lens power calculation. Current opinion in ophthalmology. 2008;19(1):13-7.

127. Sahin A, Hamrah P. Clinically relevant biometry. Current opinion in ophthalmology. 2012;23(1):47-53.

128. Root T. OphthoBook: CreateSpace Independent Publishing Platform; 2009. 180 p.

129. Grinninger P, Skalicky M, Nell B. Evaluation of healthy equine eyes by use of retinoscopy, keratometry, and ultrasonographic biometry. American journal of veterinary research. 2010;71(6):677-81.

130. Kawasaki M, Furujo T, Kuroda K, Azuma K, Okamoto Y, Ito N. Characterising keratometry in different dog breeds using an automatic handheld keratometer. The Veterinary record. 2020.

131. Featherstone HJH, C.L. Ophthalmic Examnation and Diagnostics Part 1: The eye examination and diagnostic procedures. In: Gelatt KNG, B.C.; Kern, T.J., editor. Veterinary ophthalmology. 5th ed. Ames, Iowa: Wiley-Blackwell; 2013. p. 533-613.

132. Herbig LE, Eule JC. Central corneal thickness measurements and ultrasonographic study of the growing equine eye. Veterinary ophthalmology. 2015;18(6):462-71.

133. Wolfel AE, Pederson SL, Cleymaet AM, Hess AM, Freeman KS. Canine central corneal thickness measurements via Pentacam-HR®, optical coherence tomography (Optovue iVue®), and high-resolution ultrasound biomicroscopy. Veterinary ophthalmology. 2018;21(4):362-70.

134. Belovay GW, Goldberg I. The thick and thin of the central corneal thickness in glaucoma. Eye (London, England). 2018;32(5):915-23.

135. Jeong S, Kang S, Park S, Park E, Lim J, Nam T, et al. Comparison of corneal thickness measurements using ultrasound pachymetry, ultrasound biomicroscopy, and digital caliper in frozen canine corneas. Veterinary ophthalmology. 2018;21(4):339-46.

136. Gilger BC, Whitley RD, McLaughlin SA, Wright JC, Drane JW. Canine corneal thickness measured by ultrasonic pachymetry. American journal of veterinary research. 1991;52(10):1570-2.

137. Gilger BC, Wright JC, Whitley RD, McLaughlin SA. Corneal thickness measured by ultrasonic pachymetry in cats. American journal of veterinary research. 1993;54(2):228-30.

138. Salz JJ, Azen SP, Berstein J, Caroline P, Villasenor RA, Schanzlin DJ. Evaluation and comparison of sources of variability in the measurement of corneal thickness with ultrasonic and optical pachymeters. Ophthalmic Surg. 1983;14(9):750-4.

139. Correa-Perez ME, Lopez-Miguel A, Miranda-Anta S, Iglesias-Cortinas D, Alio JL, Maldonado MJ. Precision of high definition spectral-domain optical coherence tomography for measuring central corneal thickness. Invest Ophthalmol Vis Sci. 2012;53(4):1752-7.

140. Hong JP, Nam SM, Kim TI, Seo KY, Lee SY, Meduri A, et al. Reliability of RTVue, Visante, and slit-lamp adapted ultrasonic pachymetry for central corneal thickness measurement. Yonsei Med J. 2012;53(3):634-41.

141. Ishibazawa A, Igarashi S, Hanada K, Nagaoka T, Ishiko S, Ito H, et al. Central corneal thickness measurements with Fourier-domain optical coherence tomography versus ultrasonic pachymetry and rotating Scheimpflug camera. Cornea. 2011;30(6):615-9.

142. de Korte CL, van der Steen AF, Thijssen JM. Acoustic velocity and attenuation of eye tissues at 20 MHz. Ultrasound Med Biol. 1994;20(5):471-80.

143. Tang J, Liu J. Variance of speed of sound and correlation with acoustic impedance in canine corneas. Ultrasound Med Biol. 2011;37(10):1714-21.

144. Thijssen JM, Mol HJ, Timmer MR. Acoustic parameters of ocular tissues. Ultrasound Med Biol. 1985;11(1):157-61.

145. Alario AF, Pirie CG. Central corneal thickness measurements in normal dogs: a comparison between ultrasound pachymetry and optical coherence tomography. Veterinary ophthalmology. 2014;17(3):207-11.

146. Jonas JB, Hayreh SS, Tao Y. Central corneal thickness and thickness of the lamina cribrosa and peripapillary sclera in monkeys. Archives of ophthalmology (Chicago, Ill : 1960). 2009;127(10):1395-6.

147. Medeiros FA, Sample PA, Weinreb RN. Corneal thickness measurements and frequency doubling technology perimetry abnormalities in ocular hypertensive eyes. Ophthalmology. 2003;110(10):1903-8.

148. Fogagnolo P, Rossetti L, Mazzolani F, Orzalesi N. Circadian variations in central corneal thickness and intraocular pressure in patients with glaucoma. Br J Ophthalmol. 2006;90(1):24-8.

149. Hamilton KE, Pye DC, Aggarwala S, Evian S, Khosla J, Perera R. Diurnal variation of central corneal thickness and Goldmann applanation tonometry estimates of intraocular pressure. Journal of glaucoma. 2007;16(1):29-35.

150. Broman AT, Congdon NG, Bandeen-Roche K, Quigley HA. Influence of corneal structure, corneal responsiveness, and other ocular parameters on tonometric measurement of intraocular pressure. Journal of glaucoma. 2007;16(7):581-8.

151. Kohlhaas M, Boehm AG, Spoerl E, Pursten A, Grein HJ, Pillunat LE. Effect of central corneal thickness, corneal curvature, and axial length on applanation tonometry. Arch Ophthalmol. 2006;124(4):471-6.

152. Shah S, Chatterjee A, Mathai M, Kelly SP, Kwartz J, Henson D, et al. Relationship between corneal thickness and measured intraocular pressure in a general ophthalmology clinic. Ophthalmology. 1999;106(11):2154-60.

153. Shimmyo M, Ross AJ, Moy A, Mostafavi R. Intraocular pressure, Goldmann applanation tension, corneal thickness, and corneal curvature in Caucasians, Asians, Hispanics, and African Americans. Am J Ophthalmol. 2003;136(4):603-13.

154. Goldmann H, Schmidt T. [Applanation tonometry]. Ophthalmologica. 1957;134(4):221-42.

155. Harada Y, Hirose N, Kubota T, Tawara A. The influence of central corneal thickness and corneal curvature radius on the intraocular pressure as measured by different tonometers: noncontact and goldmann applanation tonometers. Journal of glaucoma. 2008;17(8):619-25.

156. Zeng Y, Guo X, Lin J, Zeng X, Zhong Y, Cai X, et al. [Effect of tear film changes on the intraocular pressure measurement by Goldmann applanation tonometer]. Yan Ke Xue Bao. 2008;24(1):27-9.

157. Ollivier FJ, Brooks DE, Komaromy AM, Kallberg ME, Andrew SE, Sapp HL, et al. Corneal thickness and endothelial cell density measured by non-contact specular microscopy and pachymetry in Rhesus macaques (Macaca mulatta) with laser-induced ocular hypertension. Exp Eye Res. 2003;76(6):671-7.

158. Ekesten B, Torrang I. Age-related changes in ocular distances in normal eyes of Samoyeds. American journal of veterinary research. 1995;56(1):127-33.

159. Montiani-Ferreira F, Petersen-Jones S, Cassotis N, Ramsey DT, Gearhart P, Cardoso F. Early postnatal development of central corneal thickness in dogs. Veterinary ophthalmology. 2003;6(1):19-22.

160. Telle MR, Chen N, Shinsako D, Kiland JA, Oikawa K, Møller Trane R, et al. Relationship between corneal sensitivity, corneal thickness, corneal diameter, and intraocular pressure in normal cats and cats with congenital glaucoma. Veterinary ophthalmology. 2019;22(1):4-12.

161. Plummer CE, Ramsey DT, Hauptman JG. Assessment of corneal thickness, intraocular pressure, optical corneal diameter, and axial globe dimensions in Miniature Horses. American journal of veterinary research. 2003;64(6):661-5.

162. Ramsey DT, Hauptman JG, Petersen-Jones SM. Corneal thickness, intraocular pressure, and optical corneal diameter in Rocky Mountain Horses with cornea globosa or clinically normal corneas. American journal of veterinary research. 1999;60(10):1317-21.

163. Andrew SE, Ramsey DT, Hauptman JG, Brooks DE. Density of corneal endothelial cells and corneal thickness in eyes of euthanatized horses. American journal of veterinary research. 2001;62(4):479-82.

164. Osuobeni EP, Hamidzada WA. Ultrasonographic determination of the dimensions of ocular components in enucleated eyes of the one-humped camel (Camelus dromedarius). Res Vet Sci. 1999;67(2):125-9.

165. Andrew SE, Willis AM, Anderson DE. Density of corneal endothelial cells, corneal thickness, and corneal diameters in normal eyes of llamas and alpacas. American journal of veterinary research. 2002;63(3):326-9.

166. Montiani-Ferreira F, Truppel J, Tramontin MH, D'Octaviano Vilani RG, Lange RR. The capybara eye: clincial tests, anatomic and biometric features. Veterinary ophthalmology. 2008;11(6):386-94.

167. Cafaro TA, Ortiz SG, Maldonado C, Esposito FA, Croxatto JO, Berra A, et al. The cornea of Guinea pig: structural and functional studies. Veterinary ophthalmology. 2009;12(4):234-41.

168. Montiani-Ferreira F, Cardoso F, Petersen-Jones S. Postnatal development of central corneal thickness in chicks of Gallus gallus domesticus. Veterinary ophthalmology. 2004;7(1):37-9.

169. Lynch GL, Hoffman A, Blocker T. Central corneal thickness in koi fish: effects of age, sex, body length, and corneal diameter. Veterinary ophthalmology. 2007;10(4):211-5.

170. Gonzalez EM, Rodriguez A, Garcia I. Review of ocular ultrasonography. Veterinary radiology & ultrasound : the official journal of the American College of Veterinary Radiology and the International Veterinary Radiology Association. 2001;42(6):485-95.

171. Dudea SM. Ultrasongraphy of the eye and orbit. Medical Ultrasonography. 2011;13(2):171-4.

172. Rubin LF, Koch SA. Ocular diagnostic ultrasonography. Journal of the American Veterinary Medical Association. 1968;153(12):1706-16.

173. Dietrich UM. Ophthalmic Examination and Diagnostics Part 3: Diagnostic Ultrasonography. . In: Gelatt KN, Gilger BC, Kern TJ, editors. Veterinary ophthalmology. 5th ed. Ames: Wiley-Blackwell; 2013. p. 669-82.

174. Mattoon JSN, T.G. Veterinary Diagnostic Ultrasound. Philadelphia: WB Saunders; 1995.

175. Hatem RA. Ophthalmic Ultrasound. New York: Churchill Livingstone; 1996.

176. Brooks DE. Veterinary Ophthalmology. 3rd ed. Baltimore: Lippincott Williams & Wilkins; 1999.

177. Eisenberg HM. Ultrasonography of the eye and orbit. Vet Clin North Am Small Anim Pract. 1985;15(6):1263-74.

178. Pavlin CJF, F.S. Ultrasound Biomicroscopy of the Eye. New York, NY: Springer-Verlag; 1995.

179. Gibson TE, Roberts SM, Severin GA, Steyn PF, Wrigley RH. Comparison of gonioscopy and ultrasound biomicroscopy for evaluating the iridocorneal angle in dogs. Journal of the American Veterinary Medical Association. 1998;213(5):635-8.

180. Cottrill NB, Banks WJ, Pechman RD. Ultrasonographic and biometric evaluation of the eye and orbit of dogs. American journal of veterinary research. 1989;50(6):898-903.

181. Ruiz T, Campos WN, Peres TP, Goncalves GF, Ferraz RH, Nespoli PE, et al. Intraocular pressure, ultrasonographic and echobiometric findings of juvenile Yacare caiman (Caiman yacare) eye. Veterinary ophthalmology. 2015;18 Suppl 1:40-5.

182. Hamidzada WA, Osuobeni EP. Agreement between A-mode and B-mode ultrasonography in the measurement of ocular distances. Veterinary radiology & ultrasound : the official journal of the American College of Veterinary Radiology and the International Veterinary Radiology Association. 1999;40(5):502-7.

183. Boroffka SA, Voorhout G, Verbruggen AM, Teske E. Intraobserver and interobserver repeatability of ocular biometric measurements obtained by means of B-mode ultrasonography in dogs. American journal of veterinary research. 2006;67(10):1743-9.

184. Montiani-Ferreira F, Truppel J, Tramontin MH, Vilani RG, Lange RR. The capybara eye: clinical tests, anatomic and biometric features. Veterinary ophthalmology. 2008;11(6):386-94.

185. Meister U, Ohnesorge B, Körner D, Boevé MH. Evaluation of ultrasound velocity in enucleated equine aqueous humor, lens and vitreous body. BMC Vet Res. 2014;10:250-.

186. Jansson F, Sundmark E. Determination of the velocity of ultrasound in ocular tissues at different temperatures. Acta Ophthalmol (Copenh). 1961;39:899-910.

187. Oksala A, Lehtinen A. Measurement of the velocity of sound in some parts of the eye. Acta ophthalmologica. 1958;36(4):633-9.

188. Schiffer SP, Rantanen NW, Leary GA, Bryan GM. Biometric study of the canine eye, using A-mode ultrasonography. American journal of veterinary research. 1982;43(5):826-30.

189. Gorig C, Varghese T, Stiles T, van den Broek J, Zagzebski JA, Murphy CJ. Evaluation of acoustic wave propagation velocities in the ocular lens and vitreous tissues of pigs, dogs, and rabbits. American journal of veterinary research. 2006;67(2):288-95.

190. Hamidzada WA, Osuobeni EP. Ultrasound velocity in the aqueous and vitreous humours of the one-humped camel (Camelus Dromedarius). Clin Exp Optom. 1998;81(5):222-7.

191. Toni MC, Meirelles AE, Gava FN, Camacho AA, Laus JL, Canola JC. Rabbits' eye globe sonographic biometry. Veterinary ophthalmology. 2010;13(6):384-6.

192. Kassab A. Ultrasonographic and macroscopic anatomy of the enucleated eyes of the buffalo (Bos bubalis) and the one-humped camel (Camelus dromedarius) of different ages. Anat Histol Embryol. 2012;41(1):7-11.

193. Potter TJ, Hallowell GD, Bowen IM. Ultrasonographic anatomy of the bovine eye. Veterinary radiology & ultrasound : the official journal of the American College of Veterinary Radiology and the International Veterinary Radiology Association. 2008;49(2):172-5.

194. Ribeiro AP, Silva ML, Rosa JP, Souza SF, Teixeira IA, Laus JL. Ultrasonographic and echobiometric findings in the eyes of Saanen goats of different ages. Veterinary ophthalmology. 2009;12(5):313-7.

195. Bapodra P, Bouts T, Mahoney P, Turner S, Silva-Fletcher A, Waters M. Ultrasonographic anatomy of the Asian elephant (Elephas maximus) eye. Journal of zoo and wildlife medicine : official publication of the American Association of Zoo Veterinarians. 2010;41(3):409-17.

196. Murphy CJ, Mutti DO, Zadnik K, Ver Hoeve J. Effect of optical defocus on visual acuity in dogs. American journal of veterinary research. 1997;58(4):414-8.

197. Sanchez RF, Becker R, Dawson C, Escanilla N, Lam R. Calculation of posterior chamber intraocular lens (IOL) size and dioptric power for use in pet rabbits undergoing phacoemulsification. Veterinary ophthalmology. 2017;20(3):242-9.

198. Mettenleiter EM. [Sonographic diagnosis (B-mode technique) for the eyes in horses. 1. Methods and normal findings]. Tierarztl Prax. 1995;23(5):481-8.

199. Retzlaff J. A new intraocular lens calculation formula. Journal - American Intra-Ocular Implant Society. 1980;6(2):148-52.

200. Binkhorst CD. Power of the prepupillary pseudophakos. Br J Ophthalmol. 1972;56(4):332-7.

201. Mouney MC, Townsend WM, Moore GE. Association of height, body weight, age, and corneal diameter with calculated intraocular lens strength of adult horses. American journal of veterinary research. 2012;73(12):1977-82.

202. Fyodorov SN, Galin MA, Linksz A. Calculation of the optical power of intraocular lenses. Investigative ophthalmology. 1975;14(8):625-8.

203. Alpar JJF, P.U. The determination of intraocular lens power. In: Alpar JJF, P.U., editor. Fechner´s Intraocular Lenses. New York: Thieme Inc.; 1986. p. 70-99.

204. McMullen RJ, Davidson MG, Campbell NB, Salmon JH, Gilger BC. Evaluation of 30- and 25-diopter intraocular lens implants in equine eyes after surgical extraction of the lens. American journal of veterinary research. 2010;71(7):809-16.

205. Martinez-Enriquez E, Perez-Merino P, Duran-Poveda S, Jimenez-Alfaro I, Marcos S. Estimation of intraocular lens position from full crystalline lens geometry: towards a new generation of intraocular lens power calculation formulas. Sci Rep. 2018;8(1):9829.

206. Schmidt RE. Ophthalmic lesions in non-human primates. Veterinary pathology. 1971;8(1):28-36.

207. Hoffman K, Videan EN, Fritz J, Murphy J. Diagnosis and treatment of ocular coccidioidomycosis in a female captive chimpanzee (Pan troglodytes): a case study. Annals of the New York Academy of Sciences. 2007;1111:404-10.

208. Gemensky Metzler AJ, Torrence ME, Wolfe BA, Paul G. Chronic keratopathy of chimpanzees in a wildlife preserve in Kenya. 47th Annual Meeting of the American College of Veterinary Ophthalmologists; Monterey, CA2016.

209. Fujisawa M, Matsubayashi K, Soumah AG, Kasahara Y, Nakatsuka M, Matsuzawa T. Farsightedness (presbyopia) in a wild elderly chimpanzee: the first report. Geriatrics & gerontology international. 2010;10(1):113-4.

210. Sigmund AB, Cushing AC, Hendrix DVH. Ophthalmic findings in 10 captive, anesthetized chimpanzees (Pan troglodytes). Veterinary ophthalmology. 2020;23(4):760-3.

211. Hashemi H, Khabazkhoob M, Emamian MH, Shariati M, Fotouhi A. A population-based study of corneal arcus and its risk factors in Iran. Ophthalmic epidemiology. 2014;21(5):339-44.

212. Knapp S, McCulley JP, Alvarado TP, Hogan RN. Comparative ocular anatomy of the western lowland gorilla. Veterinary ophthalmology. 2007;10(6):357-62.

213. Zeiss CJ. Animals as models of age-related macular degeneration: an imperfect measure of the truth. Veterinary pathology. 2010;47(3):396-413.

214. Steinmetz A, Bernhard A, Sahr S, Oechtering G. Suspected macular degeneration in a captive Western lowland gorilla (Gorilla gorilla gorilla). Veterinary ophthalmology. 2012;15 Suppl 2:139-41.

215. Niemuth JN, De Voe RS, Jennings SH, Loomis MR, Troan BV. Malignant hypertension and retinopathy in a western lowland gorilla (Gorilla gorilla gorilla). Journal of medical primatology. 2014;43(4):276-9.

216. Beltran WA, Vanore M, Ollivet F, Nemoz-Bertholet F, Aujard F, Clerc B, et al. Ocular findings in two colonies of gray mouse lemurs (Microcebus murinus). Veterinary ophthalmology. 2007;10(1):43-9.

217. Young FA, Beattie RJ, Newby FJ, Swindal MT. The Pullman study; a visual survey of Pullman school children. I. Am J Optom Arch Am Acad Optom. 1954;31(3):111-21.

218. Young FA. THE EFFECT OF RESTRICTED VISUAL SPACE ON THE REFRACTIVE ERROR OF THE YOUNG MONKEY EYE. Investigative ophthalmology. 1963;2:571-7.

219. Augusteyn RCH, B.M.; Ho, A.; Parel, J-M. Nonhuman Primate Ocular Biometry. Invest Opththalmol Vis Sci. 2016;57:105-14.

220. Augusteyn RC, Nankivil D, Mohamed A, Maceo B, Pierre F, Parel JM. Human ocular biometry. Exp Eye Res. 2012;102:70-5.

221. Denion E, Hitier M, Guyader V, Dugue AE, Mouriaux F. Unique human orbital morphology compared with that of apes. Sci Rep. 2015;5:11528.

222. Kawana K, Tokunaga T, Miyata K, Okamoto F, Kiuchi T, Oshika T. Comparison of corneal thickness measurements using Orbscan II, non-contact specular microscopy, and ultrasonic pachymetry in eyes after laser in situ keratomileusis. Br J Ophthalmol. 2004;88(4):466-8.

223. Jansson F, Kock E. Determination of the velocity of ultrasound in the human lens and vitreous. Acta Ophthalmol (Copenh). 1962;40:420-33.

224. Gemensky Metzler A, editor Chronic keratopathy of 16 captive chimpazees in Kenya. ACVO 2016 Conference; 2016; Monterey, California.

225. Samuelson DA. Ophthalmic Anatomy. In: Gelatt KNG, B.C.; Kern, T.J., editor. Veterinary Ophthalmoogy. I. Ames, Iowa: Wiley-Blackwell; 2013. p. 39-170.

226. Grahn BHP, R.L. Veterinary Ophthalmic Pathology. In: Gelatt KNG, B.C.; Kern, T.J., editor. Veterinary ophthalmology. I. 5th ed. Ames-Iowa: Wiley-Blackwell; 2013. p. 435-522.

227. Midelfart A, Aamo B. Ocular parameters in elderly in Norway. Acta Ophthalmol (Copenh). 1994;72(1):61-6.

228. Wu SY, Leske MC. Associations with intraocular pressure in the Barbados Eye Study. Arch Ophthalmol. 1997;115(12):1572-6.

229. Kass MA, Sears ML. Hormonal regulation of intraocular pressure. Survey of ophthalmology. 1977;22(3):153-76.

230. Ziai N, Ory SJ, Khan AR, Brubaker RF. Beta-human chorionic gonadotropin, progesterone, and aqueous dynamics during pregnancy. Arch Ophthalmol. 1994;112(6):801-6.

231. Green K, Phillips CI, Cheeks L, Slagle T. Aqueous humor flow rate and intraocular pressure during and after pregnancy. Ophthalmic research. 1988;20(6):353-7.

232. Tint NL, Alexander P, Tint KM, Vasileiadis GT, Yeung AM, Azuara-Blanco A. Hormone therapy and intraocular pressure in nonglaucomatous eyes. Menopause (New York, NY). 2010;17(1):157-60.

233. Knepper PA, Collins JA, Frederick R. Effects of dexamethasone, progesterone, and testosterone on IOP and GAGs in the rabbit eye. Invest Ophthalmol Vis Sci. 1985;26(8):1093-100.

234. Tsukahara S, Sasaki T, Phillips CI, Gore SM. Subconjunctival suspension of RU486 lowers intraocular pressure in normal rabbits. Br J Ophthalmol. 1986;70(6):451-5.

235. Green K, Cheeks L, Slagle T, Phillips CI. Interaction between progesterone and mifepristone on intraocular pressure in rabbits. Current eye research. 1989;8(3):317-20.

236. Järvinen K. Icare, Global Product Manager - TONOVET & TONOLAB. Icare Finland Oy2017.

237. Sorsby A. Emmetropia and its aberrations. Med Res Counc Special Rep Serv Rep. 1959;293.

238. Merriam JC, Zheng L. The Relationship of Corneal Curvature and Axial Length in Adults. Investigative Ophthalmology & Visual Science. 2005;46(13):864-.

239. Koch DD. The posterior cornea: hiding in plain sight. Ophthalmology. 2015;122(6):1070-1.

240. Wolfel AE, Pederson SL, Cleymaet AM, Hess AM, Freeman KS. Anterior segment parameters in normal dogs using the Pentacam® HR Scheimpflug system. Veterinary ophthalmology. 2019;22(5):683-94.

241. Verneuil M, Marsot M, Ruchon C. Anterior segment parameters measured in young healthy cats using a rotating Scheimpflug camera. Veterinary ophthalmology. 2019;22(3):381-4.

242. Yüksel H, Türkcü FM, Ari Ş, Çinar Y, Cingü AK, Şahin M, et al. Anterior segment parameters of rabbits with rotating Scheimpflug camera. Veterinary ophthalmology. 2015;18(3):210-3.

243. Edelhauser HFU, J.L. The cornea and the sclera. In: Kaufman PLA, A., editor. Adler´s Physiology of the Eye: Clinical Application. 10th ed. St. Louis, Missouri: Mosby, Inc.; 2003. p. 56.

244. Hoffer KJ. Biometry of 7500 cataractous eyes. Am J Ophthalmol. 1981;99(360).

245. Olsen T, Nielsen PJ. Immersion versus contact technique in the measurement of axial length by ultrasound. Acta Ophthalmol (Copenh). 1989;67(1):101-2.

246. Shammas HJ. A comparison of immersion and contact techniques for axial length measurement. Journal - American Intra-Ocular Implant Society. 1984;10(4):444-7.

247. Hoffer KJ. Axial dimension of the human cataractous lens. Arch Ophthalmol. 1993;111(914).

248. Kiss B, Findl O, Menapace R, Wirtitsch M, Petternel V, Drexler W, et al. Refractive outcome of cataract surgery using partial coherence interferometry and ultrasound biometry: clinical feasibility study of a commercial prototype II. Journal of cataract and refractive surgery. 2002;28(2):230-4.

249. Haigis W, Lege B, Miller N, Schneider B. Comparison of immersion ultrasound biometry and partial coherence interferometry for intraocular lens calculation according to Haigis. Graefes Arch Clin Exp Ophthalmol. 2000;238(9):765-73.

250. Olsen T. Improved accuracy of intraocular lens power calculation with the Zeiss IOLMaster. Acta Ophthalmol Scand. 2007;85(1):84-7.

APPENDICES

APPENDIX 1. Ophthalmic Examination Data Collection Sheets

OPHTHALMIC EXAMINATION DATA COLLECTION SHEET

DATE & TIME (Darted): ____/____/____ ____:____ **SEX:** M / F **WEIGHT:** _____ kg

ANIMAL NAME: _____ **ORIGIN:** _____

SPECIES: *PAN TROGLODYTES* **GA PROTOCOL:** _____

DATE OF BIRTH / AGE: _____ / _____ (Time on ISO= __:__)_____

EXAMINATION TECHNIQUES / DIAGNOSTIC PROCEDURES:

☐ **TONOMETRY:** **OD: P=** ____ /____ / ____ mmHg **OS: P=** ____ /____ / ____ mmHg **Time:** ___:____

Do/Ca= ____ / ____ / ____ mmHg **Do/Ca=** ____ / ____ / ____ mmHg **Time:** ___:____

LAT RECUM: **ICare Pro=** ____ / ____ / ____ mmHg **ICare Pro=** ____ / ____ / ____ mmHg **Time:** ___:____

SUPINE: **ICare Pro=** ____ / ____ / ____ mmHg **ICare Pro=** ____ / ____ / ____ mmHg **Time:** ___:____

☐ **MYDRIACYL OU**

☐ **KERATOMETRY:** **OD:** _____ Diopters **OS:** _____ Diopters

☐ **SLIT-LAMP BIOMICROSCOPY:** **OD** **OS**

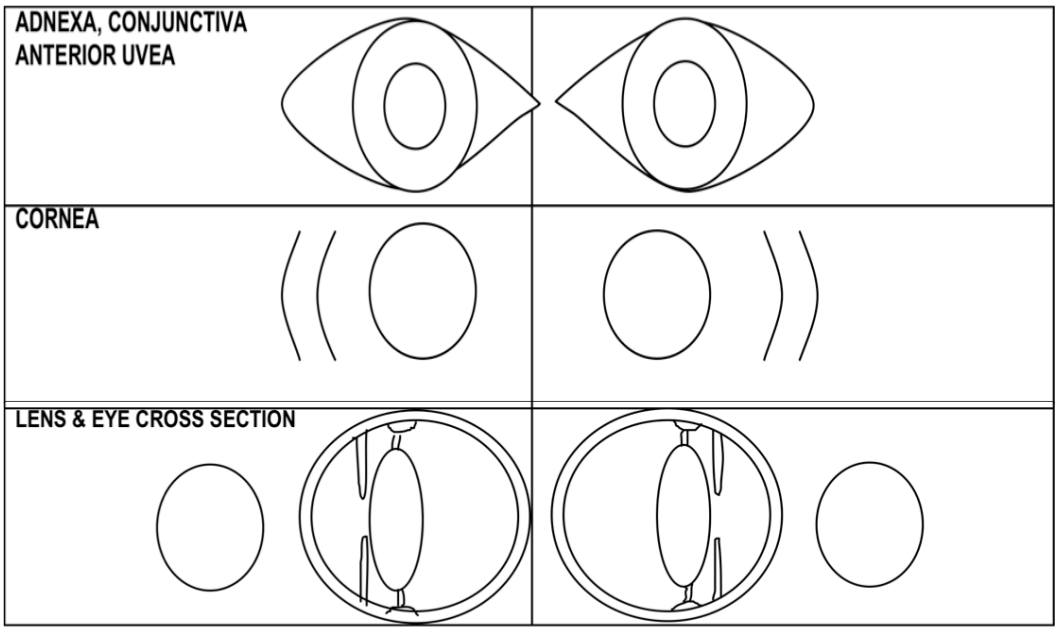

☐ **INDIRECT OPHTHALMOSCOPY:** **OD** **OS**

FUNDUS

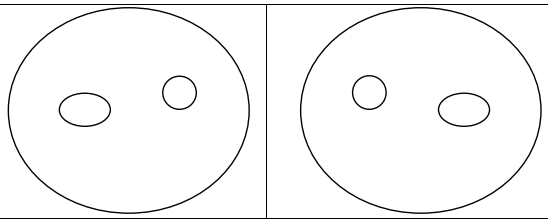

☐ **FUNDUS CAMERA / D-EYE:** **OD:** Y / N **OS:** Y / N

☐ **FLUORESCEIN:** **OD:** POS / NEG **OS:** POS / NEG

☐ **OCULAR ULTRASONOGRAPHY:**

A-SCAN (ACCUTOME) ☐

B-SCAN (M-TURBO) ☐

MEASUREMENT (CM)	OD		OS	
AXIAL GLOBE LENGTH				
ANTERIOR CHAMBER DEPTH				
LENS DEPTH				
POSTERIOR SEGMENT DEPTH				

POSTERIOR SEGMENT PATHOLOGY: **OD:** Y / N **OS:** Y / N

PHA / PHPV / RETINAL DETACHMENT / TEARS / VITREAL CHANGES / OTHER (SPECIFY):

_____

☐ **PACHYMETERY:** **OD:** _____ microns **OS:** _____ microns

COMMENTS: _____

_____

_____

_____

_____

APPENDIX 2. JGI Chimp Eden Veterinary Anaesthetic Record Data Collection Sheet

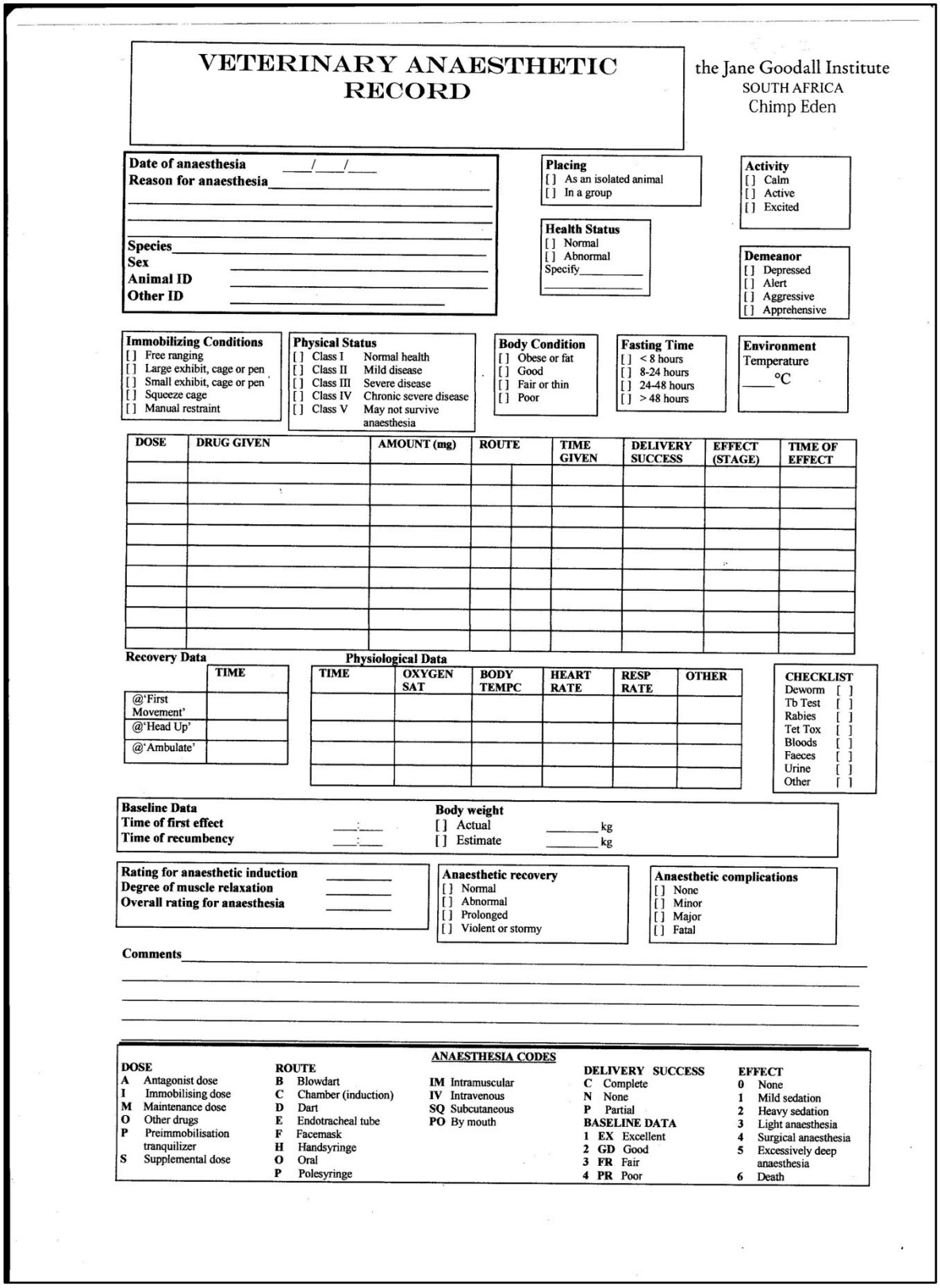

VETERINARY ANAESTHETIC RECORD

the Jane Goodall Institute
SOUTH AFRICA
Chimp Eden

Date of anaesthesia ___/___/___
Reason for anaesthesia_____
Species_____
Sex
Animal ID
Other ID

Placing
[ ] As an isolated animal
[ ] In a group

Activity
[ ] Calm
[ ] Active
[ ] Excited

Health Status
[ ] Normal
[ ] Abnormal
Specify_____

Demeanor
[ ] Depressed
[ ] Alert
[ ] Aggressive
[ ] Apprehensive

Immobilizing Conditions
[ ] Free ranging
[ ] Large exhibit, cage or pen
[ ] Small exhibit, cage or pen
[ ] Squeeze cage
[ ] Manual restraint

Physical Status
[ ] Class I Normal health
[ ] Class II Mild disease
[ ] Class III Severe disease
[ ] Class IV Chronic severe disease
[ ] Class V May not survive anaesthesia

Body Condition
[ ] Obese or fat
[ ] Good
[ ] Fair or thin
[ ] Poor

Fasting Time
[ ] < 8 hours
[ ] 8-24 hours
[ ] 24-48 hours
[ ] > 48 hours

Environment
Temperature
____°C

DOSE	DRUG GIVEN	AMOUNT (mg)	ROUTE		TIME GIVEN	DELIVERY SUCCESS	EFFECT (STAGE)	TIME OF EFFECT

Recovery Data

	TIME
@'First Movement'	
@'Head Up'	
@'Ambulate'	

Physiological Data

TIME	OXYGEN SAT	BODY TEMPC	HEART RATE	RESP RATE	OTHER

CHECKLIST
Deworm [ ]
Tb Test [ ]
Rabies [ ]
Tet Tox [ ]
Bloods [ ]
Faeces [ ]
Urine [ ]
Other [ ]

Baseline Data
Time of first effect ___:___
Time of recumbency ___:___

Body weight
[ ] Actual _____kg
[ ] Estimate _____kg

Rating for anaesthetic induction _____
Degree of muscle relaxation _____
Overall rating for anaesthesia _____

Anaesthetic recovery
[ ] Normal
[ ] Abnormal
[ ] Prolonged
[ ] Violent or stormy

Anaesthetic complications
[ ] None
[ ] Minor
[ ] Major
[ ] Fatal

Comments_____

ANAESTHESIA CODES

DOSE
A Antagonist dose
I Immobilising dose
M Maintenance dose
O Other drugs
P Preimmobilisation tranquilizer
S Supplemental dose

ROUTE
B Blowdart
C Chamber (induction)
D Dart
E Endotracheal tube
F Facemask
H Handsyringe
O Oral
P Polesyringe

IM Intramuscular
IV Intravenous
SQ Subcutaneous
PO By mouth

DELIVERY SUCCESS
C Complete
N None
P Partial

BASELINE DATA
1 EX Excellent
2 GD Good
3 FR Fair
4 PR Poor

EFFECT
0 None
1 Mild sedation
2 Heavy sedation
3 Light anaesthesia
4 Surgical anaesthesia
5 Excessively deep anaesthesia
6 Death

APPENDIX 3. JGI Chimp Eden Health Check and Assessment Data Collection Sheets

the Jane Goodall Institute
SOUTH AFRICA
Chimp Eden

HEALTH CHECK AND ASSESMENT

Animal I.D.

Name:_____ Reference no:_____

Species:_____ Sex: ☐Male ☐Female Age: ☐Adult ☐Sub-adult ☐Juvenile ☐Infant

Approx date of birth (dd/mm/yy):_____ Date of check:_____

Unique physical traits: _____

Clinical examination

1 – Visual observation (with the chimp awake in the home enclosure, without entering the enclosure)

1.1 - Skin and fur condition:

☐Normal ☐Abnormal _____

1.2 - Body condition (rough estimate):

☐1 ☐2 ☐3 ☐4 ☐5

1.3 - Ability to use all 4 limbs (without signs of lameness or imbalance):

☐Normal ☐Abnormal _____

1.4 - Head and eye movements:

☐Normal ☐Abnormal _____

1.5 - Front teeth and nostrils (abnormal discharges, unevenness or swellings):

☐Normal ☐Abnormal _____

2 – Clinical observation (with the chimp sedated)

2.1 - Weight:

_____ Kg

2.2 - Body condition (palpate the chimp over its thoracic and lumbar vertebrae):

☐1 ☐2 ☐3 ☐4 ☐5

2.3 - Eyes (straight, with no discharges, pupils even):

☐Normal ☐Abnormal _____

2.4 - Ears (clean, with no discharges, pinna not swollen) :

☐Normal ☐Abnormal _____

2.5 - Nostrils (clean, even in size) :

☐Normal ☐Abnormal _____

2.6 – Mouth (1 - just lifting up the lips: color of the gums, condition of the incisor and canine teeth; 2 – opened: examine premolar and molar teeth, check the cheek pouches and the back of the throat) :

☐Normal ☐Abnormal _____

2.7 - Jaw and throat (no swelling, check content in the cheek pouches) :

☐Normal ☐Abnormal _____

2.8 - Arms and legs (run hands down each arm and leg simultaneously checking for evenness in length and thickness of joints) :

☐Normal ☐Abnormal _____

2.9 - Fingers and toes:

☐Normal ☐Abnormal _____

2.10 - Abdomen (observe respiratory movements (respiratory rate/min: 30 – 70 min) and palpate the abdomen) :

☐Normal ☐Abnormal _____

2.11 - Thoracic auscultation (heart rate/min: 120 – 180 min) :

☐Normal ☐Abnormal _____

2.12 - External genitalia, anal and urethral orifices :

☐Normal ☐Abnormal _____

2.13 - Rectal temperature :
_____ ºC

2.14 – Body measurements

Weight (kg)	
Body length	

2.15 – Overall condition rating (1-5). Explain: _____

_____

_____

Screening tests

Samples collected: ☐Feces ☐Blood ☐Urine ☐Hair ☐Other _____

Hematology

Hemogram

WBC (mm3) _____ ☐

NEU (%) _____ ☐

LYM (%) _____ ☐

MON (%) _____ ☐

RBC (M/mm3) _____ ☐

HGB (g/dl) _____ ☐

HCT (%) _____ ☐

MCV (fl) _____ ☐

MCHC (g/dl) _____ ☐

MCH (pg) _____ ☐

PLT (m/mm3) _____ ☐

Biochemistry

Renal profile

Urea (mmol/l) _____ ☐

Creatinine (umol/l) _____ ☐

Liver function

AST (U/L) _____ ☐

ALT (U/L) _____ ☐

Glucose (mmol/l) _____ ☐

Observations:_____

_____

Fecal test
Parasitology
Number of eggs _____ EPG
Parasites: _____

Treatment: _____

TB test
Date: ____/____/____ Time of injection: _____

Eyelid: ☐Right ☐Left

Blood after injection: ☐Present ☐Not present

Reaction observed:

24h	48h	72h
☐ Grade 0	☐ Grade 0	☐ Grade 0
☐ Grade 1	☐ Grade 1	☐ Grade 1
☐ Grade 2	☐ Grade 2	☐ Grade 2
☐ Grade 3	☐ Grade 3	☐ Grade 3
☐ Grade 4	☐ Grade 4	☐ Grade 4
☐ Grade 5	☐ Grade 5	☐ Grade 5

Grade 0 – No reaction observed
Grade 1 – Bruise with extravasation of blood in the eyelid associated with the injection of tuberculin (considered negative)
Grade 2 – Varying degrees of erythema without swelling (considered negative)
Grade 3 – Varying degrees of erythema, minimum swelling or slight swelling without erythema (considered questionable)
Grade 4 – Obvious swelling, drooping of the eyelid, with varying degrees of erythema (considered positive)
Grade 5 – Swelling and/or necrosis with eyelid closed (strong positive)

Final result: ☐ Positive for TB
☐ Negative for TB

Other tests
_____

Vaccines

Vaccines administered: _____

Side effects or adverse reactions: _____